THE REALIZATION OF NARROW BAND-PASS CHARACTERISTICS USING SAMPLED DATA FILTERS

THE REALIZATION OF NARROW BAND-PASS CHARACTERISTICS USING SAMPLED DATA FILTERS

by

LOUIS BENTHIN

A Thesis

Submitted to the Faculty of Graduate Studies

in Partial Fulfilment of the Requirements

for the Degree

Master of Engineering

McMaster University

April 1968

MASTER OF ENGINEERING (1968)
(Electrical Engineering)

McMaster University
Hamilton, Ontario

TITLE: The Realization of Narrow Band-Pass Characteristics Using Sampled Data Filters

AUTHOR: Louis Benthin

SUPERVISOR: Professor S. S. Haykim

NUMBER OF PAGES: x, 122

ABSTRACT:

This thesis presents the results of an investigation of an alternative technique for the realization of narrow band-pass filters. This technique uses N parallel connected RC time-varying networks. A comparison of the performance of the 3-channel sampled data filter and one using the technique of quadrature modulation is made with respect to overall system performance.

Excellent agreement between the theoretical and experimental results are obtained for the band-pass characteristics. Design criteria are also presented in order to approach the ideal operation of an N-path sampled data filter.

ACKNOWLEDGEMENTS

I wish to thank Dr. S. S. Haykim for many stimulating discussions and encouragement given during the course of this work.

Acknowledgement is also made for the financial support given by the National Research Council of Canada.

I would like to express my sincere thanks and appreciation to my wife, Linda, whose patience and encouragement afforded the completion of this work with the minimum of stress.

Finally, I would also like to thank Mrs. T. Kammermayer for her excellent typing of this thesis.

TABLE OF CONTENTS PAGE

CHAPTER I	INTRODUCTION		1
1. 1	Historical Background		1
1. 2	Objectives		2
CHAPTER II	THEORETICAL CONSIDERATIONS		3
2. 1	Introduction		3
2. 2	The Frequency Translation Process		3
2. 3	Derivation of the System Transfer Function		8
	2. 3. 1	Analysis of the General Carrier Process	8
	2. 3. 2	Evaluation of the Modulator Constants	12
	2. 3. 3	The Sampled Data Filter Transfer Function	15
2. 4	Approach Due to Franks and Sandberg		16
	2. 4. 1	General Input-Output Relationship	16
	2. 4. 2	Transfer Function for N-Path Configuration	19
CHAPTER III	THE DESIGN OF A SAMPLED DATA FILTER SYSTEM		23
3. 1	Introduction		23
3. 2	Overall System Description		23
	3. 2. 1	The 3-Channel Sampled Data Filter	23
	3. 2. 2	The 2-Channel or Quadrature Modulation Sampled Data Filter	25
3. 3	Control and Sampling Circuits		28
	3. 3. 1	The 3-Channel Sampled Data Filter	28
	3. 3. 2	The Quadrature Modulation Sampled Data Filter	31
	3. 3. 3	The Sampling Circuit	31
3. 4	The Low-Pass and Band-Pass Filter Network		40
	3. 4. 1	The Synthesis of the Low-Pass RC Network	40
	3. 4. 2	Synthesis of the Band-Pass Network	44
3. 5	Mode of Operation		46
	3. 5. 1	The 3-Channel System	46
	3. 5. 2	The Quadrature Modulation System	53

PAGE ✓

CHAPTER IV	EXPERIMENTAL INVESTIGATION	56
4.1	Introduction	56
4.2	Channel Imperfections	57
	4.2.1 Variation in Gate-Drive Current	57
	4.2.2 Variation in Rise and Fall Time of Drive Signal	62
	4.2.3 Effect of Rise and Fall Time of Sampling Switch	67
	4.2.4 Variation in Sampling Switch Resistance	70
	4.2.5 Modulation Effects in the Sampled Data Filter	73
4.3	Variation in Sampling Frequency	83
4.4	Summary of Results on 3-Channel System	85
4.5	The Quadrature Modulation System	85
4.6	Summary and Comparison of Sampled Data Filter Systems	88
4.7	Bandwidth Variations	92
	4.7.1 Realization of Ideal Bandwidth Translation	92
	4.7.2 Bandwidth Control	95
CHAPTER V	DESIGN RECOMMENDATIONS	98
5.1	Introduction	98
5.2	Reduction of the Zero Signal Noise Component	99
5.3	Reduction of Image Component	100
5.4	Further Improvements of System Performance	100
CHAPTER VI	REMARKS AND FUTURE TRENDS	102
APPENDICES		105
APPENDIX I	CIRCUIT DETAILS	105
1.	Crystal Oscillator	105
2.	3-Stage Shift Register	106
3.	Bistable Circuit and Gate	107
4.	Tuned Amplifier	108
5.	RC-Active Band-Pass Network	109
6.	Gain/Frequency Characteristics of RC-Active Network	110

PAGE

APPENDIX II	SYNTHESIS OF THE LOW-PASS NETWORK	111
APPENDIX III	COMPUTER PROGRAMS	116
APPENDIX IV	LIST OF TEST EQUIPMENT	118
REFERENCES		120

TABLE OF ILLUSTRATIONS

FIGURE		PAGE
2. 1	Basic Multiplier	4
2. 2	Translation to Baseband	5
2. 3(a)	Spectrum of Baseband Signal	7
(b)	Double-Sideband Spectra	7
2. 4	General Carrier System	8
2. 5	Double-Polarity Amplitude Modulation	13
2. 6	N-Path Configuration	16
2. 7(a)	Symbolic Representation of F(k, s)	21
(b)	Equivalent Constant Parameter Network	21
3. 1	The 3-Channel Sampled Data Filter	24
2. 3(a)	The Complete Sampled Data Filter System	26
(b)	A Typical Printed Circuit Board	27
3. 3	The Sampled Data Filter Using the Technique of Quadrature Modulation	29
3. 4(a)	Control Circuits for the 3-Channel System	30
(b)	Control Waveforms for the 3-Channel System	32
3. 5(a)	Control Circuits for Quadrature Modulation System	33
(b)	Control Waveforms for Quadrature Modulation System	34

FIGURE		PAGE
3.6	The Sampling Circuit	36
3.7	Equalization of Source Potentials	39
3.8	Amplitude-Frequency Response of Low-Pass RC Networks	41
3.9	RC Low-Pass Filter	43
3.10	Single-Feedback RC-Active Filter	45
3.11	Basic 3-Channel System	46
3.12	Low-Pass Filter Output	49
3.13(a)	Sampled Data Filter Waveforms (3-Channel System)	51
(b)	Combined Output of Sampled Data Filter	52
3.14	Sampled Data Filter Waveforms (Quadrature Modulation System)	54
3.15	Combined Output of Quadrature Modulation System	55
(a)	With Offset Voltage V_{OS}	
(b)	Offset Voltage Nulled	
4.1	Experimental Test Facility	58
4.2	Effect of Channel Mismatch Due to Variation in Gate-Drive Current on Zero Signal Noise Component	60
4.3	Effect of Channel Mismatch Due to Variation in Gate-Drive Signal of Output Sampling Switches on Harmonic Distortion	61

FIGURE		PAGE

4.4	Effect of Gate Drive Variation of Input and Output Sampling Switches on Selectivity	63
4.5	Effect of Channel Mismatch Due to Variation in Rise & Fall Time of Gate Drive Signal on Zero Signal Noise Component	64
4.6	Effect of Channel Mismatch Due to Variation in Rise & Fall Time of Gate Drive Signal on Harmonic Distortion - Gate Drive = 5 mA	65
4.7	Effect of Channel Mismatch Due to Variation in Rise & Fall Time of Gate Drive Signal on Harmonic Distortion - Gate Drive = 3.18 mA	66
4.8	Variation in Rise & Fall Time of Sampled Signal	68
4.9	Effect of Rise & Fall Time of Input Sampling Switches on Selectivity	69
4.10	Effect of Rise & Fall Time of Output Sampling Switches on Selectivity	71
4.11	Effect of Input Switch Resistance on Selectivity	72
4.12	Effect of Output Switch Resistance on Zero Signal Noise Component	74
4.13	Effect of Output Switch Resistance on Harmonic Distortion	75

FIGURE		PAGE
4.14	Effect of Zero Signal Noise Component on Selectivity	76
4.15	Effect of Zero Signal Noise Component on Selectivity	77
4.16	Location of Image Component	79
4.17)		80
4.18)	Modulation Effects	81
4.19)		82
4.20	Effect of Sampling Frequency on Zero Signal Component	84
4.21	Variation in Rise & Fall Time of Sampled Signal	86
4.22	Effect of Rise & Fall Time of Sampling Switches on Selectivity	87
4.23	Realization of Narrow Band-Pass Characteristic Using Quadrature Modulation Technique	89
4.24	Realization of Narrow Band-Pass Characteristic Using Quadrature Modulation Technique	90
4.25	Selectivity Characteristic Using the 3-Channel System	91
4.26	Selectivity Characteristics Using the Technique of Quadrature Modulation	94
4.27	Bandwidth Variations	97

CHAPTER I

INTRODUCTION

1.1 Historical Background

The technique of narrow band-pass filtering using quadrature modulation was first discussed by Barber [1] as a means of overcoming the problems associated with the design of narrow band-pass filters at low frequencies. In a following article by Madella [2], it was proposed that the system described by Barber could be regarded, as a whole, as a set of polyphase modulating and filtering devices with the quadrature modulation system corresponding to the single-phase arrangement. It was not until 1950 that a comprehensive treatment of polyphase modulation applied to filtering problems was carried out by Macdiarmid and Tucker [3].

The study of quadrature modulation as a means of single sideband generation and reception was discussed by Weaver [4] in 1956 and practically applied for the design of electronic filters by Paris [5].

With the advent of high speed semiconductor devices, a detailed theoretical investigation was carried out by Franks and Sandberg [6], of an alternative method of realizing filtering characteristics with the modulators replaced by series sampling switches. This time-varying network consisted of N identical linear time-invariant networks connected in parallel, each operating between input and output modulators.

1.2 Objectives

This thesis presents the results of an investigation of the realization of narrow band-pass characteristics using RC time-varying networks, commonly referred to as the Sampled Data Filter. The performance of the filter due to network and system parameter variations is considered in detail and the recommendations for the design of such systems are established.

Based on the theoretical analysis of the ideal N-path Sampled Data Filter presented by Franks and Sandberg [6], a three channel Sampled Data Filter was constructed, using junction Field Effect Transistors as modulators, and its performance compared with that using the technique of quadrature modulation.

CHAPTER II

THEORETICAL CONSIDERATIONS

2.1 Introduction

In this chapter, a theoretical analysis of the sampled data filter is presented. The operation of this sampled data system relies on one fundamental theorem as applied to Time-Division-Multiplexed systems, namely, Nyquist's sampling theorem, which requires each channel to be sampled at a rate equal to at least twice the bandwidth of its input signal.

The frequency translation processes that occur within the sampled data filter are briefly discussed, followed by the derivation of the overall system transfer function using Fourier transform techniques.

2.2 The Frequency Translation Process

2.2.1 Linear modulation is essentially a multiplicative process, where the time functions that describe the modulating signal and carrier are multiplied together. This operation of multiplication is equivalent to a symmetrical translation of the baseband spectrum through a distance, ω_c, the carrier frequency, about the frequency axis. This is shown in general form below (Figure 2. 1), and is referred to as a double sideband transmission system.

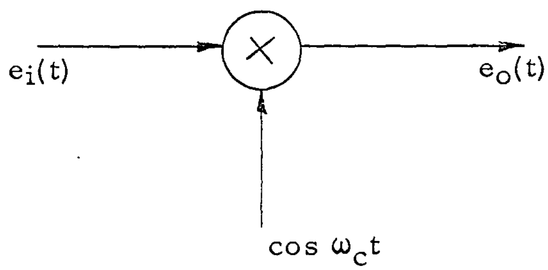

Figure 2. 1 - Basic Multiplier

The output $e_o(t) = e_i(t) \cdot \cos\omega_c t$.

The spectrum of $e_o(t)$ is its Fourier Transform, thus

$$E_o(j\omega) = \int_{-\infty}^{\infty} e_o(t) \exp(-j\omega t)\, dt$$

$$= \int_{-\infty}^{\infty} e_i(t) \cos\omega_c t \exp(-j\omega t)\, dt$$

In the sampled data filter, two translation processes are involved, namely

(i) from the carrier frequency ω_c to baseband and

(ii) from baseband to the filter centre frequency (carrier) ω_c.

2.2.2 The translation to baseband may be considered with reference to Figure 2.2.

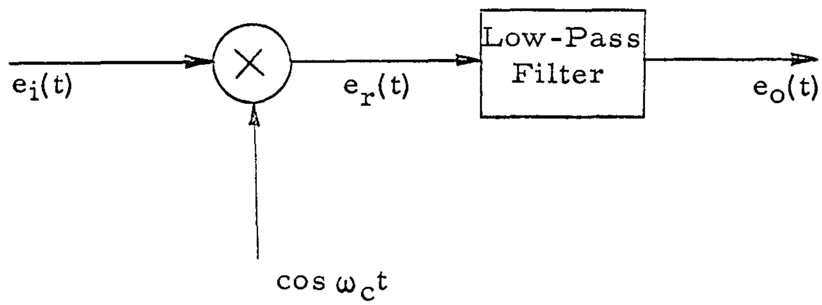

Figure 2.2 - Translation to Baseband

The cut-off frequency of the low-pass filter is $\omega_o << \omega_c$, the carrier frequency. The output from the multiplier is

$$e_r(t) = e_i(t) \cos\omega_c t$$

if $$e_i(t) = \cos\omega t, \text{ then}$$

$$e_r(t) = \cos\omega t \cdot \cos\omega_c t$$
$$= 1/2 \left[\cos(\omega + \omega_c)t + \cos(\omega - \omega_c)t\right]$$

The output from the low-pass filter is the convolution of the impulse response of the low-pass filter and the input signal, i.e.

$$e_o(t) = \int_{-\infty}^{\infty} e_r(\tau)\, h\,(t - \tau)\, d\tau$$

The spectrum of a convolution of two time functions equals the product of the spectra. Let the Fourier Transform of $e_r(t)$ be $E_r(j\omega)$ and that of $e_o(t)$ be $E_o(j\omega)$, then the output spectrum will be,

$$E_o(j\omega) = H(j\omega) \cdot E_r(j\omega)$$

Now $\quad e_r(t) = e_i(t) \cos \omega_c t$

The Fourier Transform

$$E_r(j\omega) = \int_{-\infty}^{\infty} e_i(t) \cos \omega_c t \exp(-j\omega t)\, dt$$

$$= \frac{E_i\left\{j(\omega - \omega_c)\right\} + E_i\left\{j(\omega + \omega_c)\right\}}{2}$$

Therefore

$$E_o(j\omega) = \frac{H(j\omega)}{2}\left[E_i\left\{j(\omega - \omega_c)\right\} + E_i\left\{j(\omega + \omega_c)\right\}\right]$$

The output from the low-pass filter $e_o(t)$ is confined to a region $|\omega| \leq \omega_o$. $e_o(t)$ is thus a baseband signal whose Fourier Transform $E_o(j\omega)$ is band-limited to $-\omega_o \leq \omega \leq \omega_o$, as shown in Figure 2. 3(a).

2. 2. 3 The translation from baseband to the centre frequency ω_c is carried out by multiplication of the baseband signal and the carrier signal, i. e.

$$g(t) = e_o(t) \cos \omega_c t$$

The product represents a modulated carrier, where the carrier frequency $\omega_c >> \omega_o$. The spectral components of the signal g(t) are given by its Fourier Transform.

$$G(j\omega) = \frac{1}{2}\left[E_o\left\{j(\omega - \omega_c)\right\} + E_o\left\{j(\omega + \omega_c)\right\}\right]$$

The Fourier spectrum of the modulating signal has been translated from symmetry about $\omega = 0$ to symmetry about $\pm\omega_c$. A pictorial representation of this translating process is illustrated in Figure 2. 3(a) and 2. 3(b).

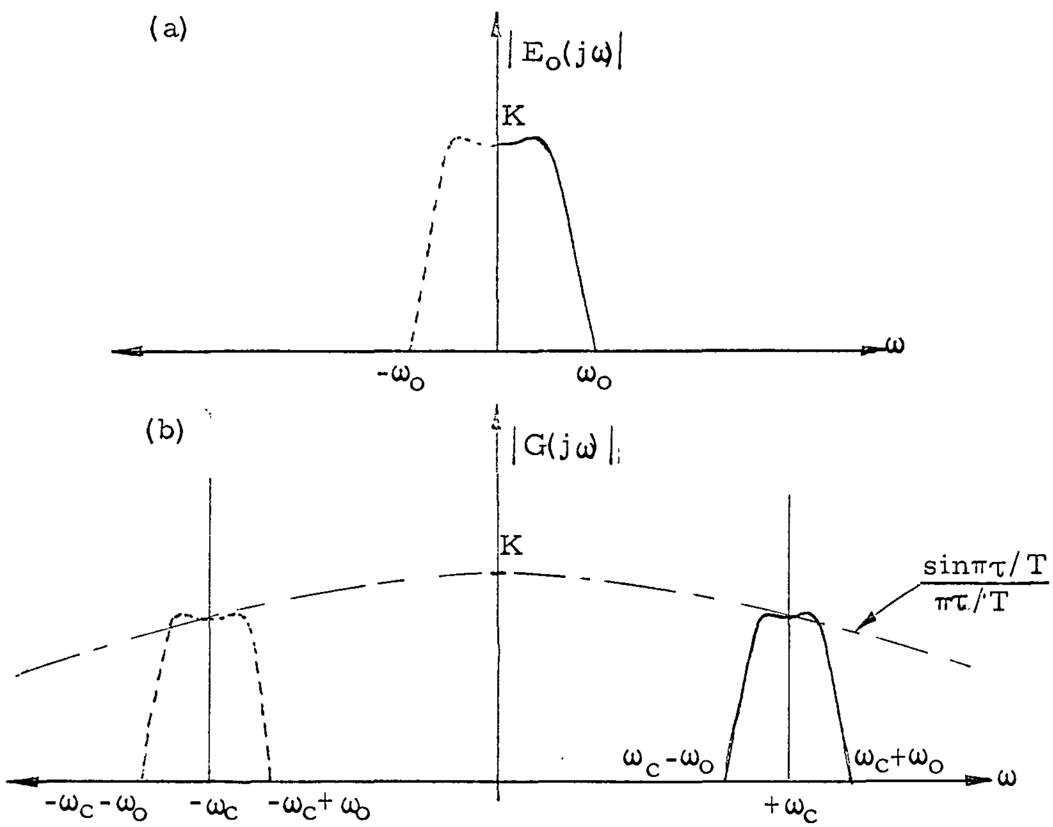

Figure 2. 3(a) - Spectrum of Baseband Signal

(b) - Double-Sideband Spectra

2.2.4 By virtue of this frequency translation process, it is possible to realize band-pass characteristics by utilizing two or more identical parallel paths containing a low-pass filter with input and output multipliers.

2.3 Derivation of the System Transfer Function

2.3.1 Analysis of the General Carrier Process

The following analysis follows closely that of Acampora [11]*. For the purpose of this analysis, a single channel of an N-path system is considered, as given in Figure 2.4 below.

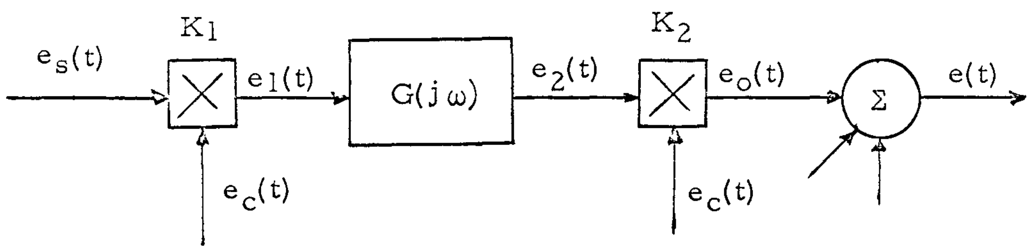

Figure 2.4 - General Carrier System

Let the input signal be $e_s(t) = \cos \omega_s(t)$, and let the nth path modulator be supplied with a 'carrier',

$$e_c(t) = \cos (\omega_c t - \frac{2\pi n}{N}).$$

Using the Fourier transform notation,

$$E_c(j\omega) = \int_{-\infty}^{\infty} e_c(t) \exp(-j\omega t)\, dt$$

* Appendix A of Acampora's article contains a number of mistakes which do not, however, seem to affect the final result.

and expressing $e_c(t)$ as

$$e_c(t) = \frac{1}{2} \left[\exp\left\{j(\omega_c t - \frac{2\pi n}{N})\right\} + \exp\left\{-j(\omega_c t - \frac{2\pi n}{N})\right\} \right]$$

we obtain,

$$E_c(j\omega) = \frac{1}{2}\int_{-\infty}^{\infty} \left[\exp\left\{-j\frac{2\pi n}{N}\right\} \exp\left\{-j(\omega-\omega_c)t\right\} + \exp\left\{j\frac{2\pi n}{N}\right\} \exp\left\{j(\omega+\omega_c)t\right\}\right] dt$$

$$= \pi \left[\delta(\omega - \omega_c) \exp\left\{-j\frac{2\pi n}{N}\right\} + \delta(\omega + \omega_c) \exp\left\{j\frac{2\pi n}{N}\right\} \right]$$

where $\delta(\omega - \omega_c)$ is a unit impulse function defined by

$$\delta(\omega - \omega_c) = \frac{1}{2\pi}\int_{-\infty}^{\infty} e^{-j(\omega - \omega_c)t}\, dt$$

The impulse function $\delta(\omega + \omega_c)$ is similarly defined.

The output from the first modulator is given by

$$e_1(t) = K_1 \cdot e_s(t) \cdot e_c(t)$$

where K_1 is the modulator gain constant. Since multiplication in the time domain corresponds to convolution in the s domain, use of the convolution integral is made to give [12]

$$E_1(j\omega) = \frac{1}{2\pi}\int_{\infty}^{\infty} K_1 E_s(j\omega_1) E_c(j\omega - j\omega_1)\, d\omega_1$$

Substituting for $E_c(j\omega)$ gives

$$E_1(j\omega) = \frac{K_1}{2}\left[\int_{\infty}^{\infty} E_s(j\omega_1)\left[\delta(j\omega - j\omega_c - j\omega_1)\right] \exp\left\{-j\frac{2\pi n}{N}\right\} d\omega_1 \right.$$

$$\left. + \int_{\infty}^{\infty} E_s(j\omega_1)\left[\delta(j\omega + j\omega_c - j\omega_1)\right] \exp\left\{j\frac{2\pi n}{N}\right\} d\omega_1 \right]$$

From which, through the use of the Sifting Integral*,

$$E_1(j\omega) = \frac{K_1}{2} \left[E_s(j\omega - j\omega_c) \exp\left\{-j\frac{2\pi n}{N}\right\} + E_s(j\omega + j\omega_c) \exp\left\{j\frac{2\pi n}{N}\right\} \right]$$

The output from the linear network $G(j\omega)$ is given by

$$E_2(j\omega) = E_1(j\omega) \cdot G(j\omega)$$

Substituting for $E_1(j\omega)$ gives

$$E_2(j\omega) = \frac{K_1}{2} \left[E_s(j\omega - j\omega_c) \exp\left\{-j\frac{2\pi n}{N}\right\} G(j\omega) + E_s(j\omega + j\omega_c) \exp\left\{j\frac{2\pi n}{N}\right\} G(j\omega) \right] \qquad 2.1$$

The output from the second modulator can be written as a convolution integral i.e.

$$E_o(j\omega) = \frac{1}{2\pi}\int_{-\infty}^{\infty} K_2 \, E_2(j\omega_1) \, E_c(j\omega - j\omega_1) \, d\omega_1$$

where K_2 is the modulator gain constant. Substituting for $E_2(j\omega)$ and $E_c(j\omega)$ into the above integral we obtain the Fourier transform of the output,

$$E_o(j\omega) = \frac{K_1 \cdot K_2}{4}\int_{-\infty}^{\infty} E_s(j\omega - j\omega_c) \, G(j\omega) \exp\left\{-j\frac{2\pi n}{N}\right\} + E_s(j\omega + j\omega_c) \, G(j\omega) \exp\left\{j\frac{2\pi n}{N}\right\}]$$

$$\times \left[\delta(\omega - \omega_c - \omega_1) \exp\left\{-j\frac{2\pi n}{N}\right\} + \delta(\omega + \omega_c - \omega_1) \exp\left\{j\frac{2\pi n}{N}\right\} \right] d\omega_1$$

$*\int_{-\infty}^{\infty} f(x)\,\delta(x - x_o)\, dx = f(x_o)$

$$E_o(j\omega) = \frac{K_1K_2}{4} \left[\left[E_s(j\omega)\ G(j\omega - j\omega_c) + E_s(j\omega)\ G(j\omega + j\omega_c)\right] \right.$$
$$+ \left[E_s(j\omega - 2j\omega_c)\ G(j\omega - j\omega_c)\ \exp\left\{-j\,\frac{4\pi n}{N}\right\} \right]$$
$$\left. + \left[E_s(j\omega + 2j\omega_c)\ G(j\omega + j\omega_c)\ \exp\left\{j\,\frac{4\pi n}{N}\right\} \right] \right]$$

where again use has been made of the Sifting integral.

The final output signal is the sum of N path outputs,

$$V(j\omega) = \sum_{n=1}^{N} E_o(j\omega)$$

Thus, for the case of a network with 3 channels, we have

$$V(j\omega) = \frac{K_1K_2}{4} \left[\left[E_s(j\omega)\ G(j\omega - j\omega_c) + E_s(j\omega)\ G(j\omega + j\omega_c) \right] \right.$$
$$+ \left[E_s(j\omega - 2j\omega_c)\ G(j\omega - j\omega_c) \sum_{n=1}^{N} \exp\left\{-j\,\frac{4\pi n}{N}\right\} \right]$$
$$\left. + \left[E_s(j\omega + 2j\omega_c)\ G(j\omega + j\omega_c) \sum_{n=1}^{N} \exp\left\{j\,\frac{4\pi n}{N}\right\} \right] \right] \quad 2.2$$

The last two terms in the above expression cancel vectorially, yielding a transfer function for the network as

$$T(j\omega) = \frac{V(j\omega)}{E_s(j\omega)} = \frac{K_1K_2}{4} \left[G(j\omega - j\omega_c) + G(j\omega + j\omega_c)\right] \quad 2.3$$

Where $G(j\omega)$ is a specific low-pass network with cut-off $\omega_o << \omega_c$, a symmetrical band-pass characteristic may be obtained. The modulator constants K_1 and K_2 are dependent upon the form of the multiplier i. e. linear or non-linear. These constants are now evaluated for the carrier system where the multipliers are of the switching type.

2.3.2 Evaluation of the Modulator Constants

The type of modulator used in the sampled data filter is that of a series sampling switch having finite sampling duration. The sampling function applied to the sampler, consists of a train of unmodulated periodic pulses of unit amplitude and mark to space ratio determined by the number of parallel identical channels used in the system. During the sampling interval the modulated pulses follow the sampled time function. This form of pulse-amplitude modulation is commonly referred to as Double-Polarity Amplitude Modulation or Exact scanning. This process is clarified in Figure 2.5.

Consider the unit sampling function of Figure 2.5 (b), where T is the period and τ the sample pulse width. This time function may be expressed in the exponential form of the Fourier series as

$$f(t) = \sum_{n=-\infty}^{\infty} C_n \exp(jn\omega_o t)$$

$$= C_o + 2 \sum_{n=1}^{\infty} |C_n| \cos(n\omega_o t - \theta_n)$$

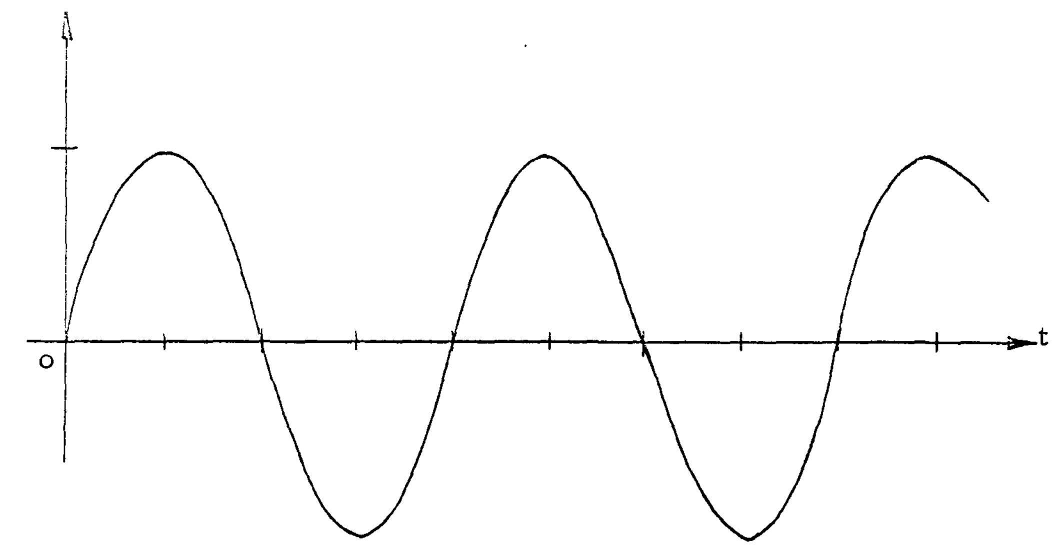

a) Input Time Function

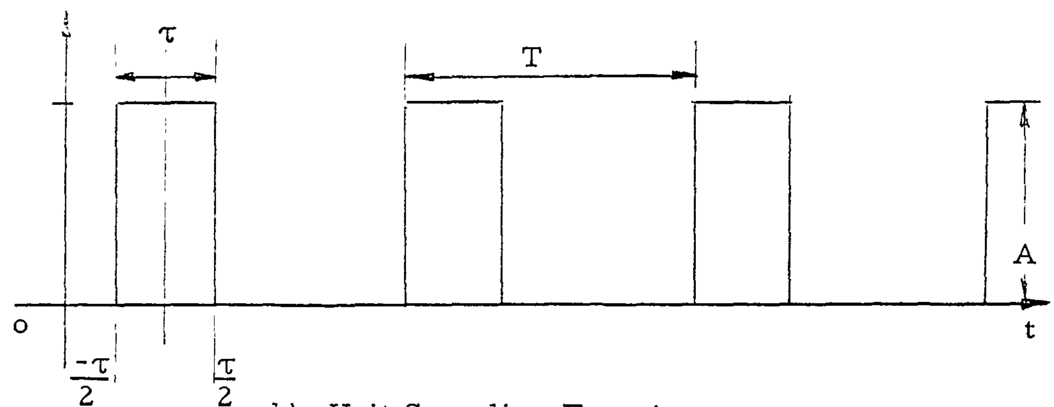

b) Unit Sampling Function

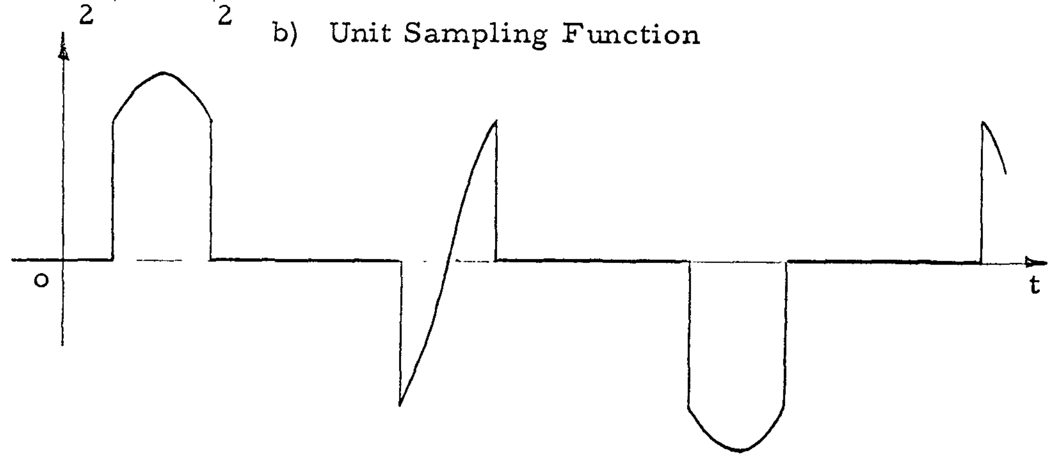

c) Double Polarity Pulses

Figure 2.5 - Double Polarity Amplitude Modulation

where $$C_n = \frac{1}{T} \int_{-T/2}^{T/2} f(t) \exp(-jn\omega_o t)\, dt, \quad n = 0, \pm 1, \pm 2 ----$$

This equation is a representation of the periodic function f(t) in the frequency domain. The function C_n is in general complex and is known as the Fourier transform of f(t). The Fourier transform of the unit sampling function considered is given by

$$C_n = F(j\omega) = \frac{1}{T} \int_{-\tau/2}^{\tau/2} A \exp(-jn\omega_o t)\, dt$$

$$= \frac{1}{T} \left[-\frac{A}{jn\omega_o} \exp(-jn\omega_o t) \right]_{-\tau/2}^{\tau/2}$$

$$= \frac{A}{T} \left[\frac{\exp(jn\omega_o\ \tau/2) - \exp(-jn\omega_o\ \tau/2)}{jn\omega_o} \right]$$

$$= \frac{2A}{n\omega_o T} \sin n\omega_o \frac{\tau}{2}$$

$$= A \frac{\tau}{T} \frac{\sin(n\omega_o\ \tau/2)}{n\omega_o\ \tau/2}$$

The exponential form of the Fourier series for the unit sampling function is now given by

$$f(t) = A\frac{\tau}{T} \sum_{n=-\infty}^{\infty} \frac{\sin n\omega_o \tau/2}{n\omega_o \tau/2} \exp(jn\omega_o t)$$

$$= A\frac{\tau}{T}\left[1 + 2\sum_{n=1}^{\infty} \frac{\sin n\omega_o \tau/2}{n\omega_o \tau/2} \cos n\omega_o t\right]$$

$$= A\frac{\tau}{T}\left[1 + 2\sum_{n=1}^{\infty} \frac{\sin n\pi \tau/T}{n\pi \tau/T} \cos n\omega_o t\right]$$

where T is the period, τ the sample pulse width and ω_o the fundamental angular frequency.

The modulator gain constants K_1 and K_2 may therefore be expressed, for the case with $n = \pm 1$, as

$$K_1 = K_2 = A\frac{\tau}{T}\left[\frac{\sin \frac{\pi\tau}{T}}{\pi\tau/T} - \frac{\sin(-\pi\tau/T)}{\pi\tau/T}\right] = \frac{A\tau}{T}\,[2a]$$

where $a = \dfrac{\sin \pi \tau/T}{\pi \tau/T}$

2.3.3 The Sampled Data System Transfer Function

The overall transfer function of the carrier system given in Figure 2.4 with $N \geq 3$ and with switching type modulators is thus given by

$$G_c(s) = \left\{\frac{A\tau}{T}\right\}^2 [a_1 \cdot G(s - j\omega_c) + a_1 \cdot G(s + j\omega_c)] \qquad 2.4$$

where $a_1 = \left[\dfrac{\sin \pi \tau/T}{\pi \tau/T}\right]^2$ and $s = j\omega$.

For N = 2, the phase relationship between the carrier frequencies of each channel is 90° resulting in the Quadrature modulation system. In this case, the last two terms of equation 2. 2 do not cancel. These unwanted components, however, may be removed by a final analog filter.

2. 4 Approach Due to Franks and Sandberg [6]

The following section presents the method, adopted by Franks and Sandberg, of the derivation of the transfer function of the sampled data network.

2. 4. 1 General Input-Output Relationship

The network considered by Franks and Sandberg is shown in block diagram form in Figure 2. 6 below.

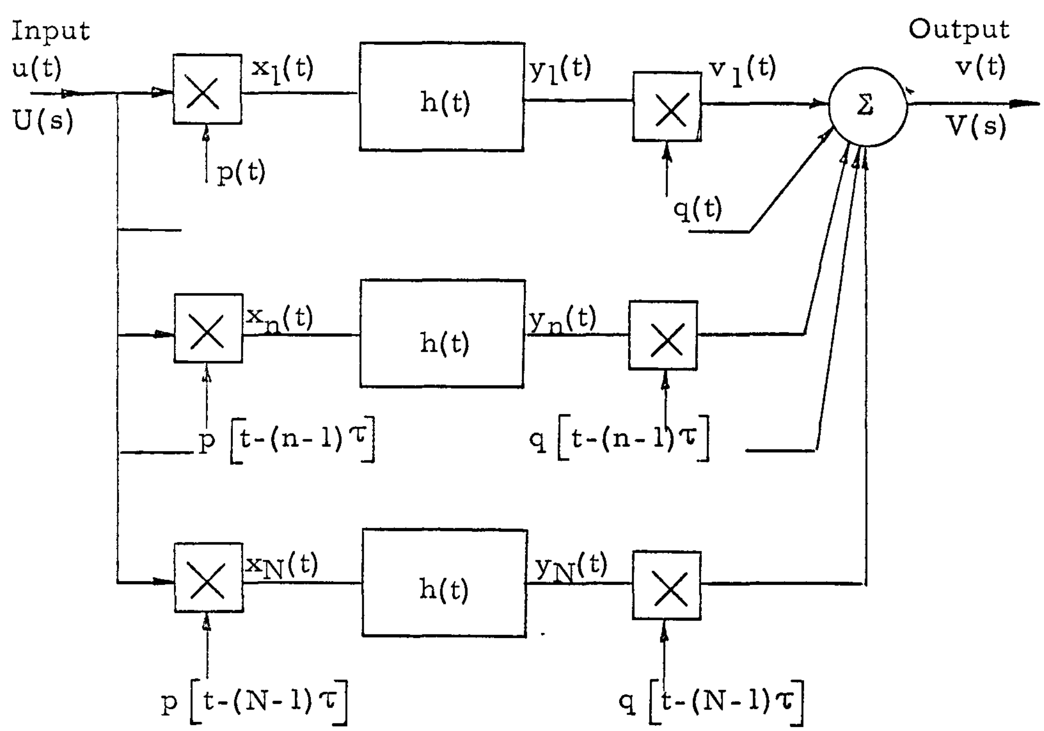

Figure 2. 6 - N-Path Configuration

The time functions $u(t)$, $v(t)$, $x_n(t)$ and $y_n(t)$ are considered to be either voltages or currents. The input modulators (multipliers) operate on the input $u(t)$ to produce the inputs

$$x_n(t) = u(t)\, p\left[t - (n - 1)\tau\right]$$

to the N identical linear time-invariant networks with impulse response $h(t)$. The outputs $y_n(t)$ are passed through output modulators, the outputs from which are then summed to produce the final output $v(t)$. The time functions $p\left[t - (n - 1)\tau\right]$ and $q\left[t - (n - 1)\tau\right]$ are periodic with period T, where $T = N\tau$ for $N \geq 3$

and $T = 2N\tau$ for $N = 2$

i. e. for the quadrature modulation system.

The periodic functions $p(t)$ and $q(t)$ can be expressed by their complex Fourier series as

$$\left.\begin{aligned} p(t) &= \sum_{m=-\infty}^{\infty} P_m \exp(j\omega_o m t) \\ \text{and} \quad q(t) &= \sum_{l=-\infty}^{\infty} Q_l \exp(j\omega_o l t) \end{aligned}\right\} \qquad (2.5)$$

where $\omega_o = \dfrac{2\pi}{T}$

$= \dfrac{2\pi}{N\tau}$ for $N \geq 3$

and $= \dfrac{\pi}{N\tau}$ for $N = 2$, the quadrature modulation system.

Define $$\left.\begin{aligned} p_n(t) &= p[t - (n-1)\tau] \\ q_n(t) &= q[t - (n-1)\tau] \end{aligned}\right\} \tag{2.6}$$

Since multiplication in the time domain corresponds to convolution in the frequency domain, it follows that the Laplace transform of the summed output

$$V(s) = \sum_{n=1}^{N} V_n(s) = \sum_{n=1}^{N} Y_n(s) * Q_n(s) \tag{2.7}$$

Using the relation

$$J(s) * \frac{1}{s-\alpha} = J(s-\alpha)$$

and equations (2.5), (2.6) and (2.7) we obtain

$$V(s) = \sum_{n=1}^{N} \sum_{l=-\infty}^{\infty} Q_l \exp[-j\omega_o(n-1)l\tau] \cdot X_n(s-jl\omega_o) \; H(s-jl\omega_o) \tag{2.8}$$

where $X_n(s)\, H(s) = Y_n(s)$

Similarly

$$X_n(s) = U(s) * P_n(s)$$

and $$X_n(s-jl\omega_o) = \sum_{m=-\infty}^{\infty} P_m \exp[-j\omega_o(n-1)m\tau] \; U[s-j(m+l)\omega_o] \tag{2.9}$$

Substituting (2.9) into (2.8) gives

$$V(s) = \sum_{n,l,m} Q_l P_m \exp[-j\omega_o(n-1)(l+m)\tau] \; H(s-jl\omega_o) \; U[s-j(m+l)\omega_o] \tag{2.10}$$

The summation over n is the following geometric series:

$$\sum_{n=1}^{N} \exp\left[-j\omega_o(n-1)(l+m)\tau\right] = N, \quad l+m = kN \qquad (2.11)$$

$$= 0, \quad \text{otherwise}$$

where k is an integer. Using (2.11) we obtain the Laplace transform of the summed output,

$$V(s) = N \sum_{k,l} Q_l P_{kN-l} H(s-jl\omega_o)\, U(s-jkN\omega_o) \qquad (2.12)$$

$$= \sum_{k=-\infty}^{\infty} F(k,s)\, U(s-jkN\omega_o) \qquad (2.13)$$

where $$F(k,s) = N \sum_{l=-\infty}^{\infty} Q_l P_{kN-l} H(s-jl\omega_o) \qquad (2.14)$$

Expressions (2.13) and (2.14) constitute the general input-output relationship for the N-path structure.

2.4.2 Transfer Function for N-Path Configuration

The quantity F(k, s) in expressions (2.13) and (2.14) completely characterizes the time-varying network of Figure 2.6. It describes operationally the relation between the input signal and output signal as is shown symbolically in Figure 2.7(a). With certain band-limiting restrictions on the input and output signals, a transfer function relation between input and output may be derived.

If the input function U(s) evaluated on the $j\omega$-axis essentially vanishes outside the interval $|\omega| < N\omega_o/2$, it follows that

$$V(j\omega) = F(0, j\omega) \cdot U(j\omega) \text{ in } |\omega| < N\omega_o/2$$

Also if $V(j\omega)$ vanishes outside the interval $|\omega| < N\omega_o/2$, then V(s) and U(s) can be related by a transfer function T(s), given by $T_{(s)} = \frac{V(s)}{U(s)}$

where $T(j\omega) = F(0, j\omega)$ in $|\omega| < N\omega_o/2$

$$= 0 \qquad \text{in } |\omega| > N\omega_o/2$$

These band limiting constraints can be accomplished by preceding and following the time-varying network with ideal low-pass filters having cut off points located at $\omega_c = N\omega_{o/2}$. With the addition of these low-pass filters, the time-varying network is equivalent to a constant parameter network having a transfer function, F(0, s), preceded and followed by ideal low-pass filters as shown in Figure 2.7(b). From equation (2.14), therefore,

$$F(0, s) = N \sum_{l=-\infty}^{\infty} P_{-l} Q_l H(s - jl\omega_o) \qquad (2.15)$$

(a)

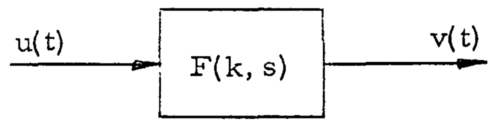

$$V(s) = \sum_{k=-\infty}^{\infty} F(k, s)\; U(s - jkN\omega_o)$$

(b)

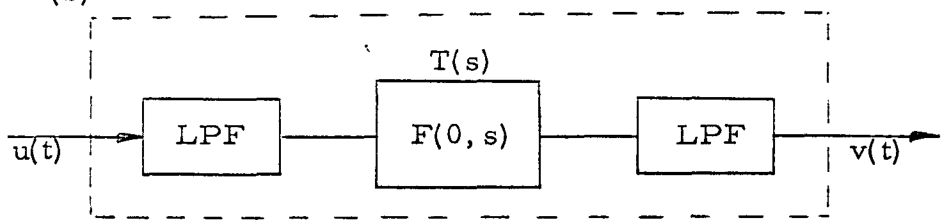

$$V(s) = U(s) \cdot T(s)$$

Figure 2.7(a) - Symbolic Representation of F(k, s)

(b) - Equivalent Constant Parameter Network

If the modulating functions are identical, i.e.

$$p(t) = q(t) = s(t)$$

then (2.15) may be rewritten as

$$F(0, s) = N \sum_{m=-\infty}^{\infty} S_m \cdot S_m^* \cdot H(s - jm\omega_o) \qquad (2.16)$$

where S_m^* is the conjugate of S_m.

Specific types of modulating functions have been considered by Franks and Sandberg, namely

a) Sinusoidal modulation

b) Jump modulation

c) Pulse modulation, which is a special case of jump modulation

The implementation of the transfer function given by equation (2.16) can be accomplished by switching function modulators i.e.

$$S(t) = \sum_{m=-\infty}^{\infty} S_m \exp(j\omega_o mt) \tag{2.17}$$

Since the transfer function relation given in equation (2.16) is valid for $|\omega| \leq N\omega_o/2$ and assuming the band-limiting filter required at the output can also provide a low-frequency cutoff (a band-pass filter); the resulting transfer function is given by, for m = ±1,

$$T(s) = N\frac{d}{T}\left[a_1 H(s-j\omega_o) + a_1^* H(s+j\omega_o)\right] \tag{2.18}$$

where $a_1 = \left[\dfrac{\sin\frac{\pi d}{T}}{\frac{\pi d}{T}}\right]^2$, a_1^* is the conjugate of a_1

d = sample pulse width

and T = the sampling period = $2\pi/\omega_o$.

The expression developed by Franks and Sandberg for the overall transfer function of the sampled data filter, given by equation (2.18) is identical to the one developed in Section 2.2 equation (2.4) in that both expressions show a low-pass to band-pass transformation of the low-pass network $G(j\omega)$.

CHAPTER III

THE DESIGN OF A SAMPLED DATA FILTER SYSTEM

3.1 Introduction

In the following chapter, the implementation of the sampled data filter analyzed in Chapter II is discussed with the modulators replaced by series sampling switches. The basic modulator is that of a switching type Field Effect Transistor with associated drive circuitry.

Both the 3-channel and quadrature modulation sampled data filters are presented, together with descriptions and characteristics of component parts and modes of operation.

3.2 Overall System Description

3.2.1 The 3-channel Sampled Data Filter

The block schematic of the 3-channel sampled data filter is given in Figure 3.1. In order to approach the theoretical model discussed previously in Chapter II, certain basic additions to the system, described by Franks and Sandberg [6], had to be made. Of these, the inclusion of a buffer stage between the input sampling switch and the

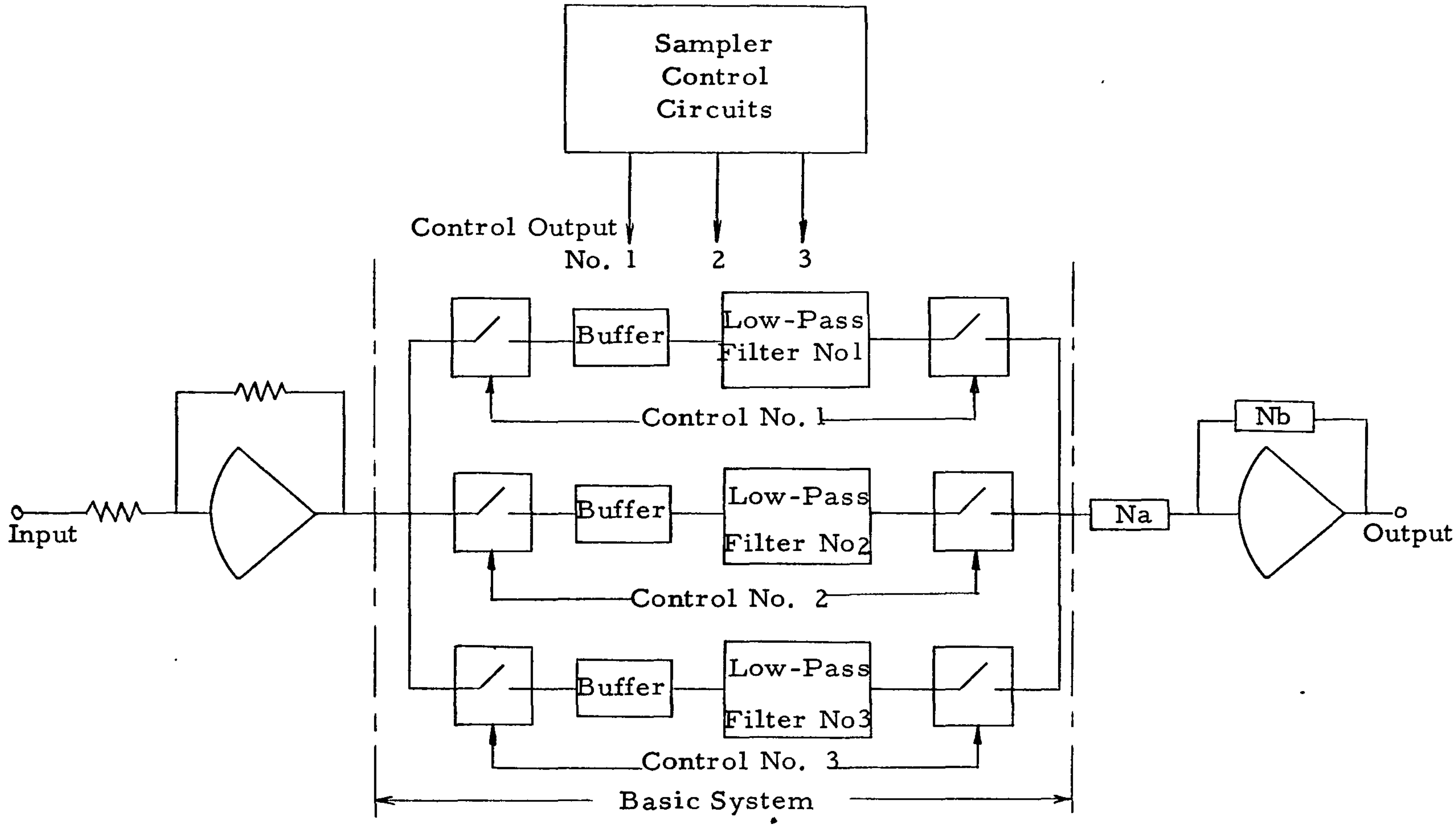

Figure 3.1 - The 3-Channel Sampled Data Filter

low-pass network is of paramount importance for the realization of the required or translated selectivity characteristics. Operational amplifiers were used at the input and output of the system to provide a low source impedance to the input sampling switches and a means of recovering the fundamental signal component with the use of a wideband RC-active filter respectively.

The complete system was constructed using both discrete and integrated circuit components on plug-in type printed circuit boards. This method of construction facilitated the modification of the 3-channel system to that using the technique of quadrature modulation, and permitted the variation of the sampler characteristics (i.e. switch resistance and switching times) with ease. The complete unit and a typical printed circuit card are shown in the photographs of Figure 3.2(a) and Figure 3.2(b).

3.2.2 The 2-channel or Quadrature Modulation Sampled Data Filter

The technique of quadrature modulation applied to sampled data filters requires a somewhat different approach to that applied to analog systems, i.e. quadrature modulation systems containing balanced ring-modulators as the multipliers.

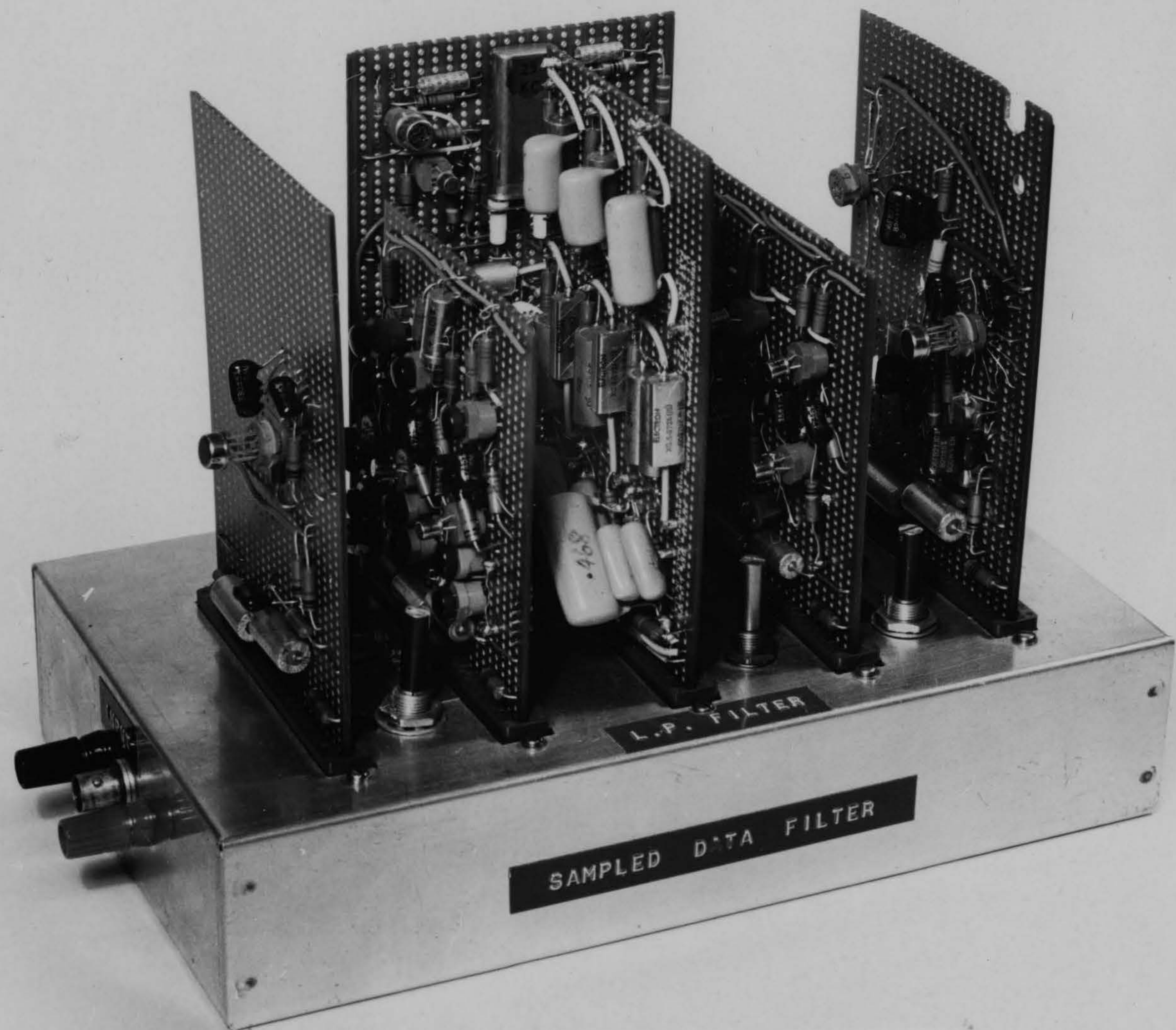

Figure 3. 2(a) - Sampled Data Filter System

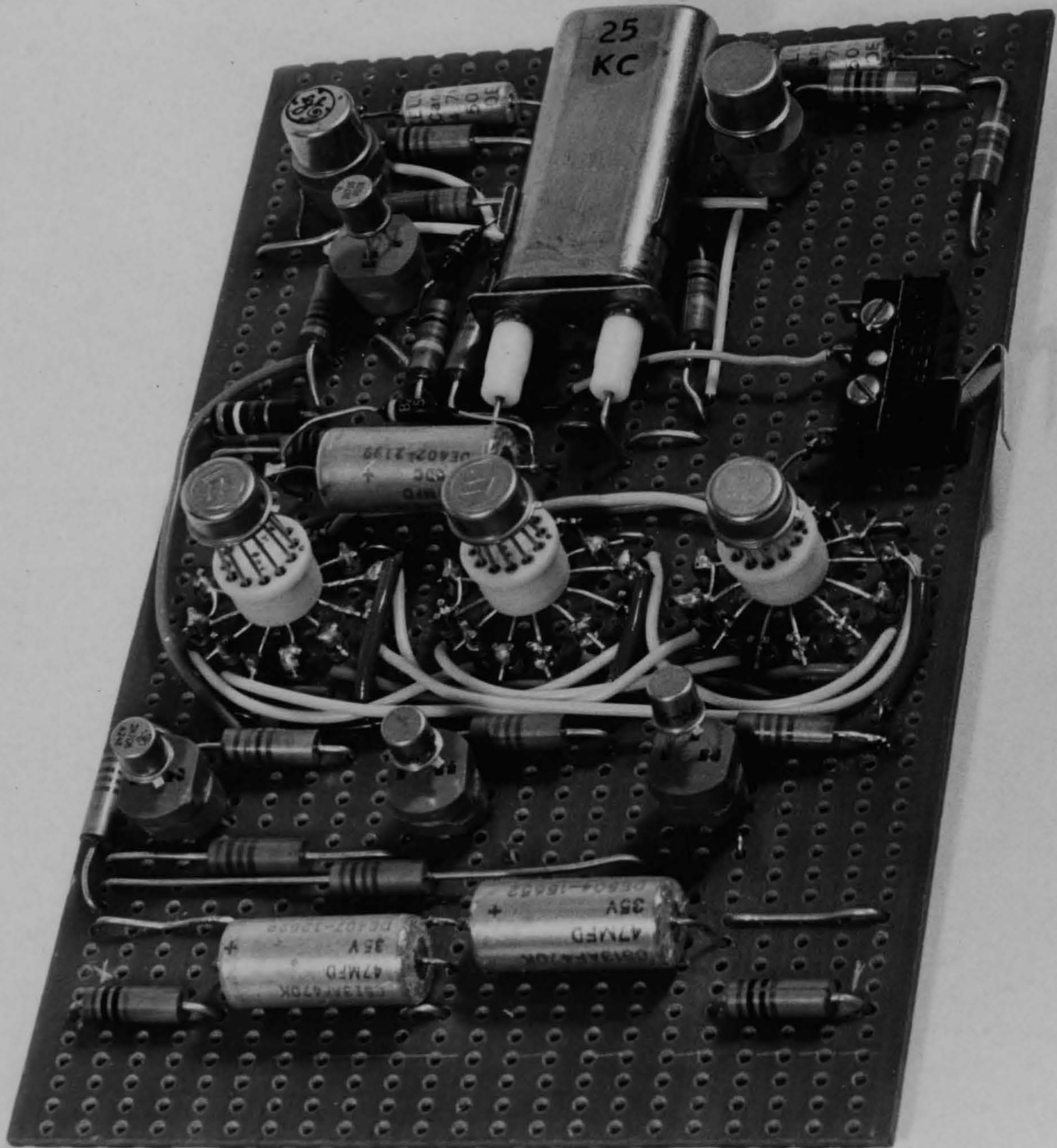

Figure 3. 2(b) - Typical Printed Circuit Card

Due to the fact that the sampling signals are 90° out of phase and that each sample width is equal to one-quarter of the period of a synchronous signal, there is a period of time equal to one-half this period during which the output sampling switches No. 1 and No. 2 are both open. This situation is highly undesirable as it results in a high output level, at the sampling or centre frequency for zero input. This is discussed in more detail in Section 3. 4.

To overcome this undesirable effect, a third output sampling switch is required, as shown in Figure 3. 3, so that for zero input to the sample data filter, the input to the broad-band filter is zero or of constant amplitude (d. c. wise) over all time.

3. 3 Control and Sampling Circuits

3. 3. 1 The 3-channel Sampled Data Filter

The block schematic of the control and sampling circuits for the 3-channel sampled data filter is given in Figure 3. 4(a). The main frequency source is that of a crystal controlled oscillator with the provision for adaptation to external frequency control. The output waveform, which is at three times the sampled data filter centre frequency, is used to drive a three stage shift-register. The outputs from this shift-register are fed to the input and output sampling circuits

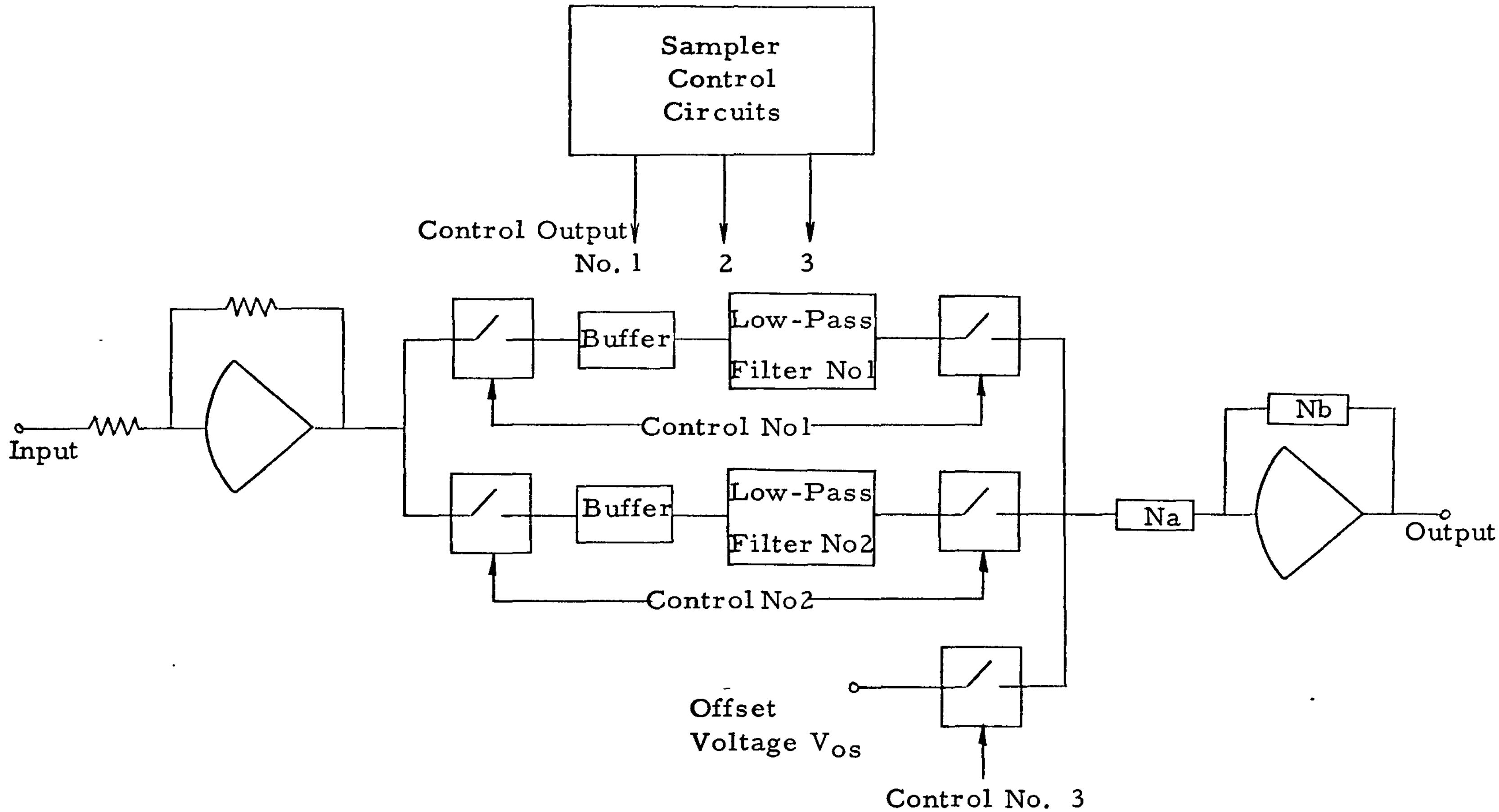

Figure 3. 3 - The Sampled Data Filter Using The Technique Of Quadrature Modulation

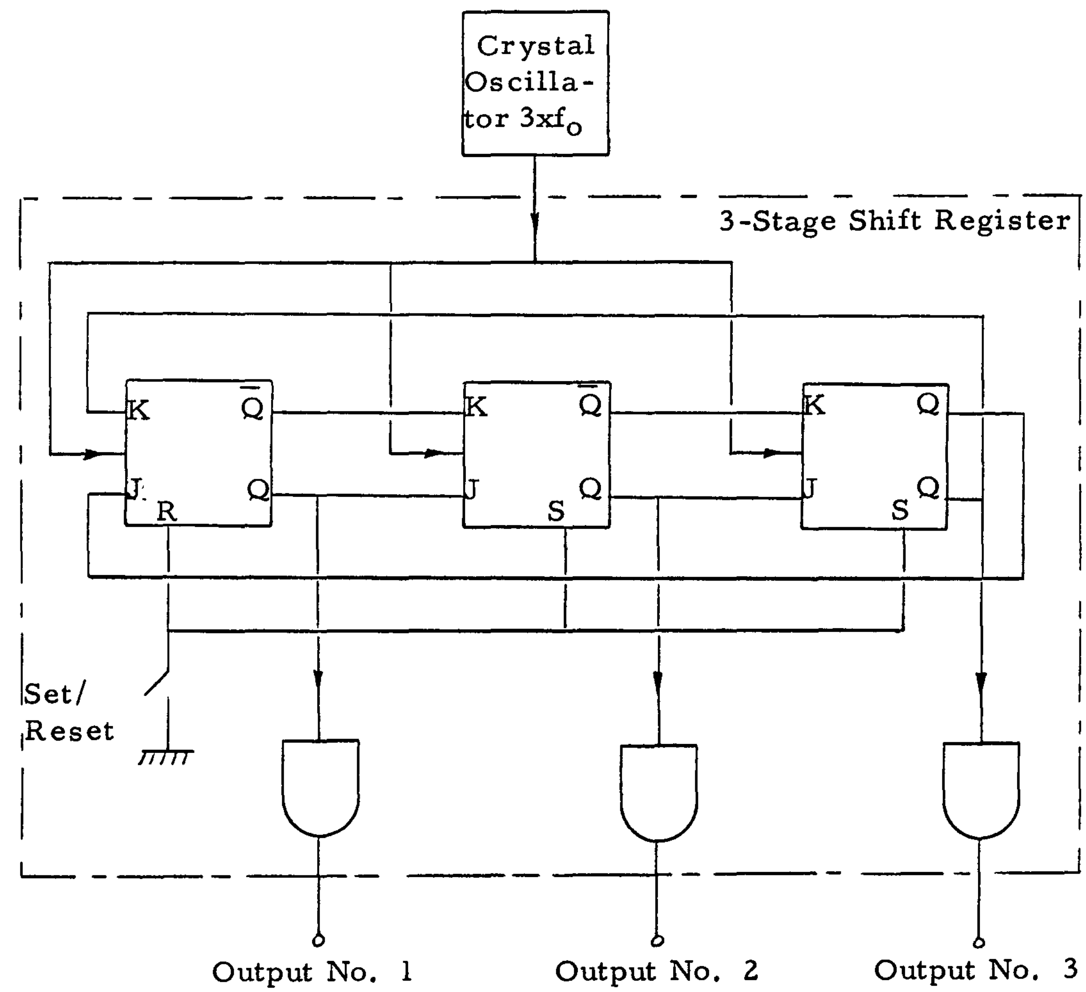

Figure 3. 4(a) - Control Circuits For 3-Channel System

of the sampled data filter. The circuit details of the crystal oscillator and the shift register are given in Appendix I for completeness. The numbers appearing at all input and output points refer to the pin-numbers appearing on the edge-connector used in conjunction with the printed circuit board. The control waveforms for the 3-channel system, showing their relative positions in time and relative amplitudes are given in Figure 3. 4(b).

3. 3. 2 The Quadrature Modulation Sampled Data Filter

The clock frequency for the quadrature modulation sampled data filter, is required to be four times the filter centre frequency. The necessary control waveforms were obtained by combining suitable bistable outputs as shown in the block schematic of Figure 3. 5(a). The circuits used for this control system are given in Appendix I and the control waveforms shown in Figure 3. 5(b).

3. 3. 3 The Sampling Circuit

The requirements for the ideal sampler or multiplier required for the sampled data filter are

(a) zero 'ON' resistance

(b) zero 'OFF' current or conductance

(c) zero switching times

(d) zero noise

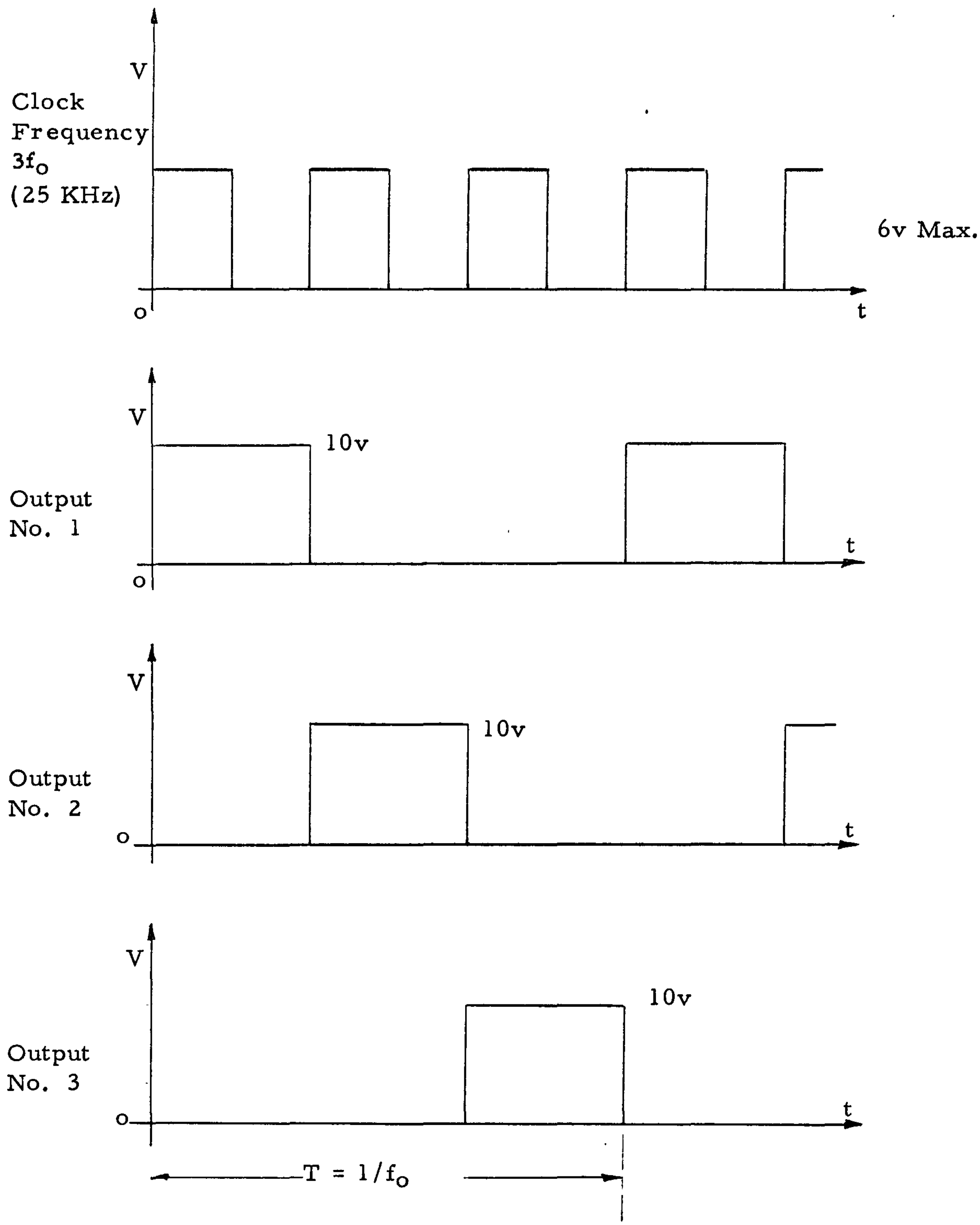

Figure 3. 4(b) - Control Waveforms For 3-Channel System

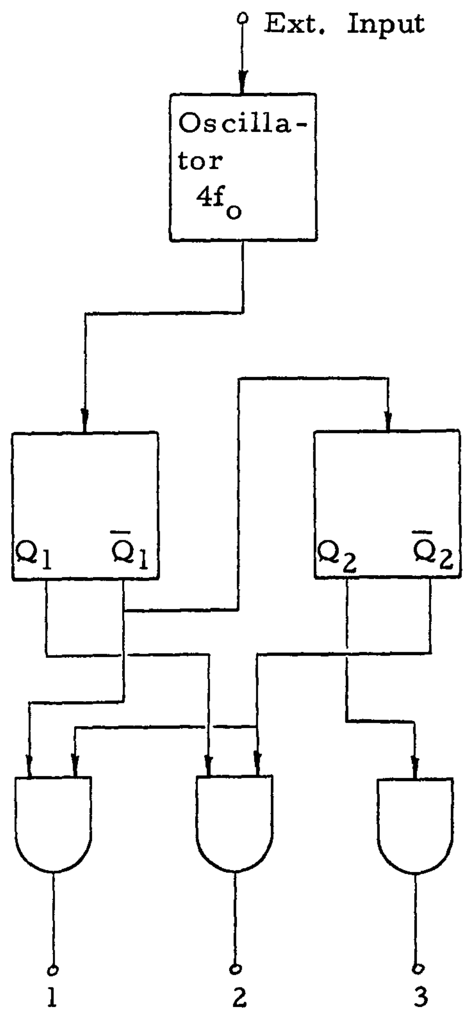

Figure 3. 5(a) - Control Circuits For Quadrature Modulation System

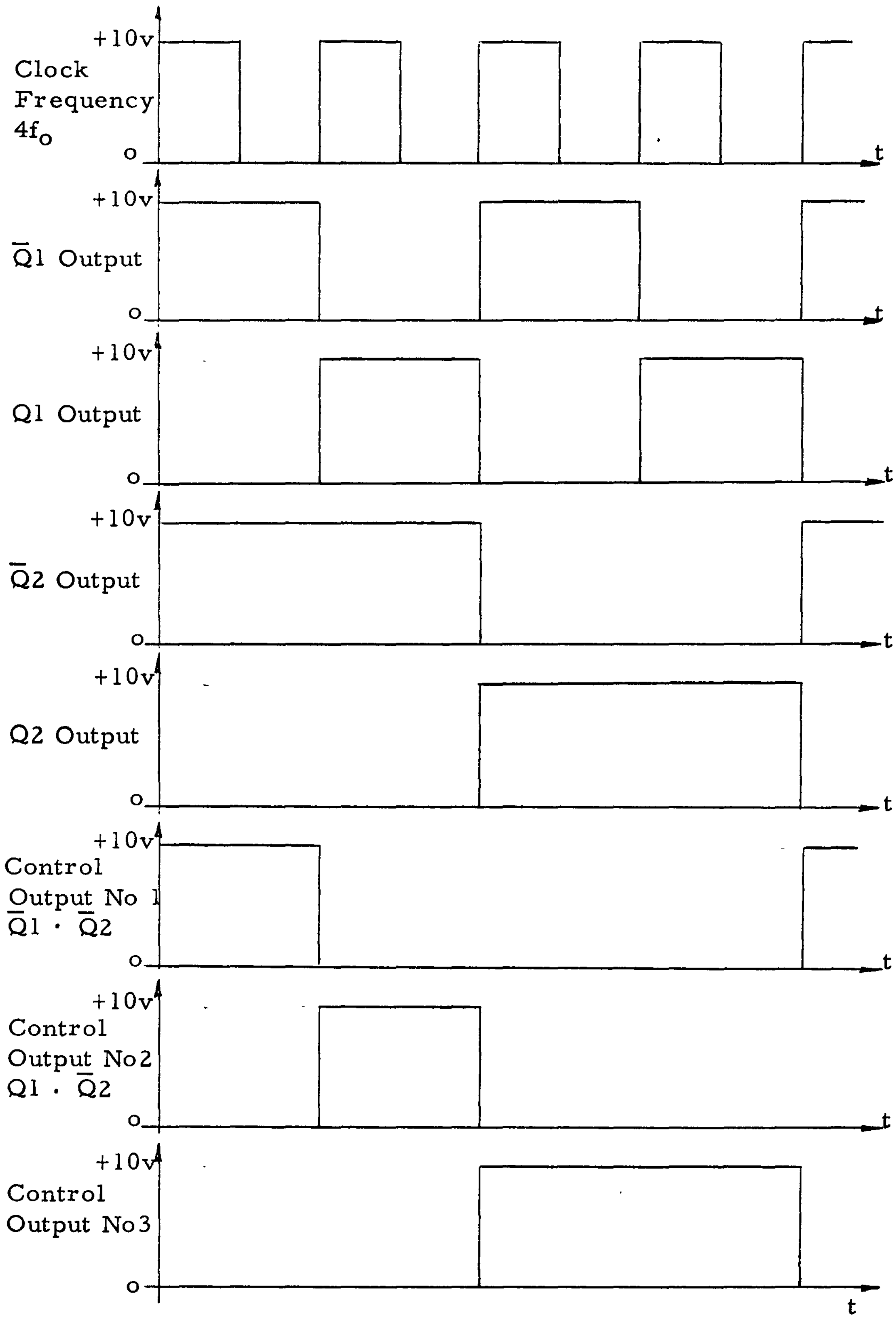

Figure 3. 5(b) - Control Waveforms For Quadrature Modulation System

The device which, perhaps, comes closest to achieving all four requirements is the Field Effect Transistor (F. E. T.) of the Metal Oxide (MOSFET) or Junction (JFET) type. The Field Effect Transistor has two characteristics which make it suitable for the operation as a sampler for the sampled data filter. The most important of these is that the FET does not have an inherent off-set voltage between the input and output terminals and secondly, since the input impedance is very high, the FET does not require a transformer type drive circuit. The sampler developed for the sampled data filter is given in Figure 3. 6. This sampler has been designed to operate over a signal frequency range from DC to 100 KHz and for signal levels up to ±4V.

The basic sampler is the P channel junction field effect transistor type 2N3376. This device has a maximum 'ON' resistance (R_{ds}) of 1. 5KΩ at 25°C. This value, although high compared to present day devices, is not detrimental to the operation or investigation of the sampled data filter. Devices having maximum 'ON' resistances of 5Ω are available, but usually some sacrifice has to be made to other device parameters, namely the pinch-off voltage (V_{po}) and the gate-drain capacitance (C_{gd}). A comparison of the pertinent FET parameters of present day devices, used for

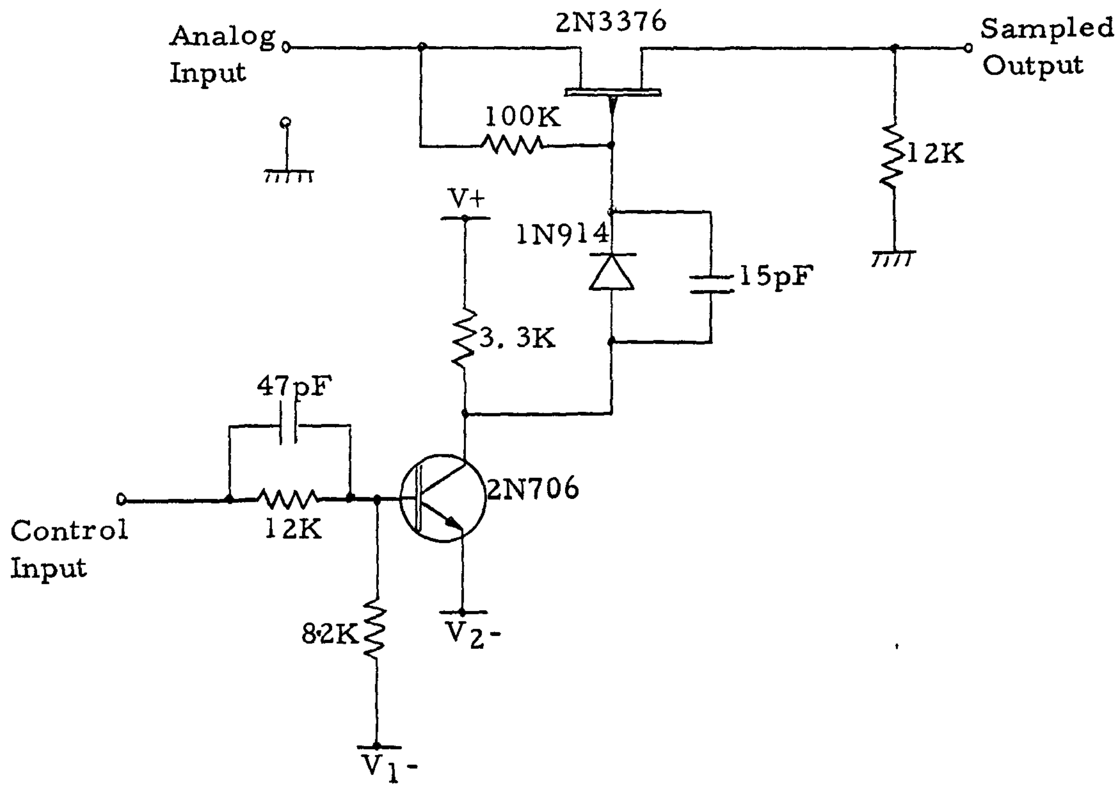

Figure 3. 6 - The Sampling Circuit

sampling applications with the 2N3376, is given in Table 3.1 below. It is seen that with the 2N3376, the requirements listed as (a), (b) and (c) for the ideal sampler are closely approached.

The sampler as given in Figure 3.6 suffers from one major disadvantage when sampling a low-level signal at high frequencies. The capacitance from gate to drain allows some of the gate drive signal to feed through to the output circuit, resulting in turn-on and turn-off transients appearing on the sampled waveform. The minimization of these transients for the output samplers in the sampled data filter, is of paramount importance since these transients result in a 'noise' component within the pass-band of the sampled data filter. The requirements for the input samplers however, need not be so severe as these are normally followed by very narrow bandwidth, low-pass sections having high rates of cut-off, thus the harmonics at multiples of the sampling frequency will be very heavily attenuated. Extensive experimentation was carried out in order to minimize these transients, so that the basic FET analog switch could be used for both the input and output samplers.

The results of the investigation showed that the harmonic components present at the output due to the switching

Type	'ON' Resistance R_{DS} (Max.)	Pinch-Off Voltage-V_{po} (Min.)	(Max.)	Gate-Drain Capacitance C_{DG}	Drain Cut-Off Current I_D Off at V_{ds}	'OFF' Resistance R_d (Min.) -Ohms	Ratio R_d/R_{ds}
2N4445	5Ω	2v	10v	25 pF	3nA at 5v	1.67×10^9	33.7×10^8
CM647	25Ω	5v	10v	5 pF	1nA at 15v	15×10^9	6×10^8
CM643	35Ω	2v	5v	5 pF	1nA at 15v	15×10^9	4.3×10^8
CM641	100Ω	1v	2.2v	5 pF	1nA at 15v	15×10^9	1.5×10^8
2N3376	1.5KΩ	1v	5v	3 pF	-0.4nA at -5v	12.5×10^9	8.3×10^6

Table 3.1 - Switching FET Characteristics at 25°C

transients, could be reduced considerably provided the signal source impedance is very low. An emitter follower was therefore introduced between the output from the low-pass filter and the output sampler. The disadvantage of including the emitter follower is the variation in the base-emitter voltage from one channel to another, which results in an excessive 'noise' component at the centre of the pass-band of the sampled data filter. An adjustment was therefore provided, to equalize the source potentials in each channel as indicated in Figure 3.7.

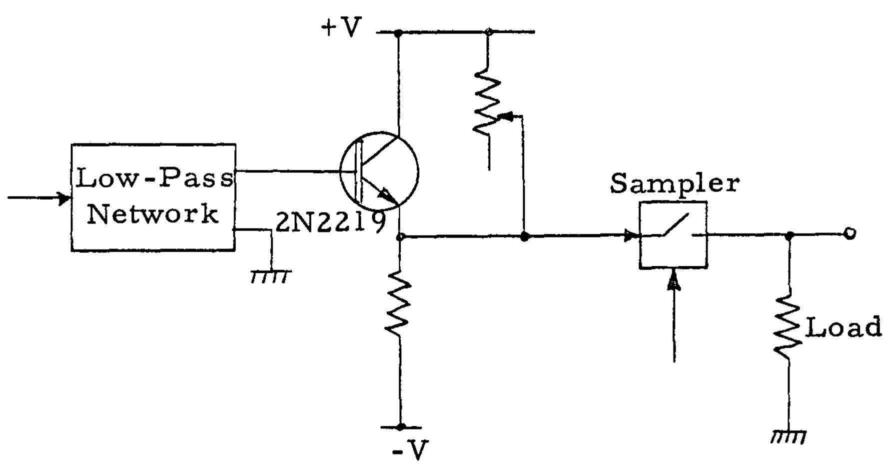

Figure 3.7 - Equalization of Source Potentials

The sampled data filter has an inherent method of reducing the harmonic components due to the switching transients, by virtue of the method employed in combining the various channel outputs. Since at any instant of time only one channel is connected to the output, the sampler outputs, when using FET's may be connected directly to a common load. This enables cancellation of the harmonic components to take place between the turn-on transient of one channel with the turn-off transient of the previous channel. Thus provided both the turn-on and turn-off transients are of equal amplitude and duration, the output will be free of any harmonic distortion due to switching transients.

3.4 The Low-Pass and Band-Pass Filter Network

3.4.1 The Synthesis of the Low-Pass RC Network

The synthesis of the low-pass RC network began with a priori knowledge of the pole-zero configuration. A third order network was chosen, since this was considered to be satisfactory for most practical applications. The method adopted for the synthesis procedure is due to E. S. Kuh [7] and is given in detail in Appendix II. This method relies on the fact that a certain ratio of load to source resistance is required and that the DC loss of the network is to be minimized. The voltage transfer function of the network was taken to be

$$G_{12}(s) = \frac{H}{(s + 1)(s + 1.5)(s + 2)}$$

The first break-point was taken to occur at 100 Hz, again for convenience, and both the theoretical and measured results compared with the straight line approximation as shown in Figure 3. 8.

Close agreement between the theoretical response and the actual network response is obtained. The maximum deviation in the characteristic of the three low-pass networks was 0. 5 dB. This deviation occurred above a frequency of 100 Hz indicating very good matching of the networks over the pass-band. The main parameters therefore, for the low-pass network are

(a) 3 dB bandwidth - 67. 5 Hz

(b) Asymptotic cut-off rate - 18 dB/octave

An alternative low-pass network having the same pole locations was designed to operate between identical source and load resistances as that given above, but with the first break-point occurring at a frequency of 10 Hz. The main parameters of this second network are therefore,

(a) 3 dB bandwidth - 7 Hz

(b) Asymptotic cut-off rate - 18 dB/octave

The element values for the low-pass network given below in Figure 3. 9 are listed in Table 3. 2.

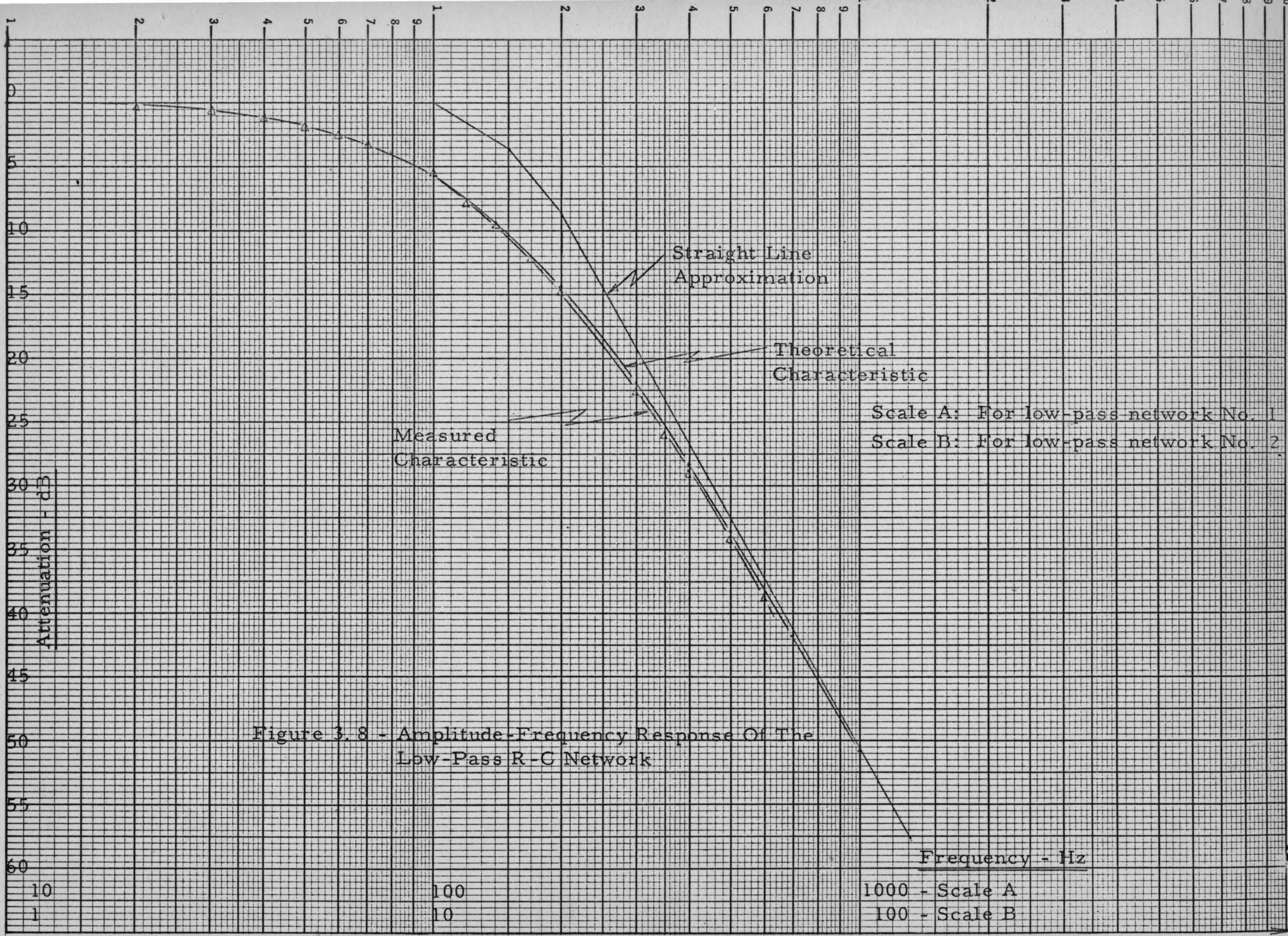

Figure 3.8 - Amplitude-Frequency Response Of The Low-Pass R-C Network

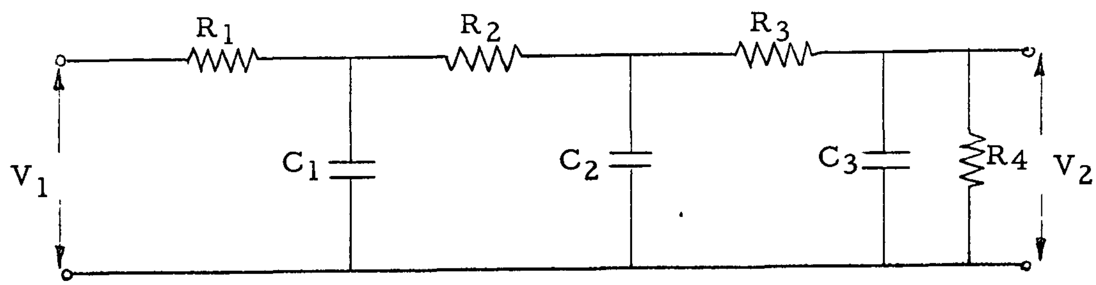

$$G_{12}(s) = \frac{V_2}{V_1} = \frac{H}{(s + 1)(s + 1.5)(s + 2)}$$

Figure 3. 9 - RC Low-Pass Filter

Element No.	Element Values (Nominal)	
	Network No. 1 Bandwidth - 67. 5 Hz	Network No. 2 Bandwidth - 7 Hz
R_1	2. 2KΩ	2. 2KΩ
R_2	24. 8KΩ	24. 8KΩ
R_3	53. 8KΩ	53. 8KΩ
R_4	12KΩ	12KΩ
C_1	0. 525 μF	5. 25 μF
C_2	0. 0624 μF	0. 624 μF
C_3	0. 1125 μF	1. 125 μF

Table 3. 2 - Element Values for RC Network

3.4.2 Synthesis of the Band-Pass Network

In order to recover the wanted signal, the combined output from the basic sampled data system is fed to a simple band-pass filter tuned to the centre frequency of the sampled data filter. To facilitate retuning of the band-pass filter to other sampling frequencies, it was decided to use an operational amplifier operating as a tuned amplifier. The 3 dB bandwidth of the tuned amplifier was designed to be approximately ten times the 3 dB bandwidth of the sampled data filter, in order that the effect of the broad band-pass filter may be ignored when measuring the selectivity characteristic of the sampled data filter. The circuit of the tuned amplifier is given in Appendix I together with the element values for centre frequencies of 8.333 KHz and 40 KHz.

For operation at one sampling frequency only, an alternative method for realizing the broad band-pass filter was carried out using RC-active network synthesis techniques. These techniques are well documented in a survey article by F. H. Blecher [8].

A new synthesis procedure of RC-active filters using unity gain current and voltage amplifiers to realize a pair of complex conjugate poles is demonstrated by S. S. Haykim [9]. However, for the proposed application, a synthesis procedure using an operational amplifier was adopted since this provided certain advantages i. e. low output impedance, high input impedance and overall gain greater than unity.

For both the tuned amplifier and RC-active network, sufficient mid-band gain was provided to compensate for the system loss due to the low-pass network, emitter followers, sampling switches and due to sampling.

The configuration of the RC-active band-pass filter* is shown in Figure 3. 10. This network is usually referred to as the 'Infinite-Gain Single-Feedback circuit', the open-circuit voltage transfer function being given by

$$\frac{E_2}{E_1} = \frac{-y_{12}a}{y_{12}b}$$

where $y_{12}a$ and $y_{12}b$ are the short circuit transfer admittances of networks Na and Nb respectively. The complete circuit of the RC-active filter together with the measured amplitude/frequency response is given in Appendix I .

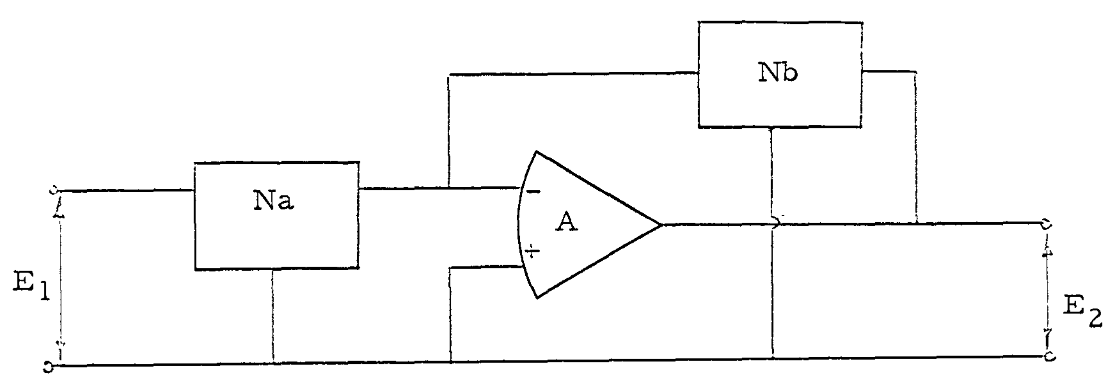

Figure 3. 10 - Single-Feedback RC-Active Filter

* From "Handbook of Operational Amplifier Active RC Networks", Burr-Brown Research Corporation, 1966.

3.5 Mode of Operation

3.5.1 The 3-channel System

For the purpose of the following discussion, a simplified version of the 3-channel system will be taken, i.e. one in which the carrier signal applied to the input and output multipliers (modulators) is of sinusoidal form instead of a switching function. This is valid since the sinusoid considered is the fundamental component of the switching function.

Consider the basic three channel system given in Figure 3.11 below:

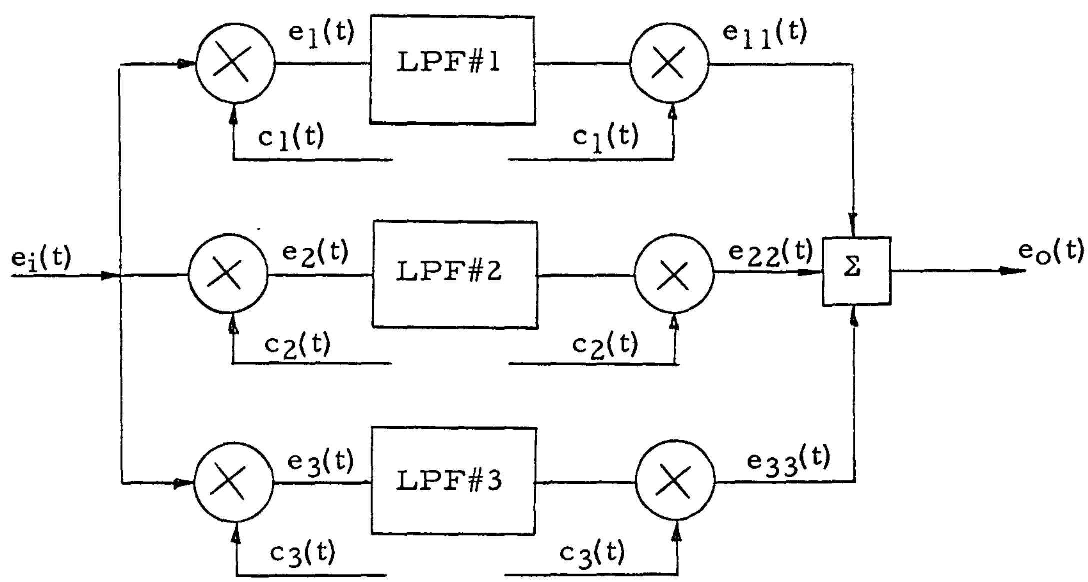

Figure 3.11 - Basic 3-channel System

Let the input to the system be represented by:

$$e_i(t) = E \cos(\omega t + \theta)$$

where ωt represents the frequency and θ the phase of the signal of amplitude E. Let the carrier frequencies for the input and output modulators be represented by $\cos \omega_c t$ for channel number 1, $\cos \omega_c t + \frac{2\pi}{3}$ for channel number 2, and $\cos \omega_c t + \frac{4\pi}{3}$ for channel number 3.

The output from the first modulator in channel number 1 is

$$e_1(t) = e_i(t) \cos \omega_c t$$

$$= E \cos (\omega t + \theta) \cos \omega_c t$$

$$= \frac{E}{2} \left\{ \cos(\omega_c t + \omega t + \theta) + \cos(\omega_c t - \omega t - \theta) \right\} \quad \text{-3. 1}$$

Similarly for the modulator output in channel number 2 is

$$e_2(t) = e_i(t) \cos (\omega_c t + \frac{2\pi}{3})$$

$$= E \cos (\omega t + \theta) \cos (\omega_c t + \frac{2\pi}{3})$$

$$= \frac{E}{2} \left\{ \cos(\omega_c t + \omega t + \frac{2\pi}{3} + \theta) + \cos (\omega_c t - \omega t + \frac{2\pi}{3} - \theta) \right\}$$

-3. 2

and for the modulator output in channel number 3 is

$$e_3(t) = e_i(t) \cos (\omega_c t + \frac{4\pi}{3})$$

$$= \frac{E}{2} \left\{ \cos (\omega_c t + \omega t + \frac{4\pi}{3} + \theta) \right.$$

$$\left. + \cos (\omega_c t - \omega t + \frac{4\pi}{3} - \theta) \right\} \quad \text{-3. 3}$$

These expressions now represent the upper and lower sideband modulation products.

For frequencies of the input signal close to the carrier frequency, the upper sideband products will be located at approximately $2\omega_c$ and the lower sideband products appear to be wrapped around the origin and superimposed upon themselves. These lower sideband products are referred to as the baseband signal in Section 2.2 when discussing the frequency translation process. The signals represented by equations (3.1), (3.2) and (3.3) are passed through low-pass filters which remove the upper sideband products and provide sharp cut-off characteristics for the lower sideband products. The low-pass filter output waveform in each channel may be represented pictorially as shown in Figure 3.12. It is seen that this waveform extends from a high frequency through zero back to a high frequency. This spectrum becomes the symmetrical band-pass characteristic obtainable at the final output.

The output from the low-pass filters may be represented by

$$\frac{E}{2} \cos (\omega_c t - \omega t - \theta) \text{ for channel No. 1}$$

$$\frac{E}{2} \cos (\omega_c t - \omega t + \frac{2\pi}{3} - \theta) \text{ for channel No. 2}$$

and $$\frac{E}{2} \cos (\omega_c t - \omega t + \frac{4\pi}{3} - \theta) \text{ for channel No. 3}$$

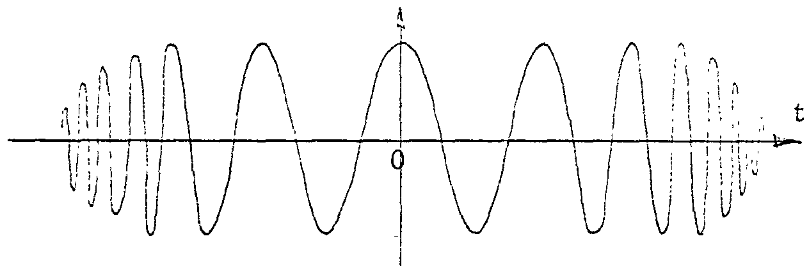

Channel No. 1

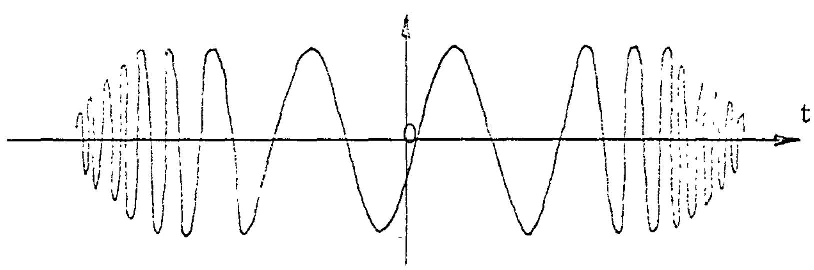

Channel No. 2

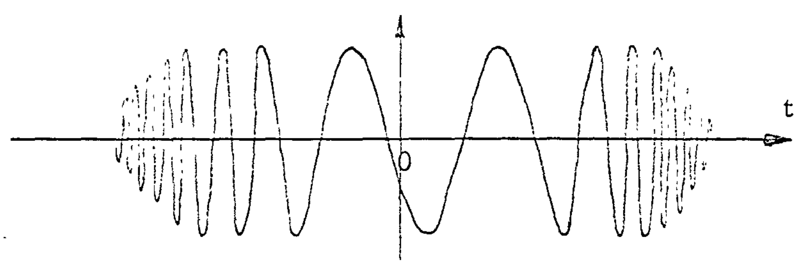

Channel No. 3

Figure 3.12 - Low-Pass Filter Output

These signals are now fed to the output modulators which are driven in synchronism with the input modulators. The output from channel No. 1 will therefore be

$$e_{11}(t) = \frac{E}{2} \cos (\omega_c t - \omega t - \theta) \cos \omega_c t$$
$$= \frac{E}{4} \left\{ \cos (2\omega_c t - \omega t - \theta) + \cos (\omega t + \theta) \right\} \qquad -3.4$$

Similarly the output from channel No. 2 will be

$$e_{22}(t) = \frac{E}{2} \cos (\omega_c t - \omega t + \frac{2\pi}{3} - \theta) \cos (\omega_c t + \frac{2\pi}{3})$$
$$= \frac{E}{4} \left\{ \cos (2\omega_c t - \omega t + \frac{4\pi}{3} - \theta) + \cos (\omega t + \theta) \right\} \qquad -3.5$$

and for channel No. 3

$$e_{33}(t) = \frac{E}{2} \cos (\omega_c t - \omega t + \frac{4\pi}{3} - \theta) \cos (\omega_c t + \frac{4\pi}{3})$$
$$= \frac{E}{4} \left\{ \cos (2\omega_c t - \omega t + \frac{8\pi}{3} - \theta) + \cos (\omega t + \theta) \right\} \qquad -3.6$$

Summing equations (3.4), (3.5) and (3.6) provides the final output $e_o(t) = \frac{3E}{4} \cdot \cos (\omega t + \theta)$.

Let us consider an in-phase synchronous signal applied to the sampled data filter. For this situation, the waveforms at various points throughout the system are given in Figure 3.13(a) and Figure 3.13(b). The waveform shown in Figure 3.13(b) is now applied to the broad band-pass filter such that the input signal (which is the fundamental component of this waveform) may be recovered.

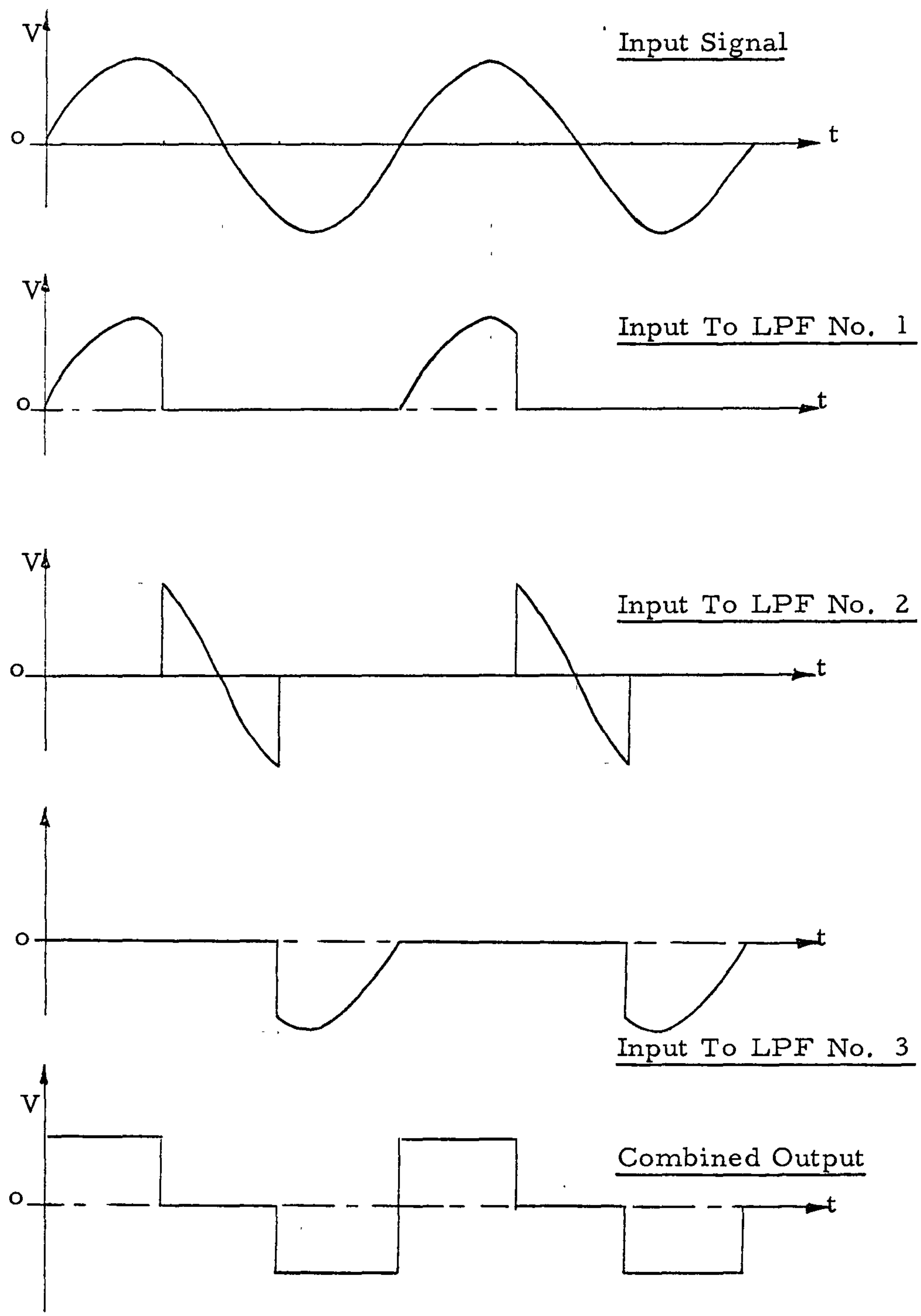

Figure 3.13(a) - Sampled Data Filter Waveforms (3-Channel System)

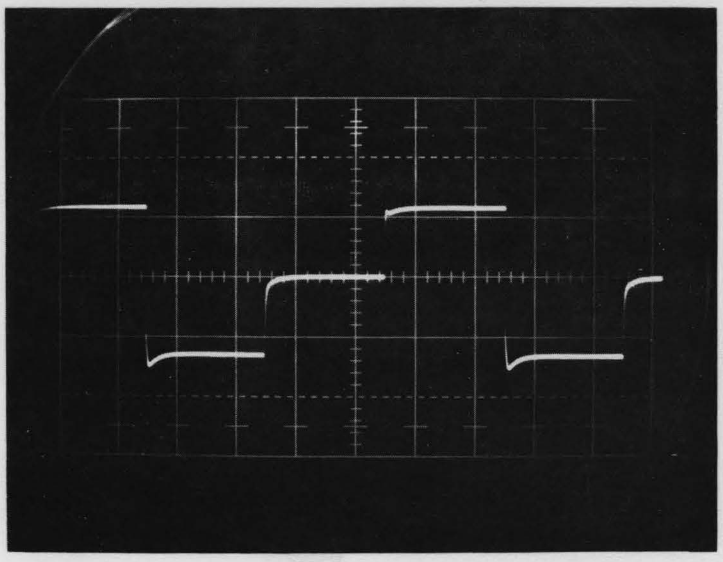

Frequency = 8333 Hz

Vertical Scale = 0.05 v/cm

Horizontal Scale = 20μS/cm

Figure 3.13(b) - Combined Output of Sampled Data Filter

3.5.2 The Quadrature Modulation System

The operation of this system is identical to that of the 3-channel system except for the fact that the carrier signals applied to the input and output modulators in the two channels are displaced by 90°. The waveforms associated with the quadrature modulation system are displayed in Figure 3.14 and are representative for an in-phase synchronous signal.

In the situation where the outputs from the low-pass filters have a DC offset voltage, the combined output will appear as shown in Figure 3.15(a). During the time the output samplers are 'ON', the input to the broad band-pass filter will be varying about this offset voltage (V_{OS}). For the time the samplers are 'OFF', the input to the broad band-pass filter will assume the potential determined by the operational amplifier characteristics, which in the ideal case will be zero volts. The broad band-pass filter will therefore recover both the wanted signal and the fundamental component due to the offset voltage V_{OS}. To overcome this problem of offset voltage, which is only present in the quadrature modulation system, a third output sampling switch is introduced as shown in Figure 3.3. This has the effect of connecting the input of

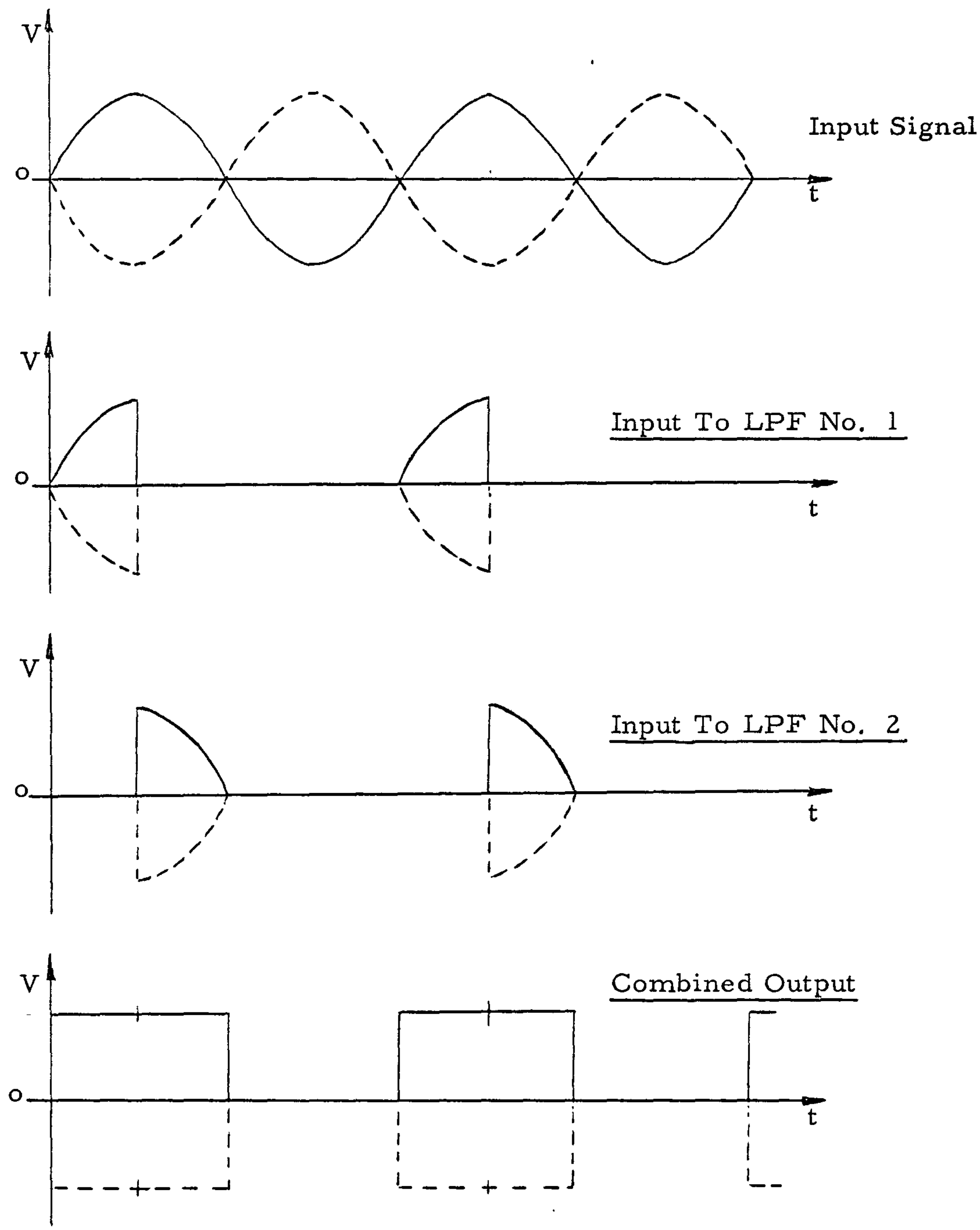

Figure 3. 14 - Sampled Data Filter Waveforms (Quadrature Modulation System)

the broad band-pass filter to the offset voltage for the period during which the output sampling switches in channel Nos. 1 and 2 are both 'OFF'. The waveform presented to the final band-pass filter will be as shown in Figure 3.15(b) and only the signal component will therefore be recovered.

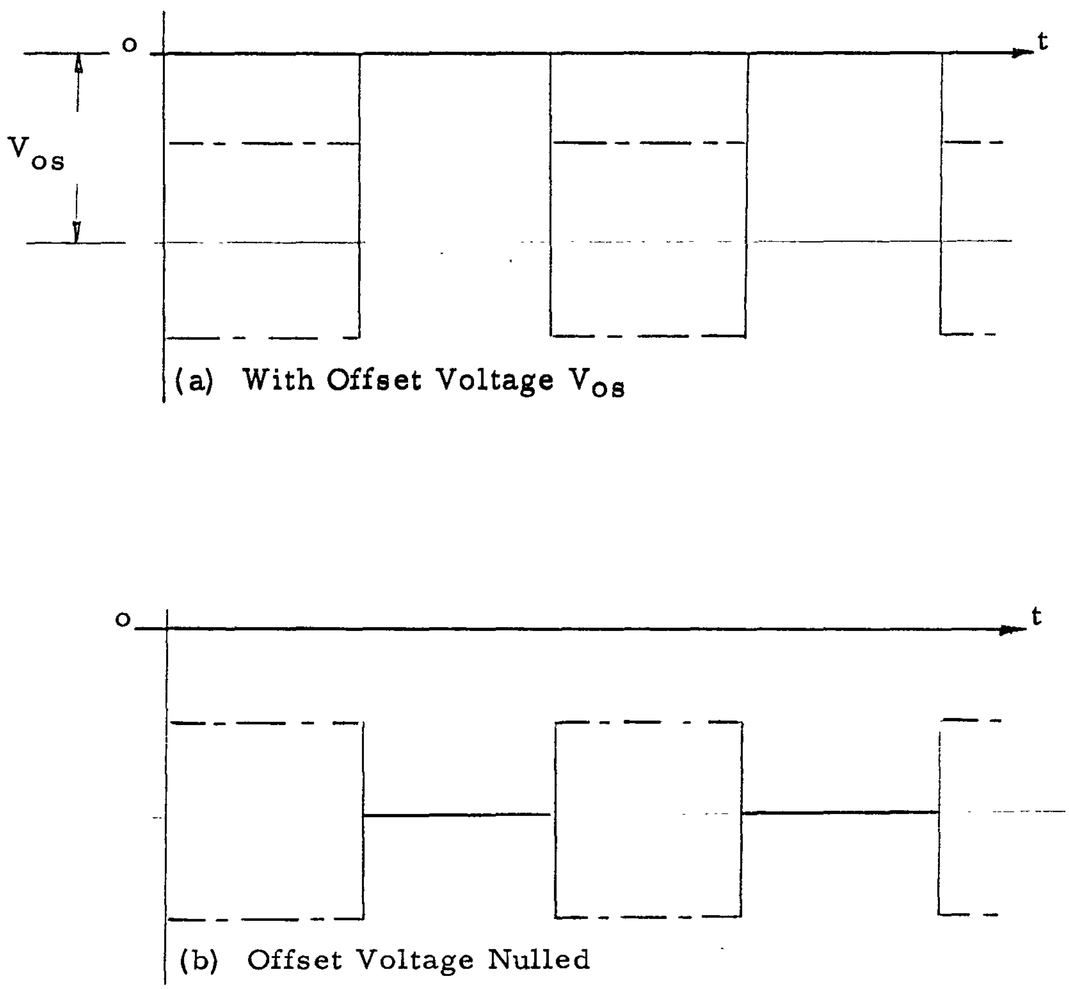

Figure 3.15 - Combined Output Of Quadrature Modulation System

CHAPTER IV

EXPERIMENTAL INVESTIGATION

4.1 Introduction

The sampled data filter described in Chapter III was constructed and extensive measurements performed on the system in an attempt to establish certain design criteria. These design criteria are based on the effect of system parameter variations on the overall sampled data filter characteristic. In the ideal system, an exact low-pass to band-pass transformation of the low-pass filter characteristic is achieved. This transformation process is examined in detail with respect to

(a) Channel imperfections,

(b) Variations in sampling frequency, and

(c) Different number of channels - the quadrature modulation system.

The effect of these system parameter variations on the overall performance together with the results obtained are discussed in detail below. The 3-channel system is first examined in detail in order to establish the sources of error which influence the overall system performance. A comparison is then made between the band-pass characteristics of the 3-channel system and the sampled data filter using the quadrature modulation technique.

The measuring set up for carrying out this investigation is given in the photograph of Figure 4. 1 and the necessary test equipment listed in Appendix IV.

4. 2 Channel Imperfections

4. 2. 1 Variation in the Gate-Drive Current

The effect of variation in the gate-drive current to both the input and output samplers with respect to the overall system performance was investigated. As stated in Section 3. 2. 3, under ideal conditions, with the turn-on transient being of equal magnitude and duration as the turn-off transient, the distortion due to switching transients at the sampler output will be zero. These transients are dependant upon both the gate drive current (gate-drive source impedance) and the rise and fall times of the gate drive waveform. Variation in the gate-drive current alters the turn-off transient only whereas by varying the rise and fall times of the gate drive waveform simultaneously, affects both the turn-on and turn-off transients due to the sampler. Where cancellation of the harmonic components of the switching transients is not complete, the system will exhibit an output for zero input at

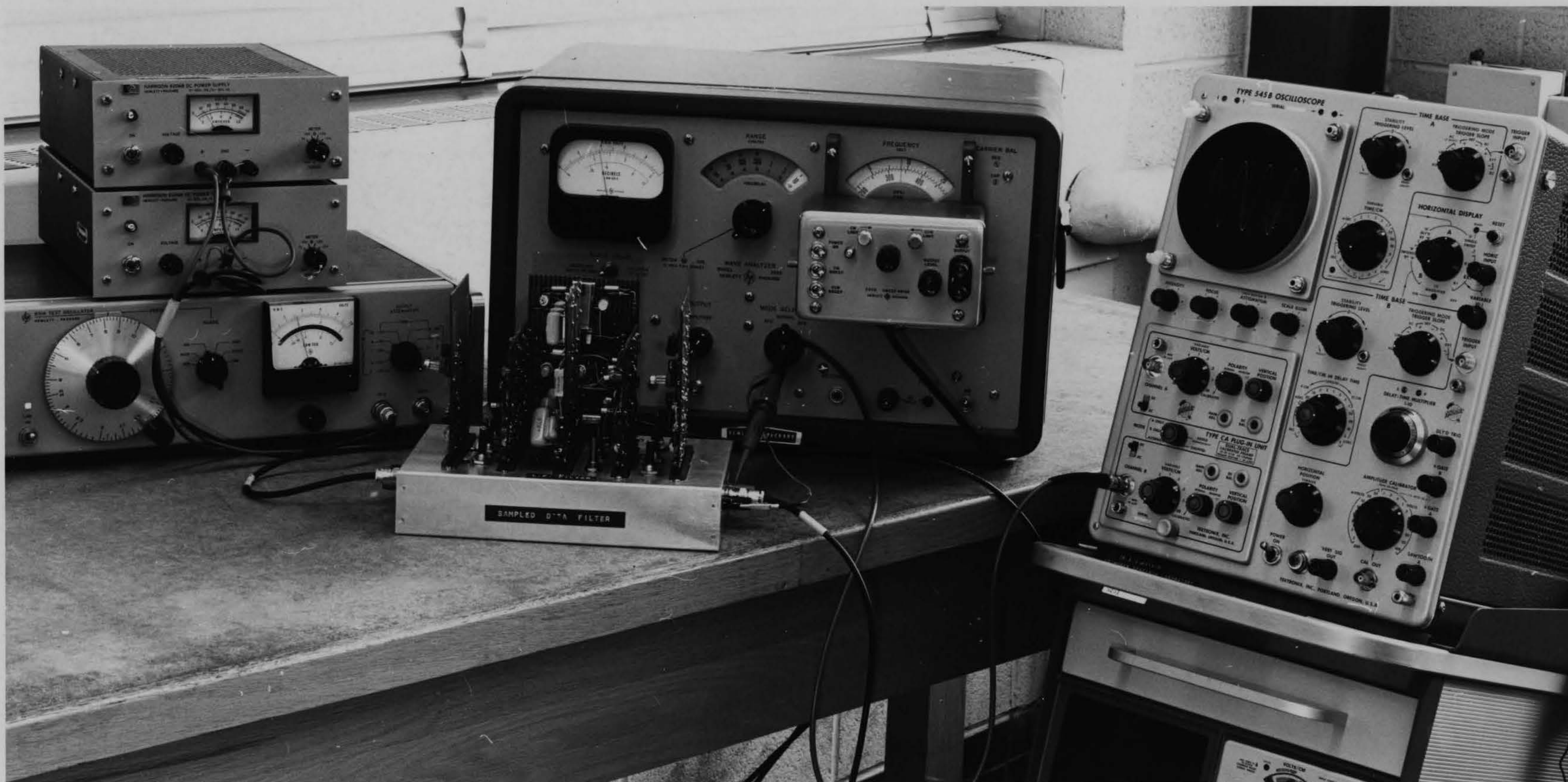

Figure 4. 1 - Experimental Test Facility

multiples of the sampling frequency. This output at the fundamental of the sampling frequency is referred to as the 'Zero Signal Noise Component' - (V_z). The variation of this component, as measured on a wave analyzer, with gate drive current is given in Figure 4. 2. The gate drive to the samplers in channel Nos. 2 and 3 was held constant at 5 mA.

The graphs given in Figure 4. 2 clearly show that any variation between the gate drive current of the input sampling switches has negligible effect on the zero signal component. The output sampling switches, however, have a direct effect on this component due to the fact that the switching transients appear directly on the output of the sampled data filter. In order to minimize this component therefore, it is of utmost importance to provide equal gate-drive currents to the output samplers.

The variation in the amplitudes of the harmonic components of the switching transients, due to the variation in gate drive current is similar to the variation in the zero signal component as demonstrated by the graphs given in Figure 4. 3. For the 3-channel system however, the harmonic component at 3fo and 6fo etc. should ideally be zero. Since we have non-ideal sampling switches, there will be a finite but constant value at multiples of 3fo. The amplitudes of these

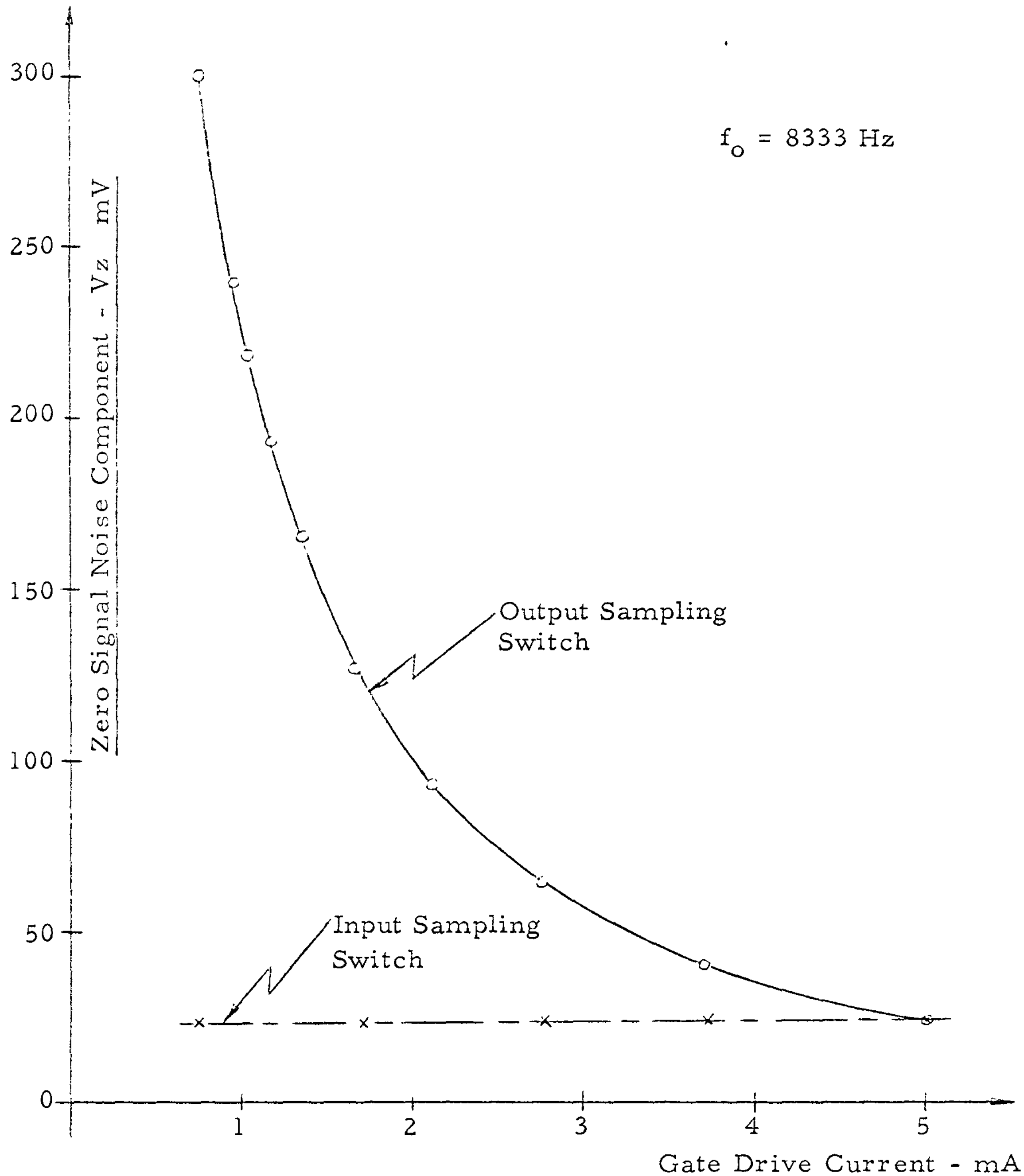

Figure 4. 2 - Effect Of Channel Mismatch Due To Variation In Gate Drive Current On Zero Signal Noise Component

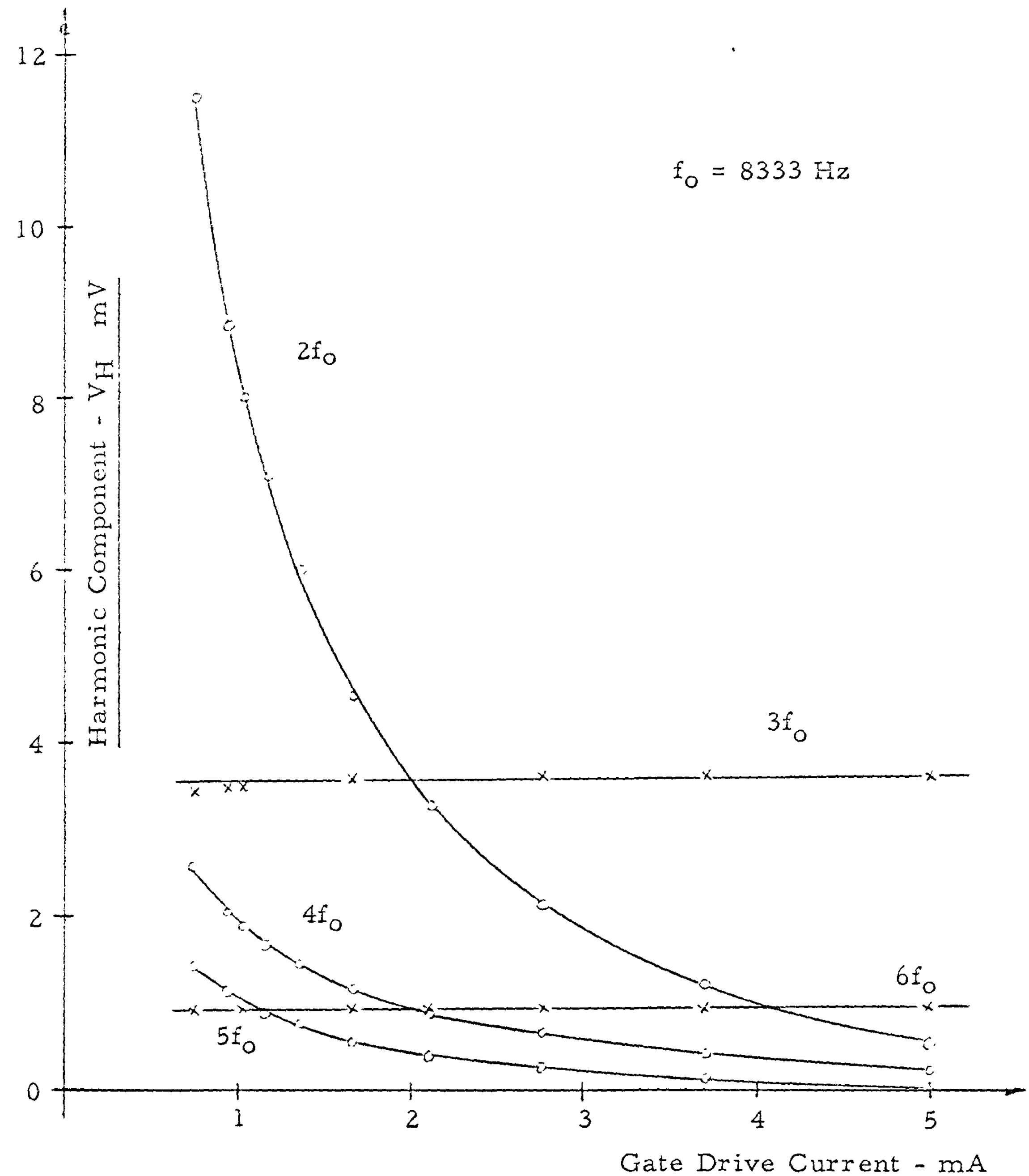

Figure 4. 3 - Effect Of Channel Mismatch Due To Variation In Gate Drive Signal Of Output Sampling Switches, On Harmonic Distortion

harmonics could be reduced considerably by a more elaborate broad band-pass filter, i. e., one having greater cut-off rates than that of a single stage RC-network.

The effect of variation in gate drive current, to both the input and output sampling switches, on the sampled data filter selectivity characteristics is seen in Figure 4. 4. No change in the 3 dB bandwidth is experienced and the asymptotic cut-off rate of 18 dB/octave is achieved.

4. 2. 2 Variation in Rise and Fall Time of Drive Signal

As discussed in Section 4. 2. 1, the variation in gate drive current affected the turn-off transient only. In order to determine the effect of variation in both turn-on and turn-off transients, the rise and fall times of the gate drive waveform were varied at a number of settings of gate drive current. The results obtained are given in Figure 4. 5, Figure 4. 6 and Figure 4. 7, where it is seen that the zero signal component and the harmonic distortion increases with increasing rise and fall times. Again the distortion is primarily due to the output sampling switches, as is to be expected. Thus in order to minimize the zero signal component and its harmonics, is to ensure that the rise and fall times of the gate drive signal in each channel are equal to each other.

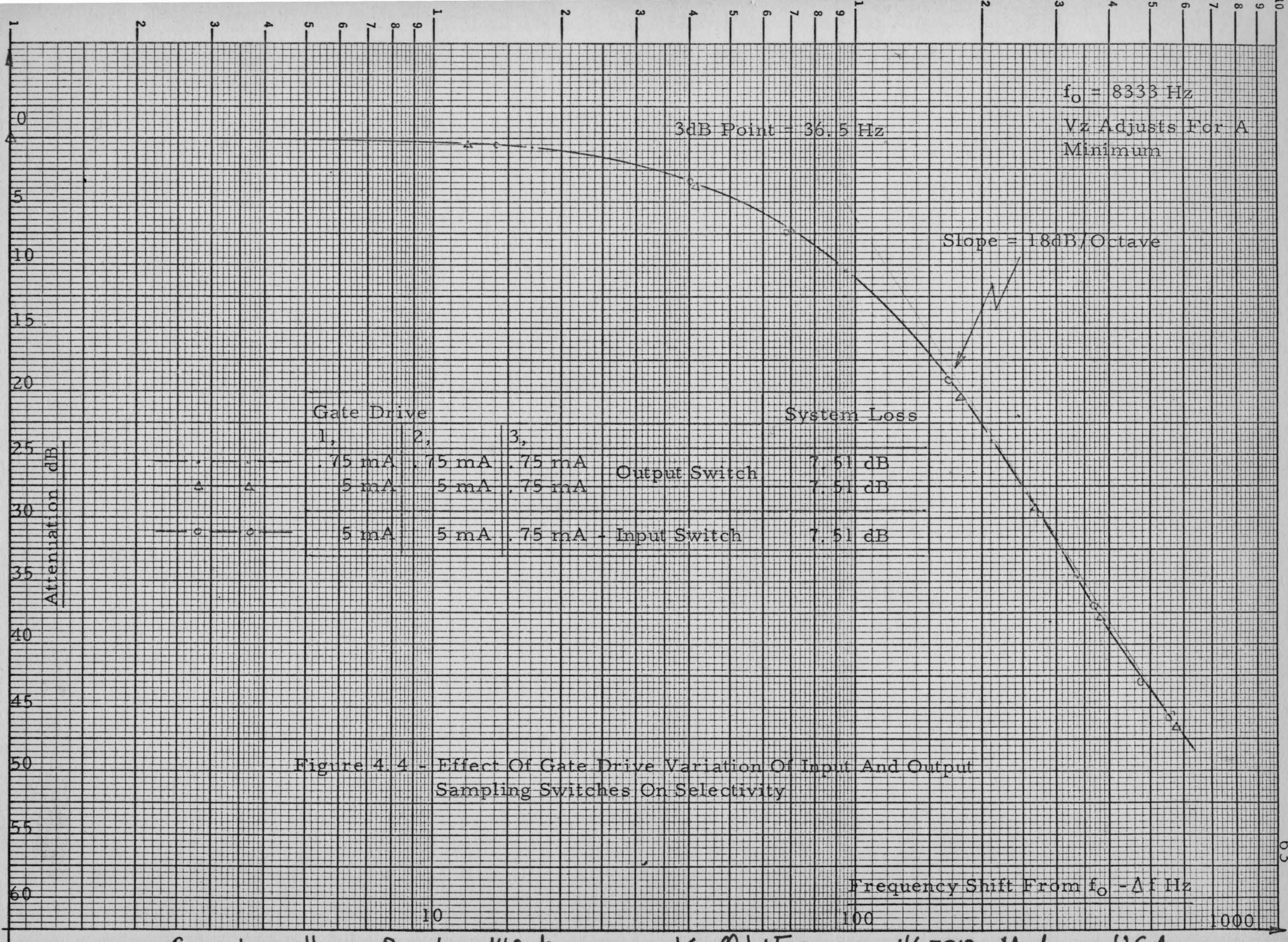

Figure 4.4 - Effect Of Gate Drive Variation Of Input And Output Sampling Switches On Selectivity

Semi-logarithmic 3 cycles x 140 divisions Keuffel & Esser co. 46 5813 Made in U.S.A.

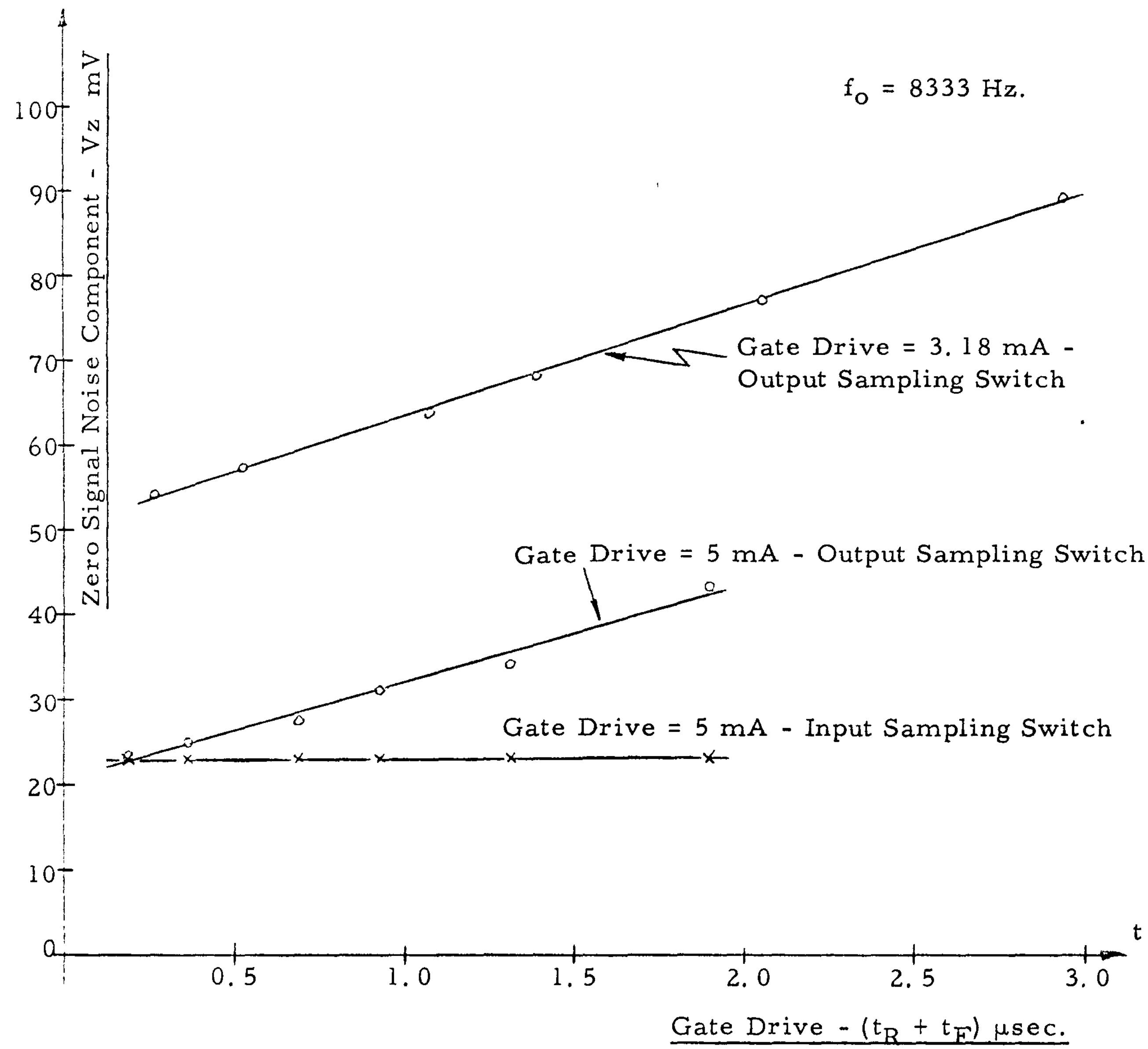

Figure 4.5 - Effect Of Channel Mismatch Due To Variation In Rise & Fall Time Of Gate Drive Signal On Zero Signal Noise Component

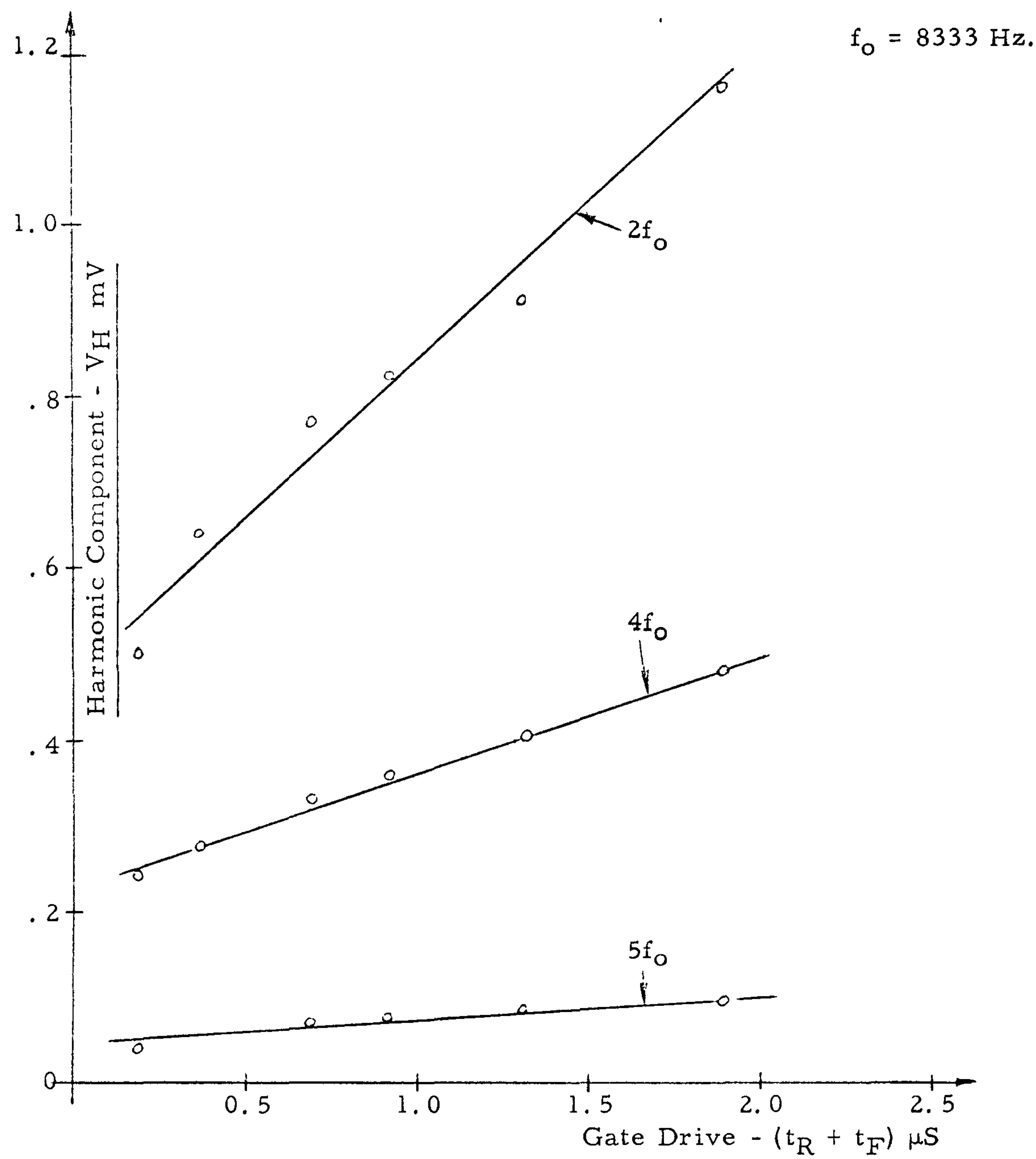

Figure 4.6 - Effect Of Channel Mismatch Due To Variation In Rise & Fall Time Of Gate Drive Signal On Harmonic Distortion - Gate Drive = 5 mA.

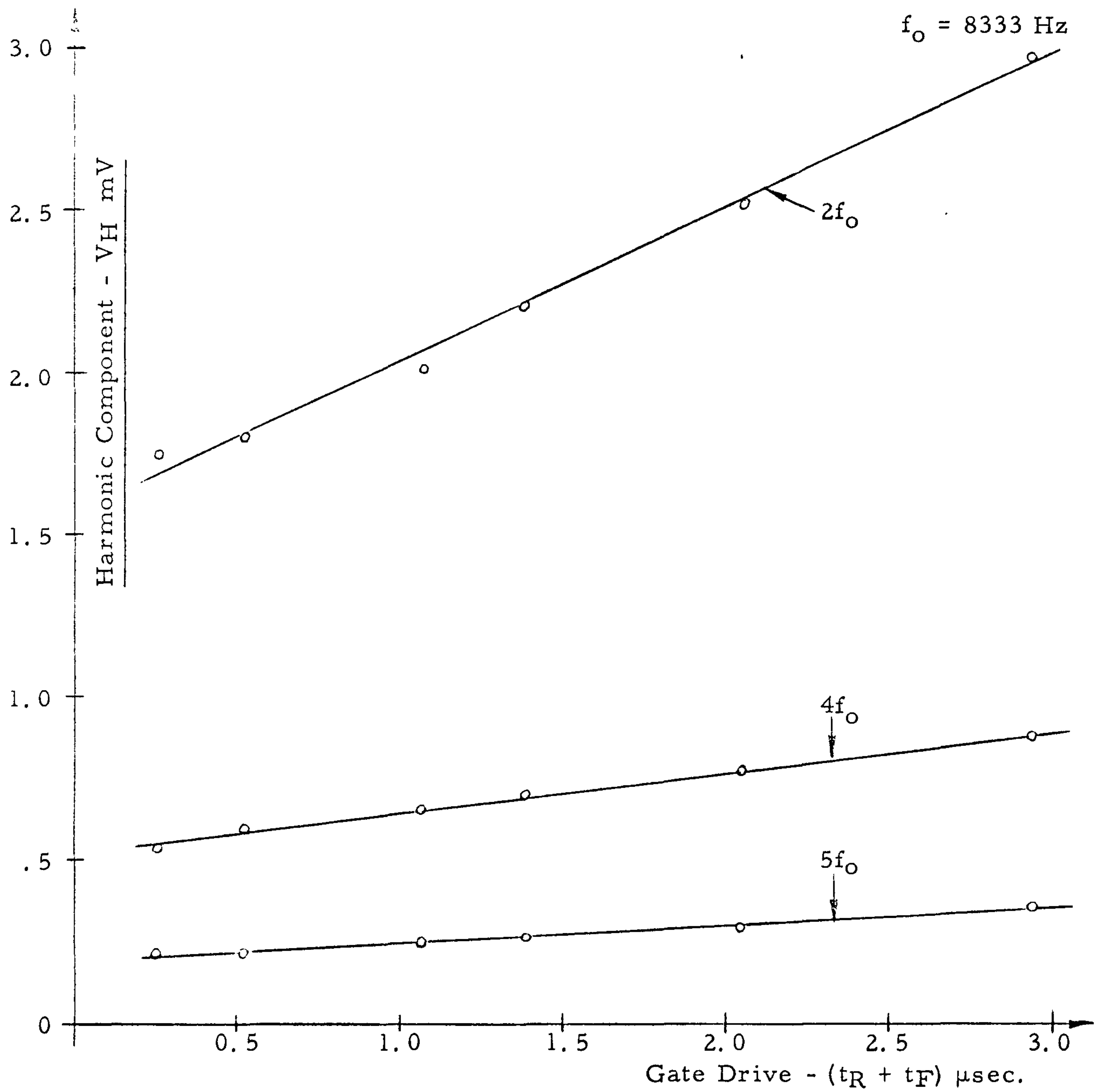

Figure 4.7 - Effect Of Channel Mismatch Due To Variation In Rise & Fall Time Of Gate Drive Signal On Harmonic Distortion - Gate Drive = 3.18 mA

4.2.3 Effect of Rise and Fall Time of Sampling Switch

The effect of variation in the rise and fall time of the sampling switches was considered next. The degree to which the rise and fall times were varied can be seen from the photographs of the sampled signal as shown in Figure 4.8. The rise and fall time was degraded in one channel only and the effect of this on the selectivity and harmonic distortion of the sampled data filter investigated. As can be deduced, the variation in the switching times of the input sampling switches has negligible effect on the zero signal noise component and its harmonics. It is to be expected however, that the overall system loss should increase since less energy is transmitted through one of the channels. The effect of the switching times of the input sampling switches on the selectivity characteristics and the overall loss at the passband centre is given in Figure 4.9. No change in the selectivity characteristics is found and a slight increase in system loss is experienced.

The effect of mismatch in the rise and fall times of the output sampling switches is more pronounced. The switching times of the samplers are determined by the time constant due to the load resistance and output capacitance. Since this output capacitance appears in parallel with all channels, each sampling switch will therefore experience the same rise and

(a)* Scale:-
Horizontal = 20μS/cm
Vertical = 0.5v/cm

Frequency = 8333 Hz

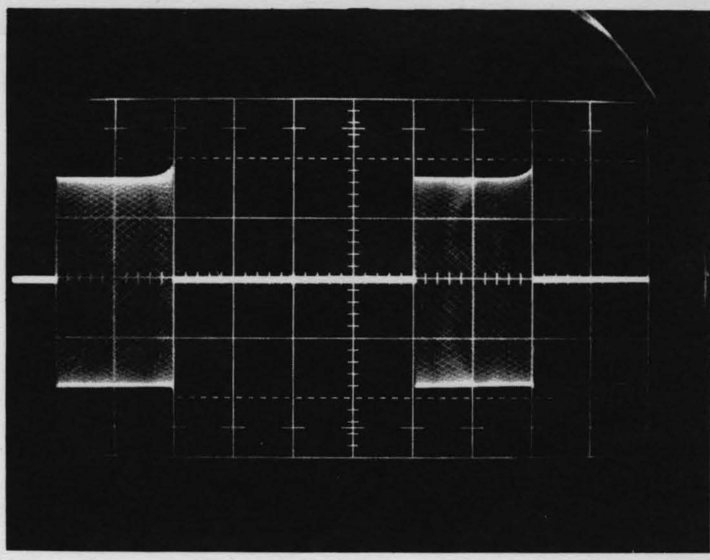

(b)* Scale:-
Horizontal = 20μS/cm
Vertical = 0.5v/cm

Frequency = 8333 Hz

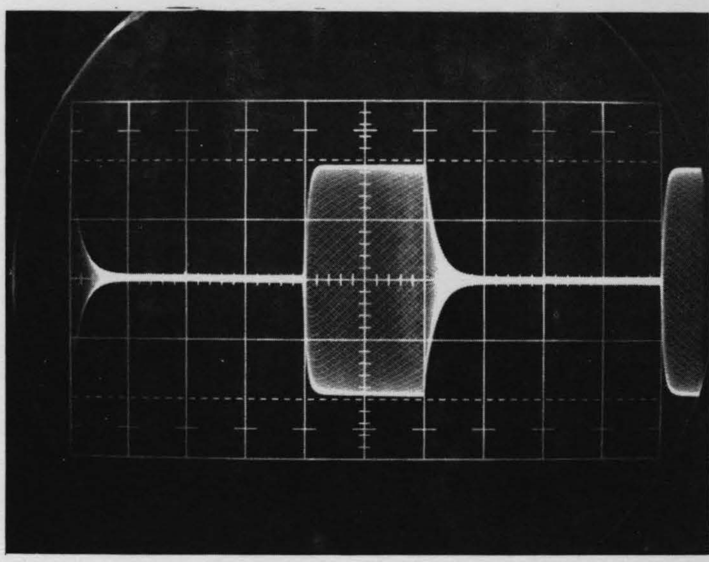

* Oscilloscope not synchronized to carrier.

Figure 4.8 - Variation in Rise and Fall Time of Sampled Signal

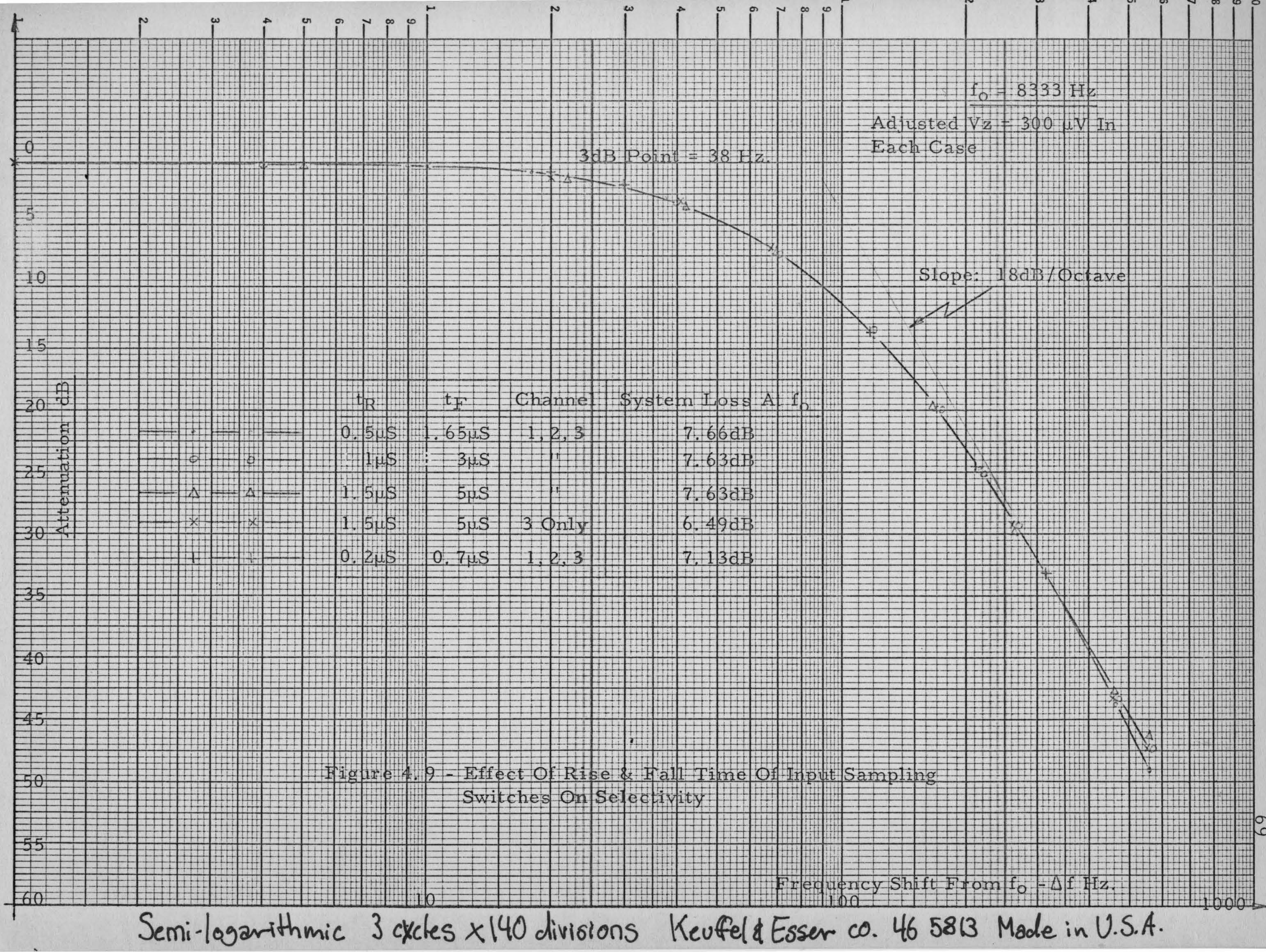

Figure 4.9 - Effect Of Rise & Fall Time Of Input Sampling Switches On Selectivity

fall time. For this situation the only noticeable effect will be the increase in overall system loss. The selectivity characteristics and the change in system loss is given in Figure 4. 10.

4. 2. 4 Variation in Sampling Switch Resistance

The main effect of any variation between the 'on' resistances of the sampling switches in each channel, is to increase the zero signal noise component, which is at the centre frequency, and all of its harmonics. The effect of input switch resistance variation on this component and its harmonics is negligible as these are followed by narrow band low-pass filters having a high value of insertion loss. If the passive low-pass filter is replaced by an RC-active filter of the same order but with the addition of gain, then the effect of input switch resistance variation will become more pronounced. For this reason, therefore, it is desirable to maintain the sampling switch 'on' resistance as small as possible, compatible with the signal, drive and load requirements.

In Figure 4. 11, the effect of input switch resistance variation is shown to be negligible on the selectivity characteristic. The system loss however, is increased with increase in 'on' resistance due to the reduction in signal amplitude applied to the low-pass filter.

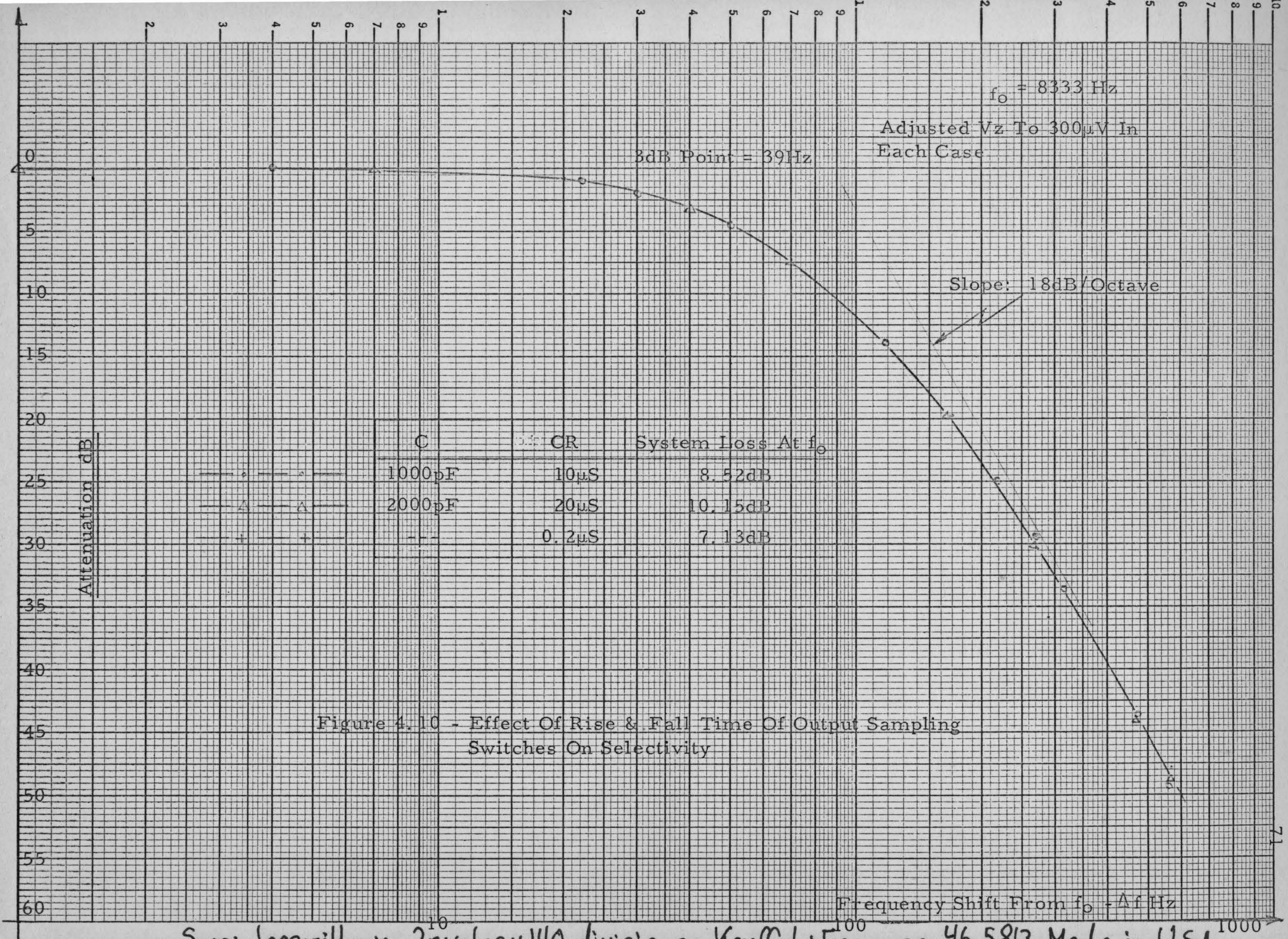

Figure 4.10 - Effect Of Rise & Fall Time Of Output Sampling Switches On Selectivity

Semi-logarithmic 3cycles x 140 divisions Keuffel & Esser co. 46 5813 Made in U.S.A.

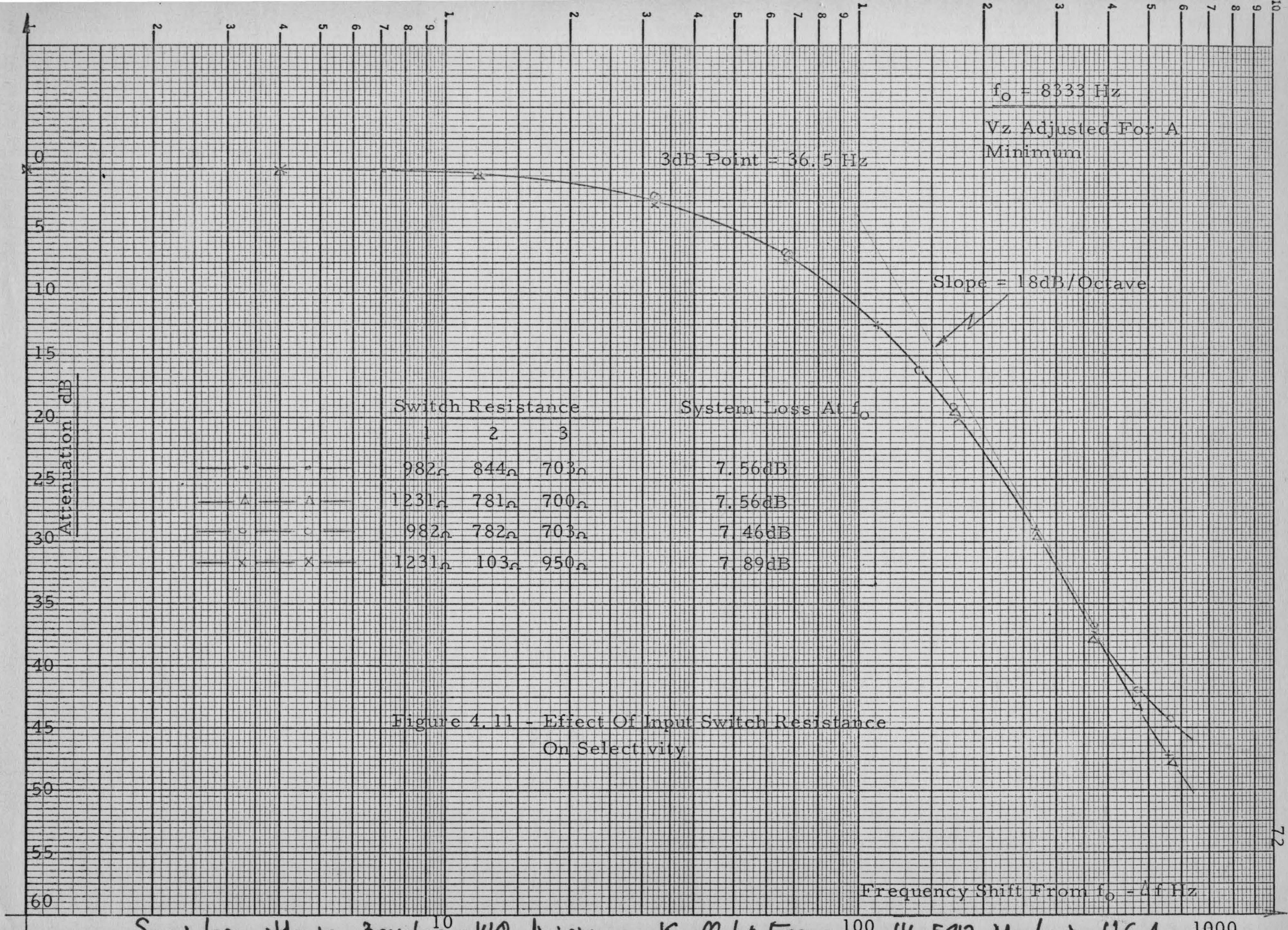

Figure 4.11 - Effect Of Input Switch Resistance On Selectivity

For the sampled data filter system with passive low-pass sections, the variation in output switch resistance has a direct bearing on the overall system performance as can be seen in Figure 4.12 and Figure 4.13. In order to minimize the effect of switch resistance, it is necessary that this 'on' resistance be a small fraction of the load resistance.

Throughout the foregoing discussion, it can be seen that the main emphasis has been centred on the zero signal noise component. The magnitude of this component directly affects the maximum amount of stop-band attenuation available from the sampled data filter. In this context, the stop-band attenuation is defined as

$$\text{Attenuation} = 20 \log \frac{\text{output signal}}{\Sigma(\text{Zero signal noise components})}$$

The effect of this component on the sampled data filter characteristics is seen in Figure 4.14 and Figure 4.15. From these it can be seen that increasing the zero signal noise component reduces the available stop-band attenuation. In addition, Figure 4.14 and Figure 4.15 show that a symmetrical bandpass characteristic and asymptotic cut-off rate of 18 dB/octave are maintained.

4.2.5 Modulation Effects in the Sampled Data Filter

During the course of the experimental investigation into the selectivity characteristics, an anomaly in the

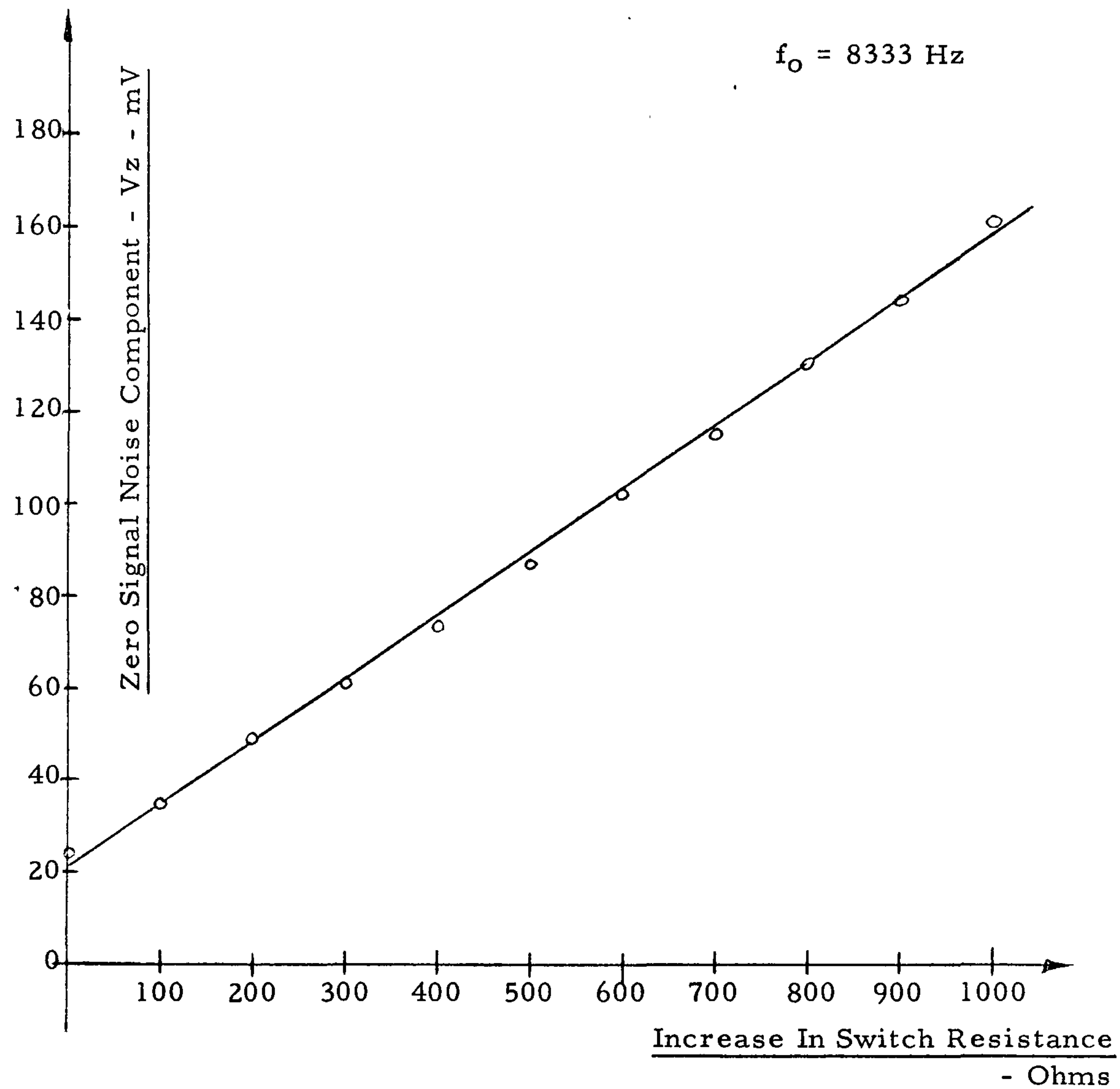

Figure 4.12 - Effect Of Output Switch Resistance On Zero Signal Noise Component

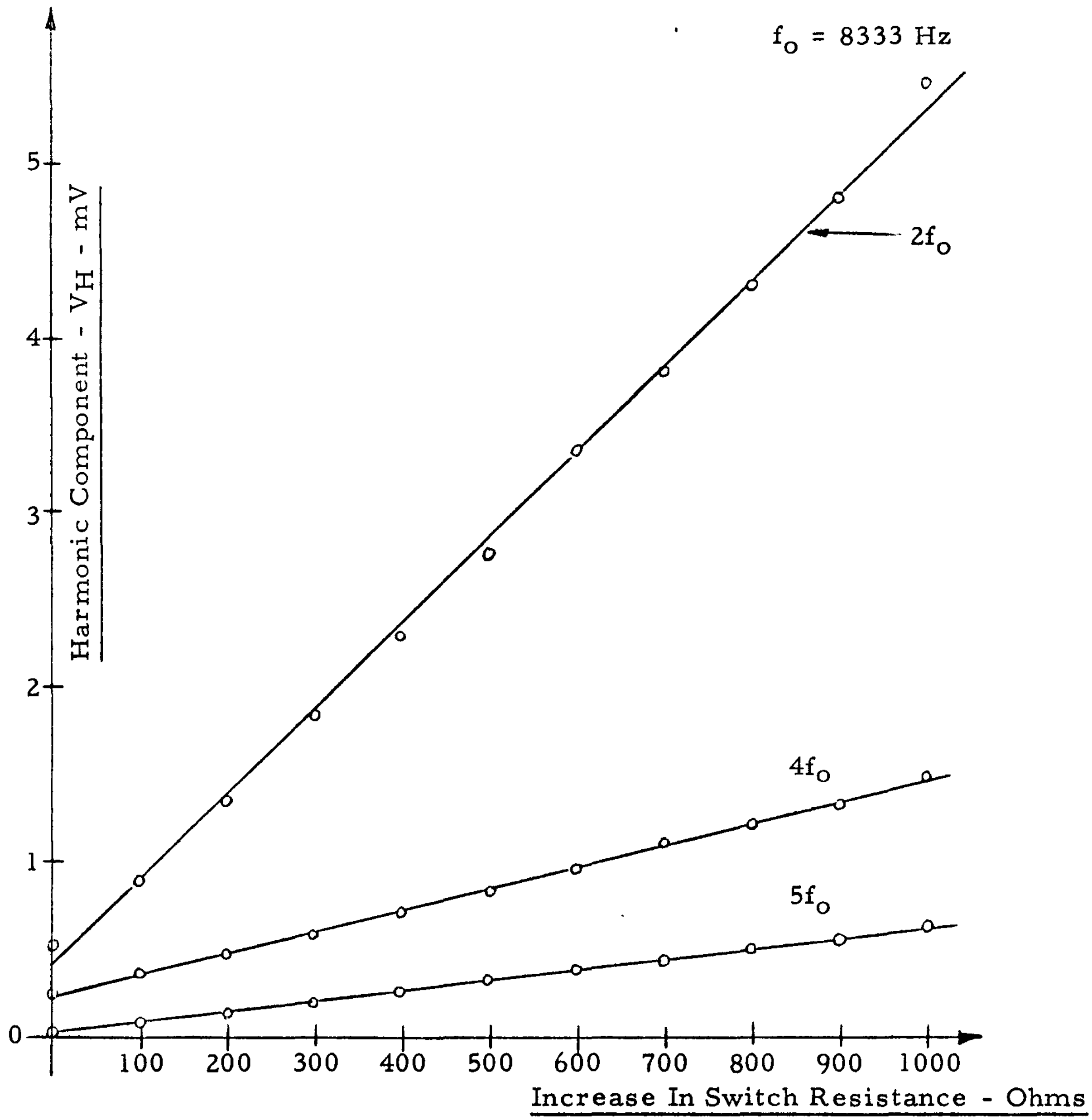

Figure 4.13 - Effect Of Output Switch Resistance On Harmonic Distortion

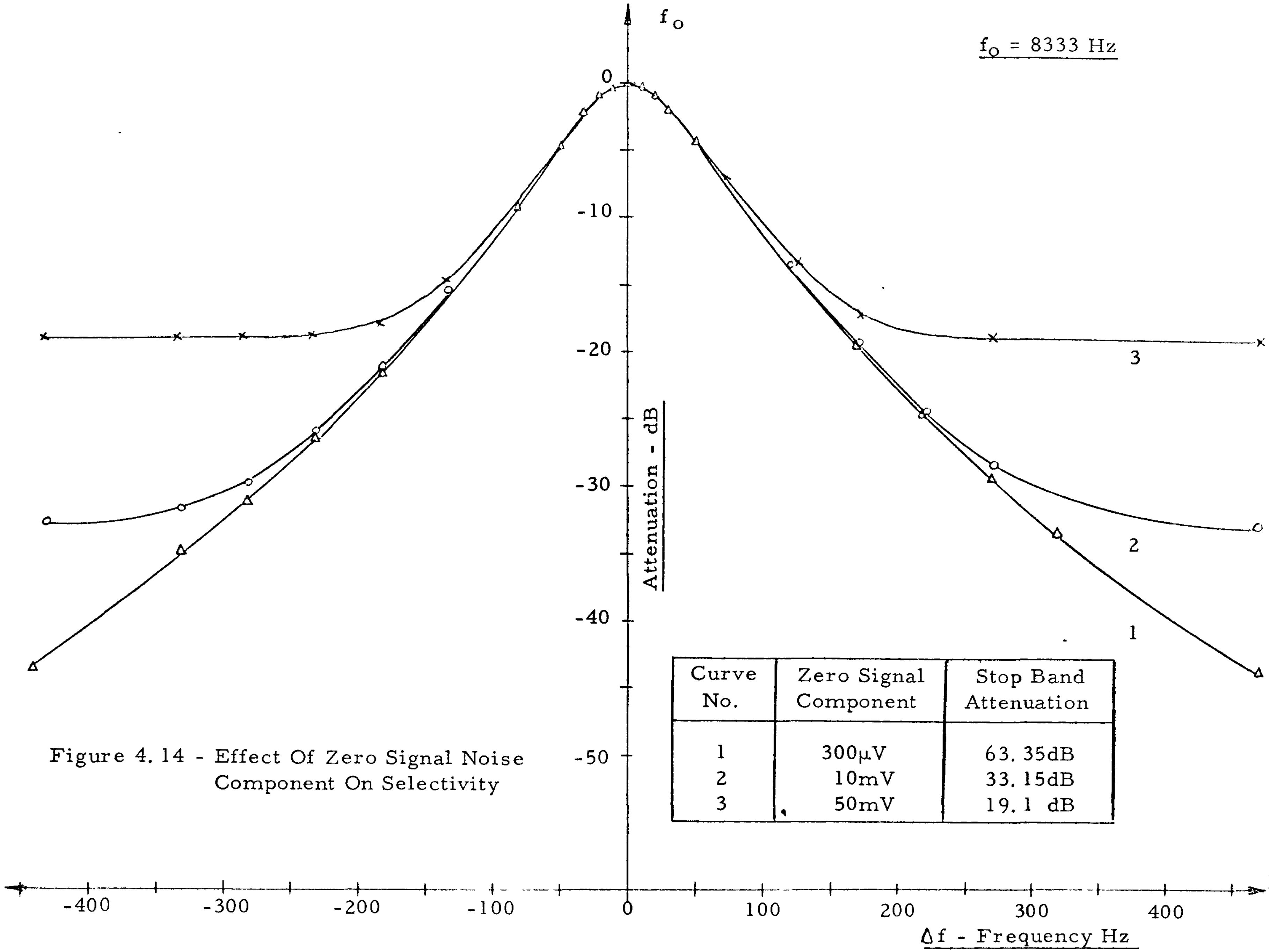

Curve No.	Zero Signal Component	Stop Band Attenuation
1	300µV	63.35dB
2	10mV	33.15dB
3	50mV	19.1 dB

Figure 4.14 - Effect Of Zero Signal Noise Component On Selectivity

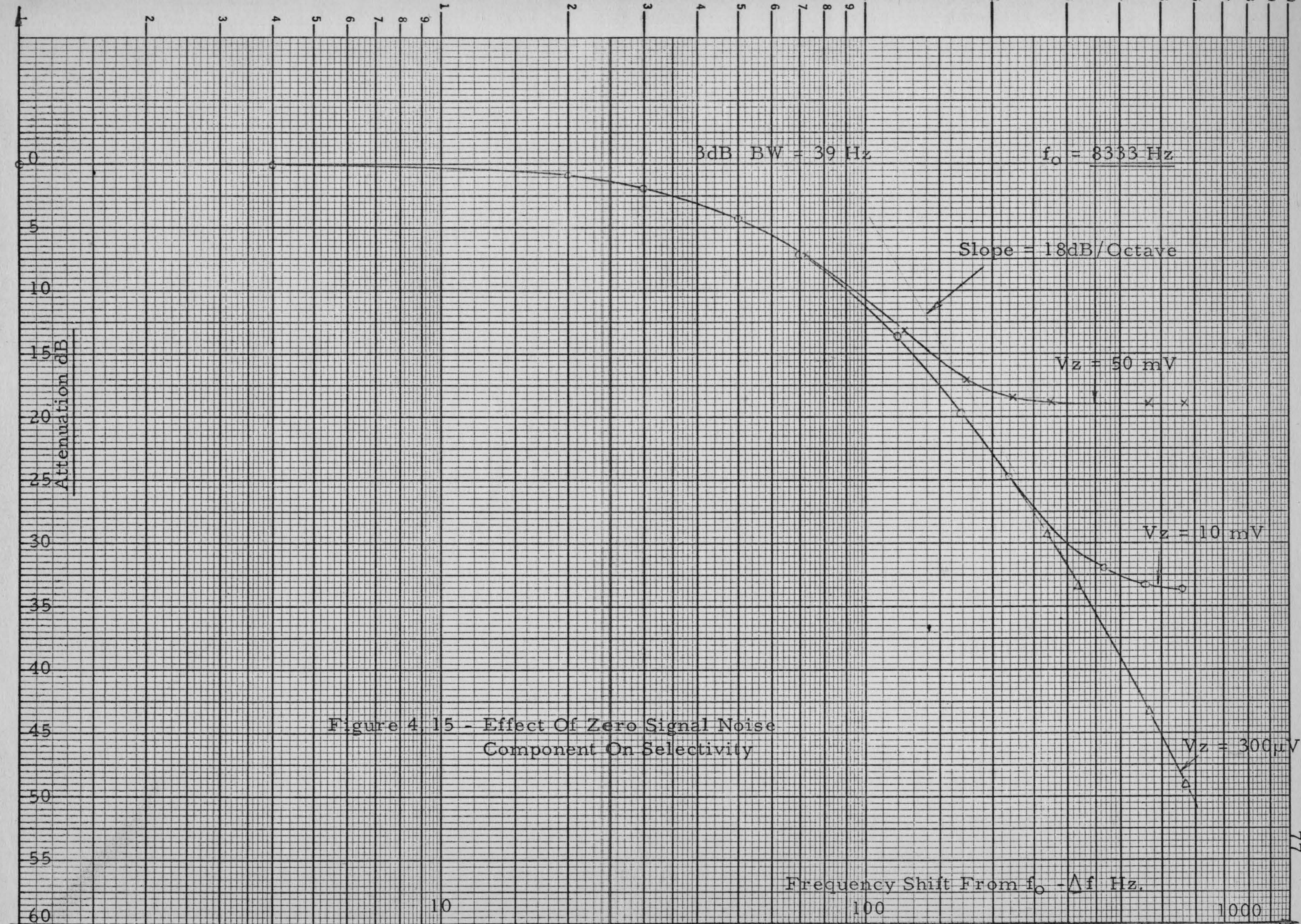

Figure 4.15 - Effect Of Zero Signal Noise Component On Selectivity

Semi-logarithmic 3 cycles x 140 divisions Keuffel & Esser co. 46 5813 Made in U.S.A.

performance of the sampled data filter was observed. This took the form of a modulation of the wanted signal.

Consider an in-phase synchronous input signal of unit amplitude. The outputs from the three channels are given by equations 3.4, 3.5 and 3.6 from Section 3.4. These equations are repeated here for convenience, and are as follows.

$$e_{11}(t) = \frac{E}{4}\left\{\cos\,(2\omega_c t - \omega t) + \cos\omega t\right\} \qquad 4.1$$

$$e_{22}(t) = \frac{E}{4}\left\{\cos\,(2\omega_c t - \omega t + \frac{4\pi}{3}) + \cos\omega t\right\} \qquad 4.2$$

$$e_{33}(t) = \frac{E}{4}\left\{\cos\,(2\omega_c t - \omega t + \frac{8\pi}{3}) + \cos\omega t\right\} \qquad 4.3$$

Adding equation 4.1, 4.2 and 4.3 gives $e_o(t) = \frac{3E}{4}\cos\omega t$.

Thus under ideal conditions the output will consist of the wanted signal $\cos\omega t$ only. If the gain/frequency characteristics of the low-pass networks are not identical, or if the signal applied to these networks are not of equal magnitude, cancellation of the first terms in the above equations will not be carried out. The net result is the appearance of an image component of $\cos(2\omega_c t - \omega t + \theta)$ within the pass-band of the sampled data filter. The location of the image component with respect to the signal and zero signal component is given in Figure 4.16.

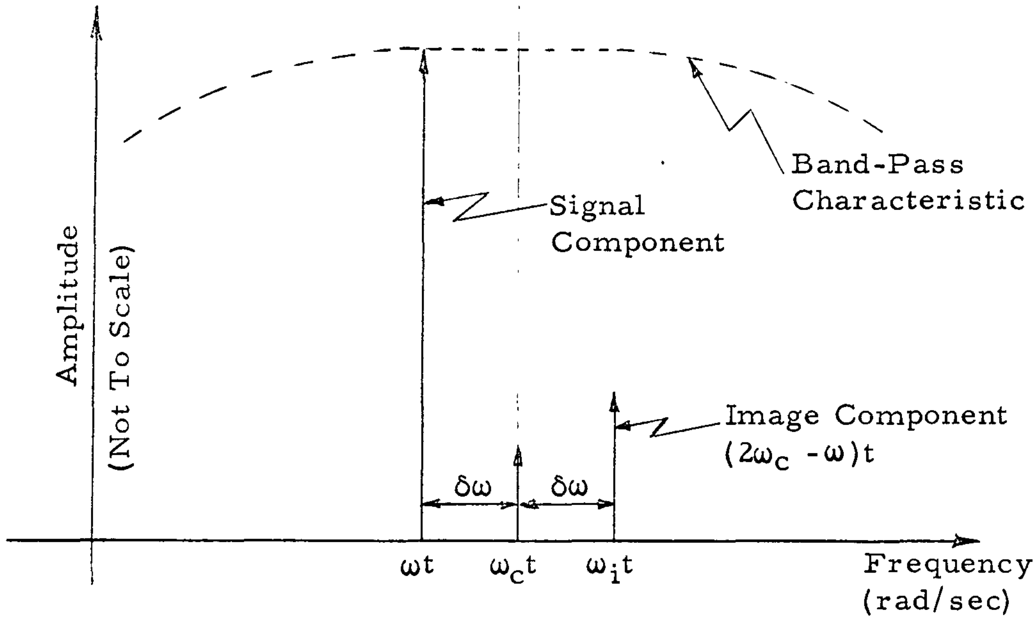

Figure 4. 16 - Location of Image Component

The location of the image component was verified experimentally and was found to be approximately 40 dB below the wanted signal. Depending on the relative amplitudes of the image and zero signal noise component the frequency and amplitude of the modulation varied accordingly. This effect is shown in the photographs of Figure 4. 17 to Figure 4. 19.

The image component was reduced further by adjusting the input signal amplitude to the low-pass filters. This reduction, however, could only be achieved at one frequency for one particular input level, suggesting that the image component is a direct result of unbalance between the gain/frequency characteristics of the low-pass filters. In order to

(a) Scale:-

Horiz(upper) = 50μS/cm
Horiz(lower) = 2mS/cm
Vertical = 0.5v/cm

Frequency = 8334 Hz

V_z = 150μV

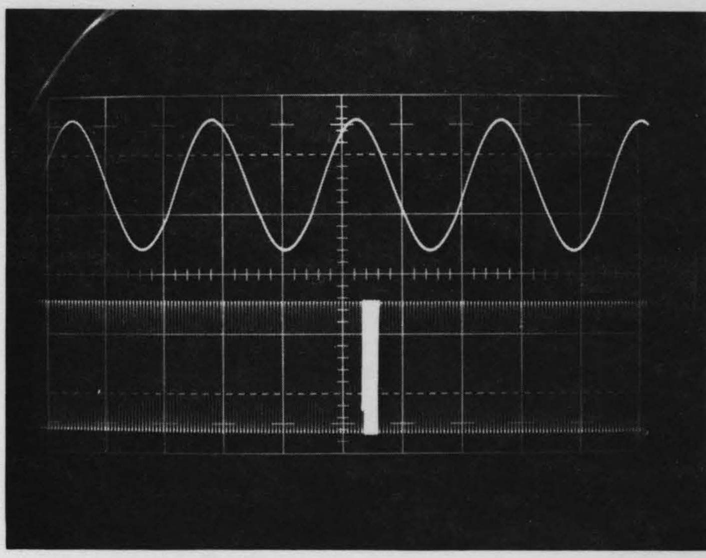

(b) Scale:-

Horiz(upper) = 50μS/cm
Horiz(lower) = 1mS/cm
Vertical = 0.1v/cm

Frequency = 8200 Hz

V_z = 150μV

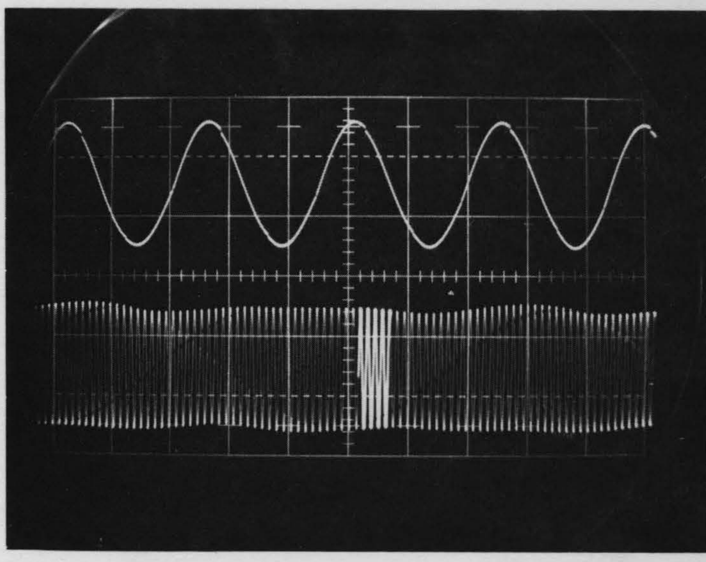

Figure 4.17 - Modulation Effects

(a) Scale:-
Horizontal = lmS/cm
Vertical = 0. 05v/cm

Frequency = 8000 Hz

V_z = 10mV > V_s (Signal)

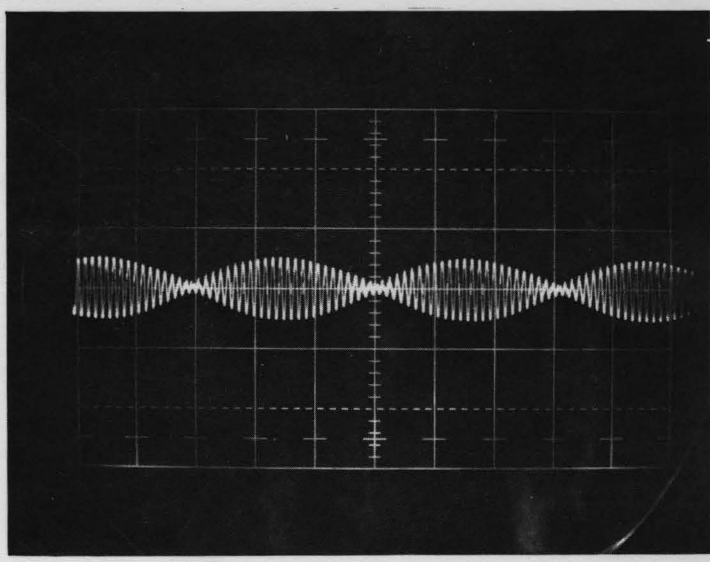

(b) Scale:-
Horizontal = 2mS/cm
Vertical = 0. lv/cm

Frequency = 8200 Hz

V_z = 10mV < V_s (Signal)

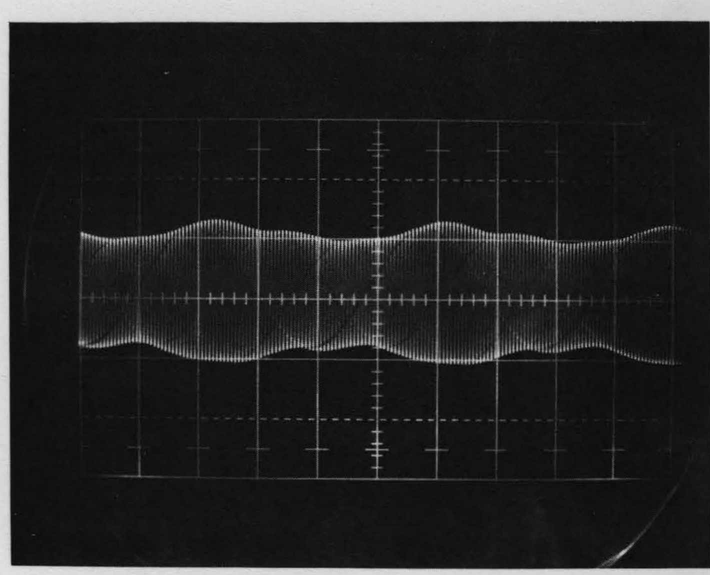

Figure 4. 18 - Modulation Effects

(a) Scale:-

Horiz(upper) = 0. 1mS/cm
Horiz(lower) = 2mS/cm
Vertical = 0. 2v/cm

Frequency = 8200 Hz

V_z = 50mV $\triangleq V_s$ (Signal)

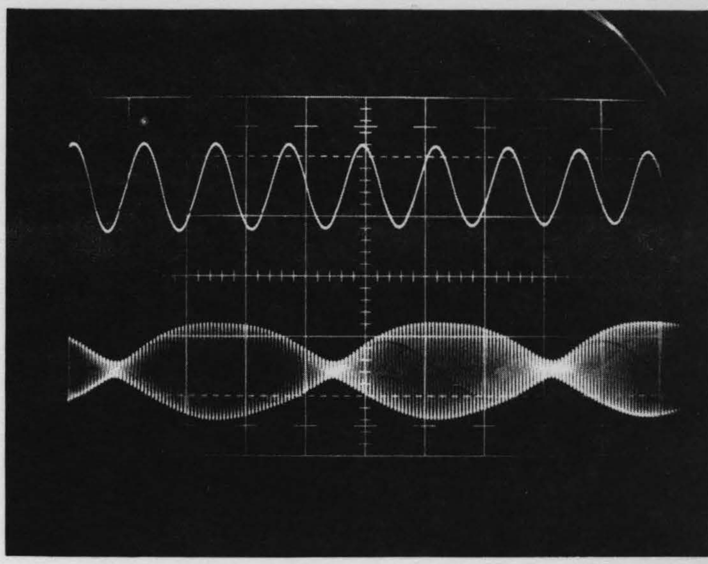

(b) Scale:-

Horiz(upper) = 0. 1mS/cm
Horiz(lower) = 2mS/cm
Vertical = 0. 1v/cm

Frequency = 8000 Hz

V_z = 50mV > V_s (Signal)

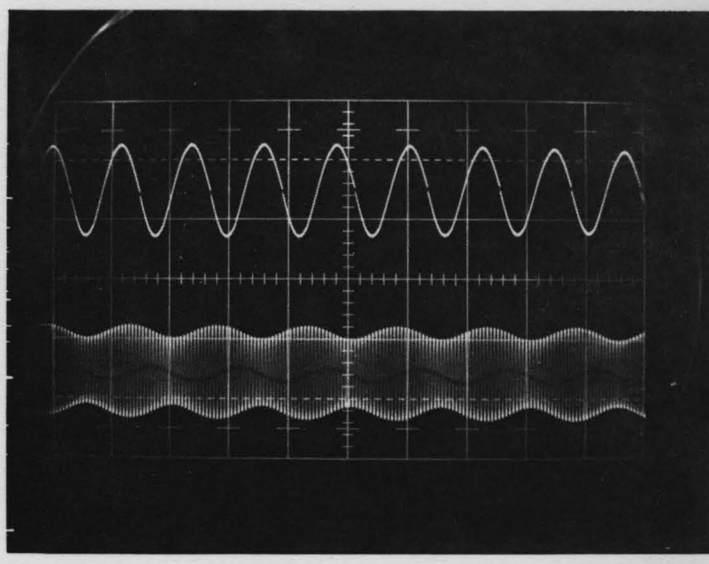

Figure 4. 19 - Modulation Effects

minimize this component, therefore, it is important to maintain accurate balance between these low-pass filters.

4.3 Variation in Sampling Frequency

The effect of sampling frequency variation on the overall system performance was considered next. The zero signal noise component was measured over a frequency range suitable for the measuring equipment (up to 50 KHz) after having set this component to some convenient value at the low frequency. As is to be expected, the zero signal component increases linearly with increase in sampling frequency above 15 KHz, as demonstrated in Figure 4.20. The departure from linearity below a sampling frequency of 15 KHz could be due to more effective cancellation of the switching transients. For the system operating as a single band-pass filter, this increase in zero signal component should be of no concern, since it may be reduced considerably by proper matching of the individual channels. However, if the sampled data filter is to operate over a wide frequency range, then this component must be minimized in order to achieve the minimum desirable stop band attenuation over the required frequency range.

The extent to which the rise and fall time of the sampled signal was degraded at a sampling frequency of 40 KHz

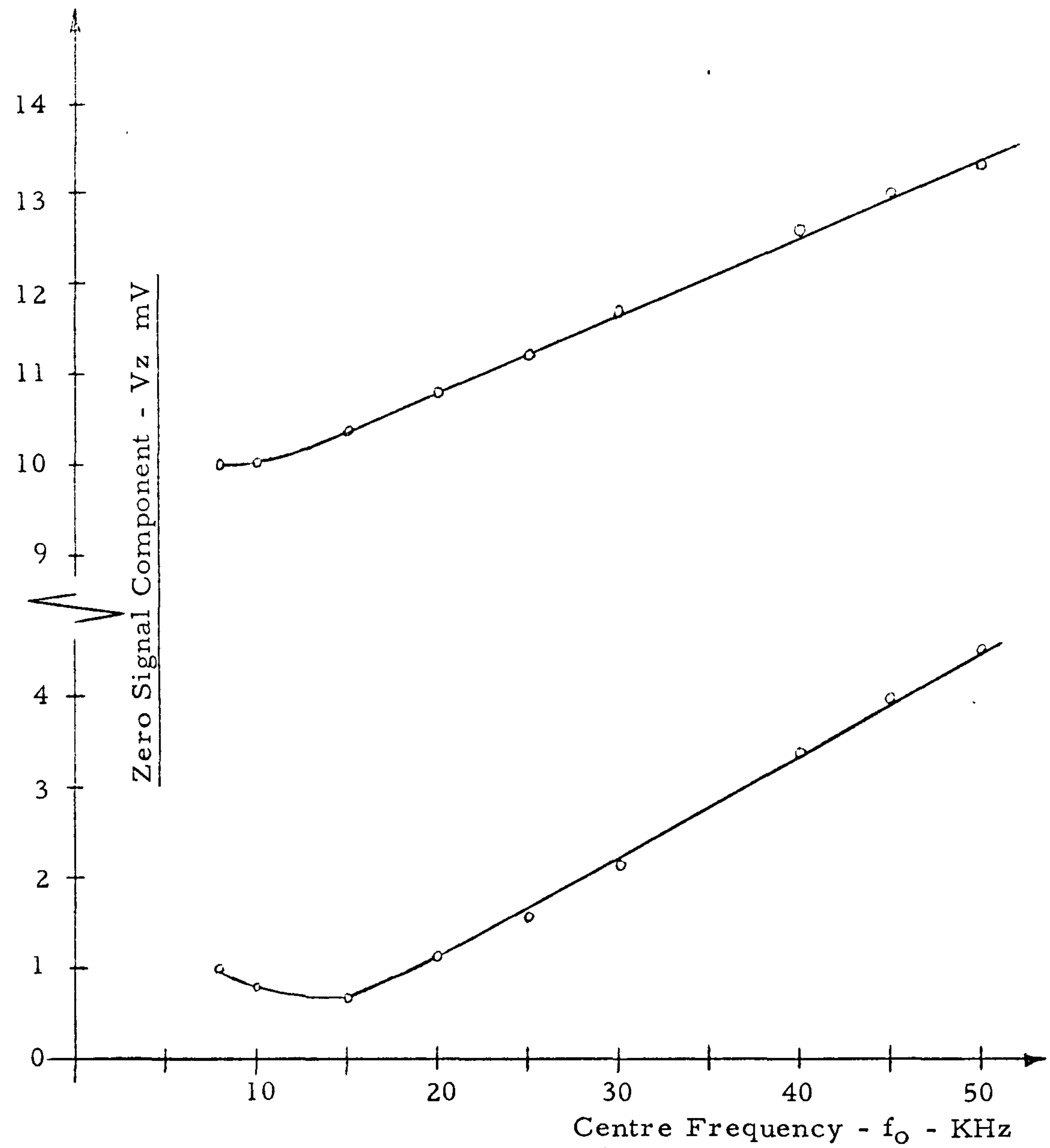

Figure 4. 20 - Effect Of Sampling Frequency On Zero Signal Component

is shown in the photographs of Figure 4. 21. The effect of this degradation on the selectivity characteristics is shown in Figure 4. 22 where it is seen that the asymptotic cut off rate of 18 dB/octave is achieved.

4. 4 Summary of Results on 3-channel System

From the experimental investigation carried out on the 3-channel sampled data filter, any imperfections within the system, resulted in the appearance of two unwanted components at the output of the sampled data filter, namely

1. The zero signal noise component and its harmonics
2. The image component.

These two components give rise to the modulation of the output signal as demonstrated in Figures 4. 17 to 4. 19. The depth of modulation being determined by the degree of mismatch between the various channels and the output signal amplitude.

4. 5 The Quadrature Modulation System

Selected measurements of the quadrature modulation sampled data filter were carried out. These included the selectivity characteristics for two different low-pass networks. The gain/frequency characteristics of these networks are given in Figure 3. 8.

(a)* Scale:-

Horizontal = 5μS/cm
Vertical = 0.5v/cm

Frequency = 40 KHz

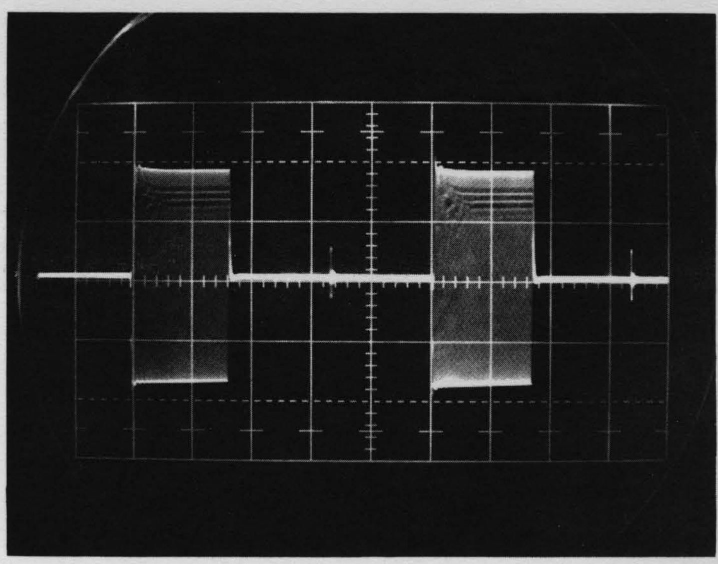

(b)* Scale:-

Horizontal = 5μS/cm
Vertical = 0.5v/cm

Frequency = 40 KHz

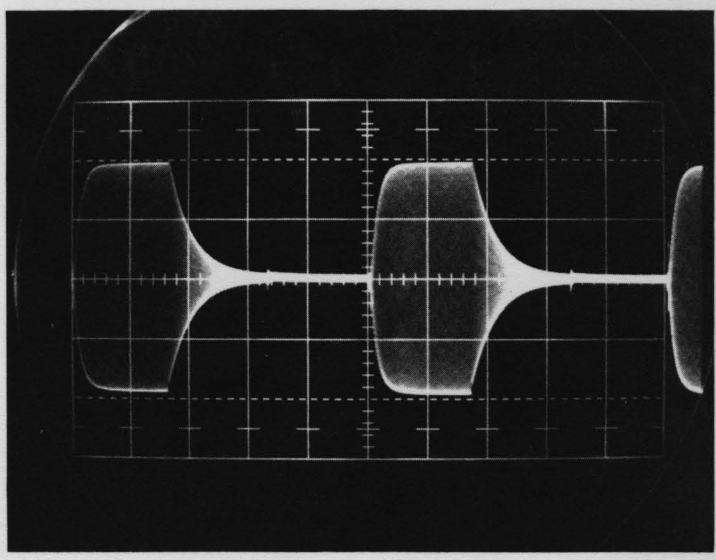

* Oscilloscope not synchronized to carrier.

Figure 4.21 - Variation in Rise and Fall Time of Sampled Signal

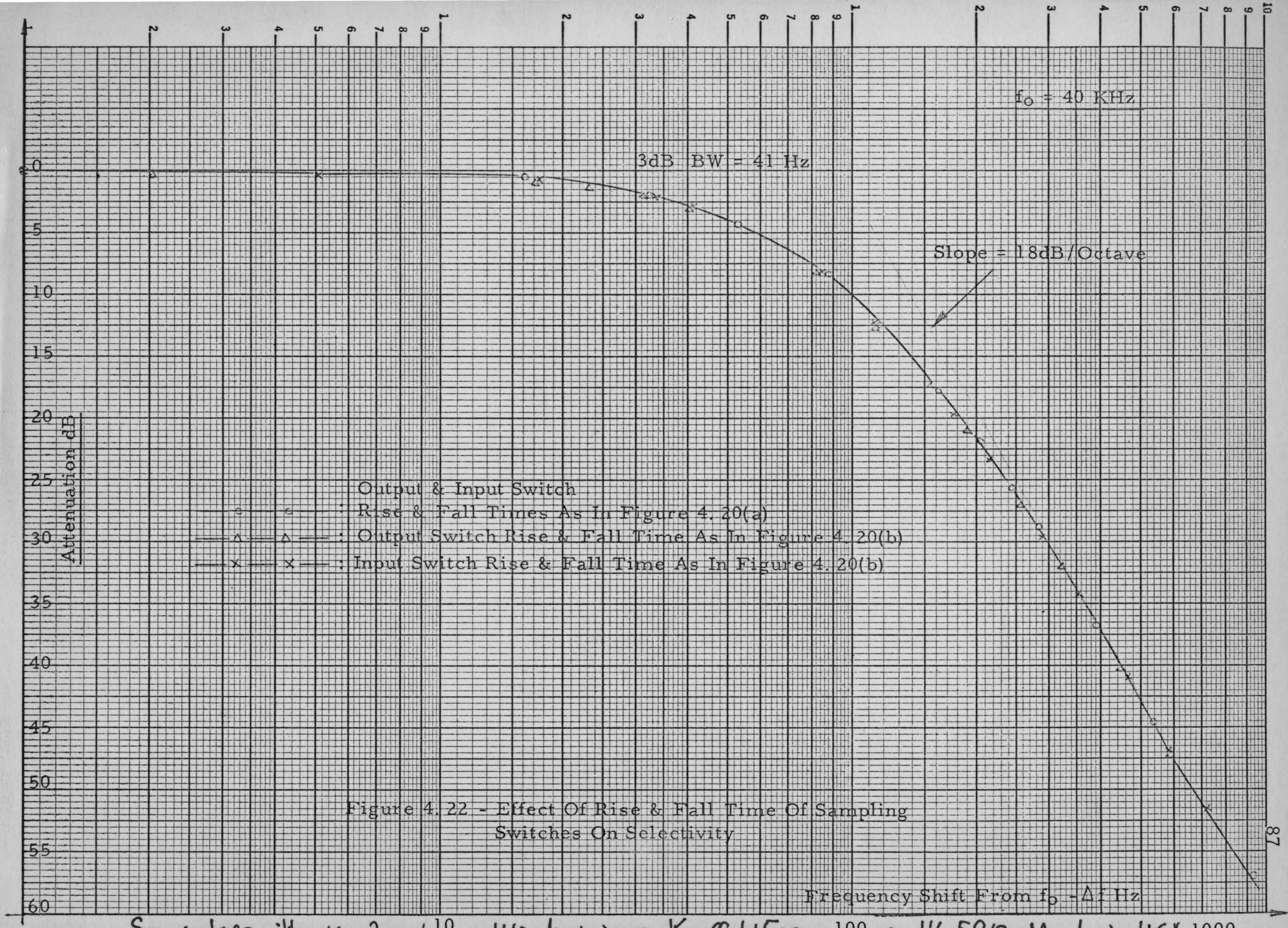

Figure 4. 22 - Effect Of Rise & Fall Time Of Sampling Switches On Selectivity

Measurements of the zero signal noise component and image component showed these to be of the same order as those measured on the 3-channel system. The main effect of this zero signal noise component is to decrease the available stop band attenuation for the same level of input signal. This is due to the increase in the pass band loss of the sampled data filter. The increase in loss over the 3-channel system amounted to approximately 6 dB, which is to be expected, since the signal is sampled for a time equivalent to one half the fundamental period whereas in the 3-channel system the signal is sampled over the complete period.

Figure 4. 23 demonstrates that a symmetrical band-pass characteristic is maintained and Figure 4. 24 shows that the asymptotic cut-off rate of 18 dB/octave is approached.

4. 6 Summary and Comparison of Sampled Data Filter Systems

Measurements of the zero signal noise component and image component were carried out on the quadrature modulation sampled data filter. Selectivity characteristics were obtained for two different low-pass networks.

A comparison of the pertinent parameters together with the results obtained for the zero signal noise and image component are summarized in Table 4. 1, below. From this

Figure 4. 23 - Realization Of Narrow Band-Pass Characteristic Using Quadrature Modulation Technique

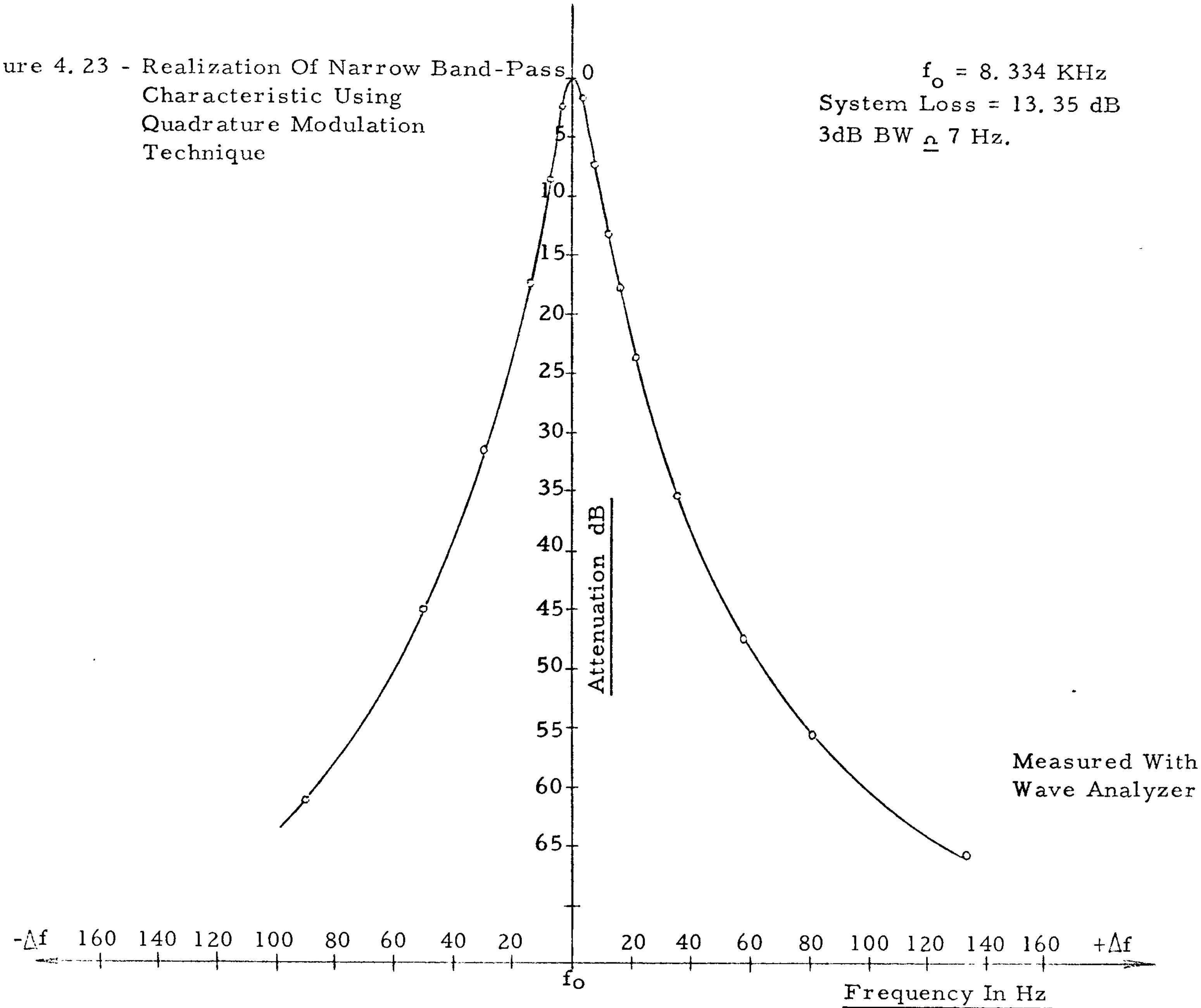

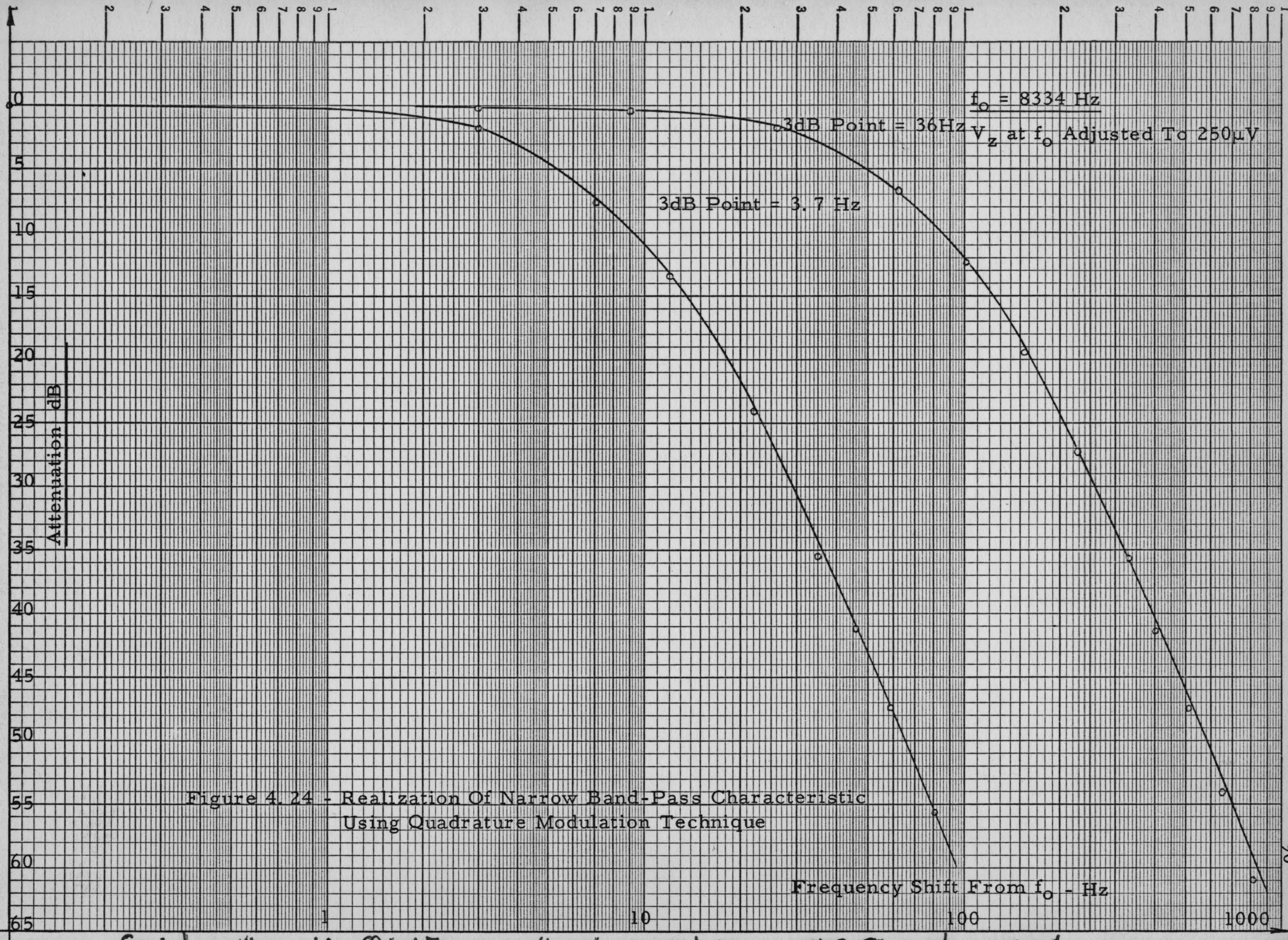

Figure 4.24 - Realization Of Narrow Band-Pass Characteristic Using Quadrature Modulation Technique

Semi-logarithmic Keuffel & Esser CO. 4 cycles X 70 divisions 358-81 Made in U.S.A

Table 4.1

PARAMETER / SYSTEM	LOW-PASS FILTER		BAND-PASS CHARACTERISTICS				
	3dB BANDWIDTH	RATE OF CUT-OFF	3dB BANDWIDTH	RATE OF CUT-OFF	ZERO SIGNAL COMPONENT*	IMAGE COMPONENT	STOP-BAND ATTENUATION
3-CHANNEL SYSTEM	67.5 Hz	18dB/ OCTAVE	135 Hz	18dB/ OCTAVE	$\ngtr$ 2mV	$\nless$ 35dB	51.5dB
2-CHANNEL OR QUADRATURE MODULATION SYSTEM	67.5 Hz	18dB/ OCTAVE	135 Hz	18dB/ OCTAVE	$\ngtr$ 2mV	$\nless$ 35dB	41.8dB
	7 Hz		14 Hz	18dB/ OCTAVE	$\ngtr$ 2mV	$\nless$ 35dB	42.25dB

Input To Both Systems Constant At IV RMS

$f_o = 8333$ Hz

* Gain Of RC-Active Network $\simeq$ 40dB.

table, it is seen that little advantage can be gained, for most applications, in utilizing the 3-channel system instead of the quadrature modulation system.

4.7 Bandwidth Variations

4.7.1 Realization of Ideal Bandwidth Translation

From the measurements taken of the selectivity characteristics on the 3-channel and quadrature modulation sampled data filter, it is seen that an exact low-pass to band-pass transformation was not obtained. A one to one correspondence between the low-pass and band-pass 3 dB bandwidth was realized, whereas theory dictates a two to one correspondence in the bandwidth translation process. This anomaly was further investigated and was found to be due to interaction of the low-pass networks with the input sampling switches. This was rectified by introducting a buffer stage between the input sampler and the low-pass network in order to realize the ideal system more closely.

The results obtained, with this modification, for both the 3-channel and quadrature modulation system show that an exact low-pass to band-pass translation is achieved; these are given in Figure 4.25 and Figure 4.26 respectively.

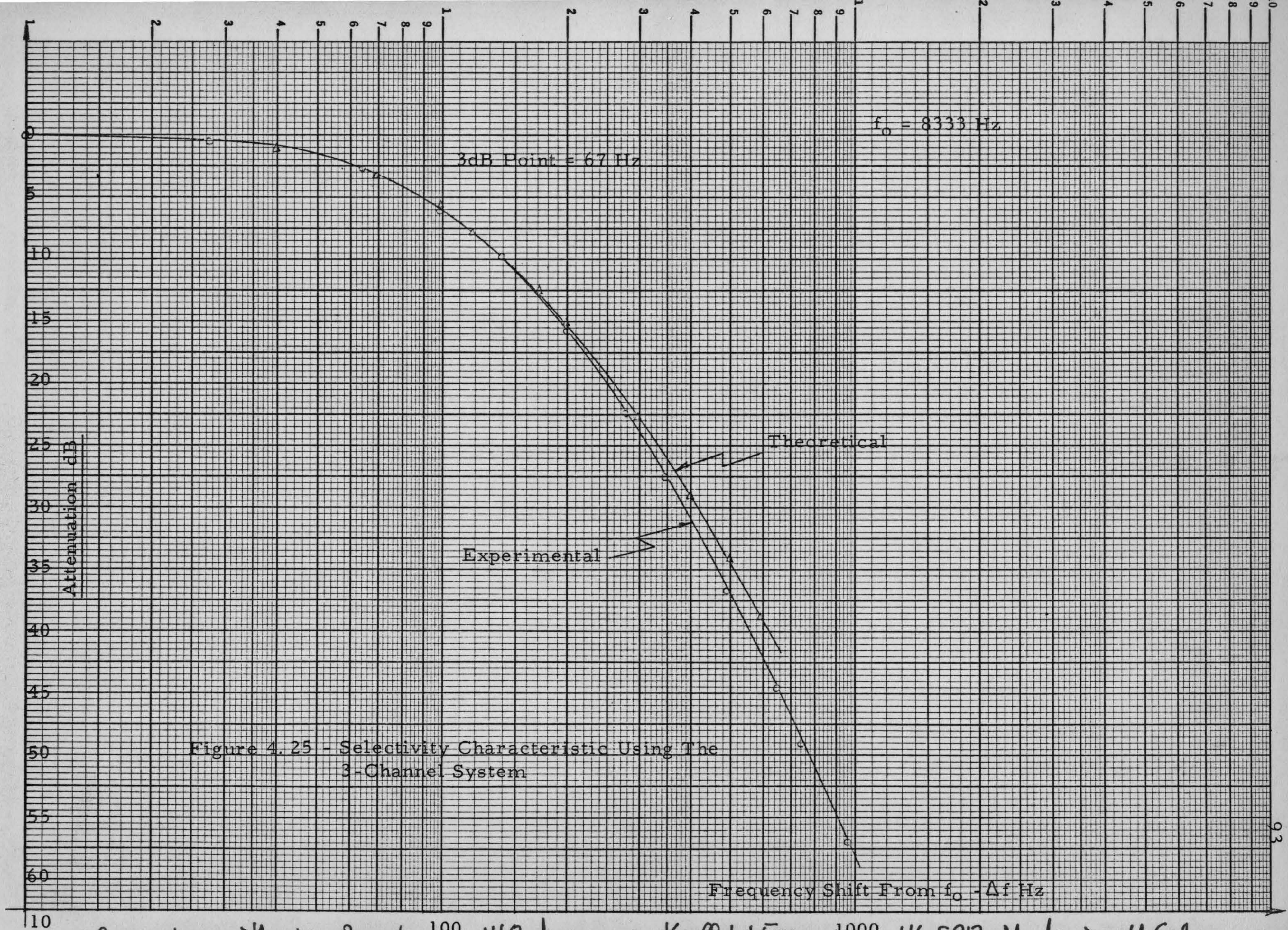

Figure 4. 25 - Selectivity Characteristic Using The 3-Channel System

Semi-logarithmic 3 cycles × 140 divisions Keuffel & Esser Co. 46 5813 Made in U.S.A.

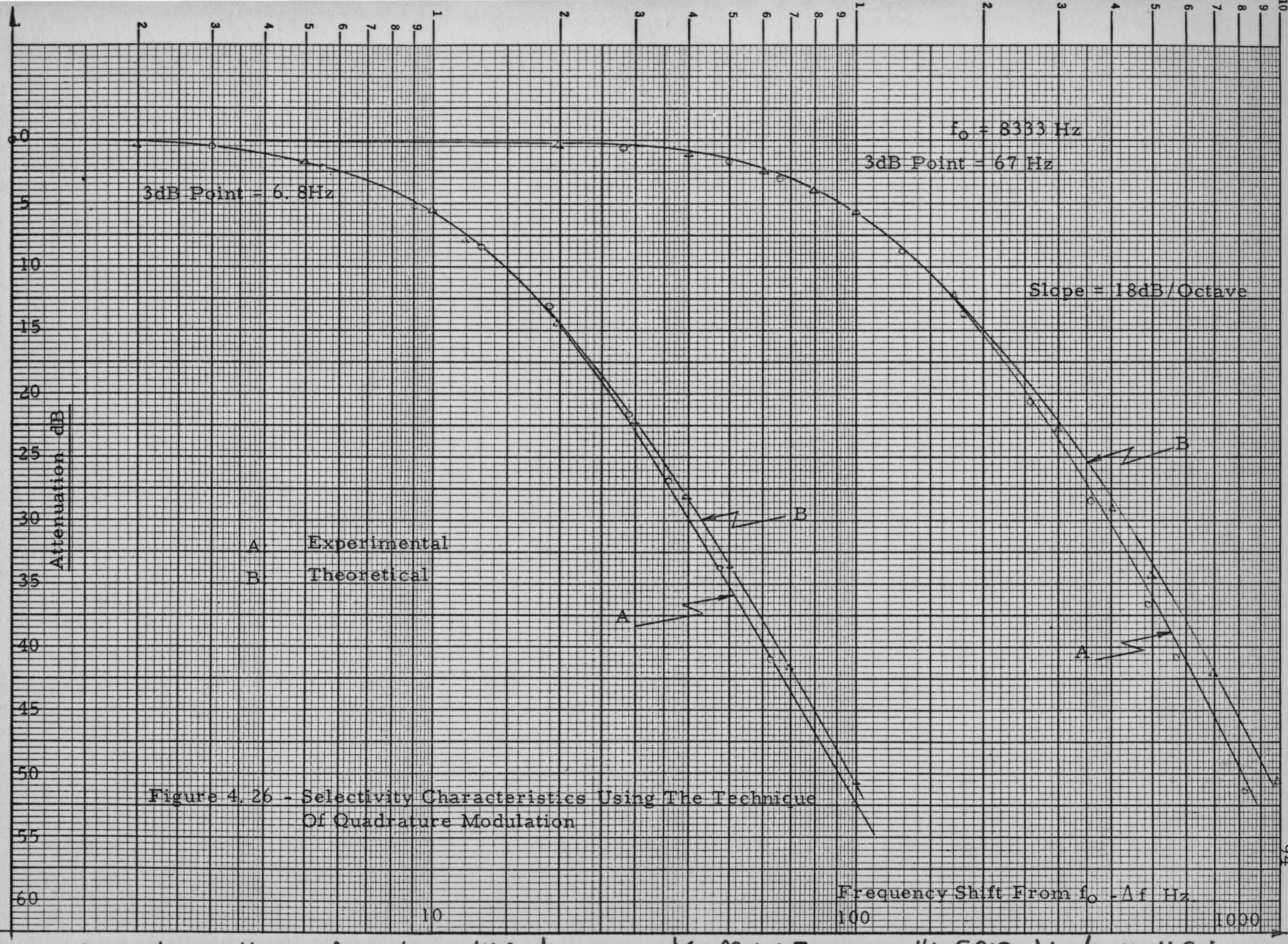

Figure 4.26 - Selectivity Characteristics Using The Technique Of Quadrature Modulation

The slight increase in loss at the high frequencies, when using the low-pass network of bandwidth 70 Hz, is attributed to the broad band-pass filter having a greater effect at these frequencies than within the pass-band.

4.7.2 Bandwidth Control

From the preceding discussion concerning the variation in the 3dB bandwidth of the sampled data filter, the question arises whether some form of bandwidth control can be achieved. Due to the interaction found between the input sampling switch and low-pass filter it seemed logical to alter the characteristics of one or the other to provide this control. The easiest characteristic to change was the switching function. The normal control waveforms for both the input and output sampling switches are given in Figure 3.5. Complementary control was applied to the sampling switches, and initial results indicated a reasonable change in the 3dB bandwidth. The disadvantage of this method however was the drastic increase in the pass-band loss and increase in modulation of the output signal.

A more suitable arrangement would be to control the parameters of an active or passive network, connected between the input sampling switches and low-pass networks, so as to control the reflection coefficient. In this manner it is possible to control the bandwidth over a 2:1 range as demonstrated by curves No. 1 and No. 4, of Figure 4.27.

An alternative method which is very easily implemented, is to alter the pole positions of the low-pass network by either switching alternative elements into the network or by using the variable resistance characteristics of a field-effect device.

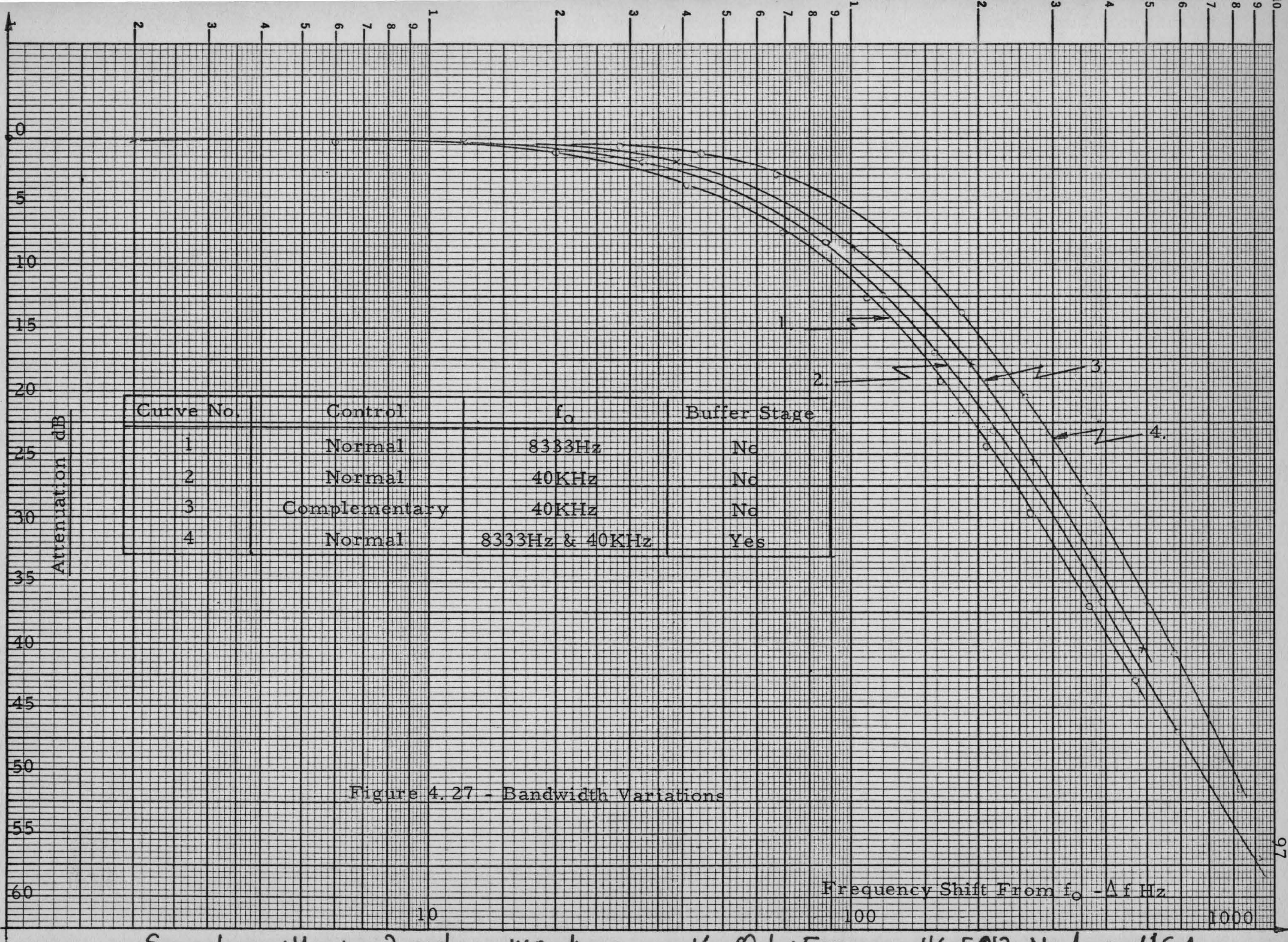

Curve No.	Control	f_o	Buffer Stage
1	Normal	8333Hz	No
2	Normal	40KHz	No
3	Complementary	40KHz	No
4	Normal	8333Hz & 40KHz	Yes

Figure 4.27 - Bandwidth Variations

CHAPTER V

DESIGN RECOMMENDATIONS

5.1 Introduction

In order to realize narrow band-pass filter characteristics operating over a frequency range, say from 1 KHz to 100 KHz, using RC time-varying networks, the following design recommendations must be borne in mind so that the optimum overall system performance of the sampled data filter may be obtained. This optimum system performance is based on the minimization of

a) the image component and

b) the zero signal component and its harmonics.

Both of these unwanted components are present in the system as a result of the imperfections associated with each channel and manifest themselves in the modulation of the wanted signal. The minimization of both the zero signal noise component and image component can be achieved by following the recommendations, in the design of a sampled data filter, given below.

5.2 Reduction of the Zero Signal Noise Component

The reduction of this component is important in order to obtain the maximum amount of stop-band attenuation of the sampled data filter for a given signal input. This applies to both the 3-channel and quadrature modulation system.

From the results of a qualitative analysis of the sampled data filter, this unwanted component is found to be the direct result of mismatch in the output sampling switches. This mismatch may take the form of variations in the gate drive signal and variations in the 'ON' resistances of the sampling switches. Thus in order to reduce this component to acceptable levels, it is necessary to keep this variation in 'ON' resistance a small percentage of the load resistance. This implies the use of field effect devices having 'ON' resistances equal to less than say 1% of the load resistance. For a typical load of $10K\Omega$, this condition can easily be met and exceeded with present day devices.

The control of the gate drive signal can easily be implemented with the use of high speed digital logic circuits. Typical switching times of digital integrated circuits are of the order of 10nS which is an improvement by a factor of 10 over the discrete system used during the investigation, resulting in a further reduction of the zero signal noise component and its harmonics.

Unbalance between the low-pass networks will also introduce the zero signal noise component. In order for these networks to have zero effect on this component, the dc loss of each network must be made identical with each other.

5.3 Reduction of the Image Component

The amplitude of the image component encountered in the sampled data filter is a direct function of unbalance of the amplitude and phase-frequency characteristics in the individual low-pass networks. Balance to within 2% was obtained for the low-pass network providing an image component not less than 35dB below the output signal. In order to reduce the image component further, so that its effect may be neglected, is to provide low-pass networks matched to say 0.5% or better. This tolerance figure is easily obtainable with available discrete components and thin-film technology [10].

5.4 Further Improvements of System Performance

The use of an RC-active low-pass network instead of a passive network would provide certain advantages. The foremost of these is the fact that if an operational amplifier is used as the active network, a low output impedance is provided to the output sampling switches which is necessary to reduce the switching transient component at a frequency of

3x the sampling frequency. Each sampling switch may also be conveniently presented with identical offset voltages as these are easily controlled when using an operational amplifier. For the quadrature modulation system, the third output sampling switch may be eliminated when utilizing an operational amplifier as the active element, since in this case the offset voltage may now be adjusted to zero volts or to the voltage determined by the virtual ground point of the broad band-pass active filter.

The other advantage of using an active low-pass network is that gain may be provided to compensate for the equivalent loss due to a passive network. Provided the low-pass networks are accurately balanced, the effect will be to improve the signal-to-noise ratio at the final output. The 'noise' referred to here is the zero signal noise component and its harmonics. An increase in the stop-band attenuation will result.

CHAPTER VI

REMARKS AND FUTURE TRENDS

6.1 An alternative technique for the realization of narrow band-pass characteristics has been investigated. This technique makes use of RC time-varying networks resulting in the so-called 'N-path filter'. The distortion inherent in the sampled data filter has been examined qualitatively in two different configurations, namely the 3-channel system and the system using the technique of quadrature modulation.

The process of bandwidth translation has been examined quantitatively for both systems, and excellent agreement between theoretical and experimental results were obtained. Based upon the experimental investigation, certain design criteria necessary for the optimum design of a sampled data filter have been presented. The design recommendations are based on the minimization of the zero signal noise component and the image component.

The zero signal noise component can be compared to the carrier leak associated with analog multipliers (balanced ring modulators). In the systems described in Chapter III, the zero signal noise component was adjusted to greater than 60dB below the output signal which is comparable to that obtained in analog systems.

The main attraction of the sampled data filter is the fact that the centre frequency may be easily controlled without altering the prescribed band-pass characteristics. The basis of these characteristics is in the synthesis of the low-pass network.

6.2 With the rapid advancement of integrated circuit technology, the reduction of the sampled data filter into integrated circuit form would be the next phase of its development. This technique using thin-films, has already been described by Galpin [10] for the realization of a single-sideband demodulator.

Numerous references on the design of narrow band-pass filters using commutated low-pass networks have been cited. These band-pass filters have been referred to in the literature as quadrature function filters, sampled data filters and N-path filters.

Since commutated low-pass networks yield a band-pass characteristic, is it possible to obtain a band-stop characteristic with commutated networks? This question has been answered to some degree by Acampora [11]. Acampora has considered alternative path networks i. e. the high-pass filter, the all-pass network and the band-pass filter. The results obtained from the theoretical analysis presented by Acampora are listed below:

1) Commutated high-pass filters do not lend themselves to a band-stop filter. The maximum attenuation of the resultant notch being 6dB.

2) Surprisingly, it is the all-pass network which provides a notch filter.

3) Commutated band-pass filters result in a pair of adjacent band-pass filters with a notch between them that grows deeper as the sampling frequency increases.

It is recommended that further work be carried out on the sampled data filter, using all-pass networks in order to realize prescribed band-stop characteristics. This would enable the design of complementary filters to be carried out.

APPENDICES

APPENDIX I

CIRCUIT DETAILS

1. Crystal Oscillator

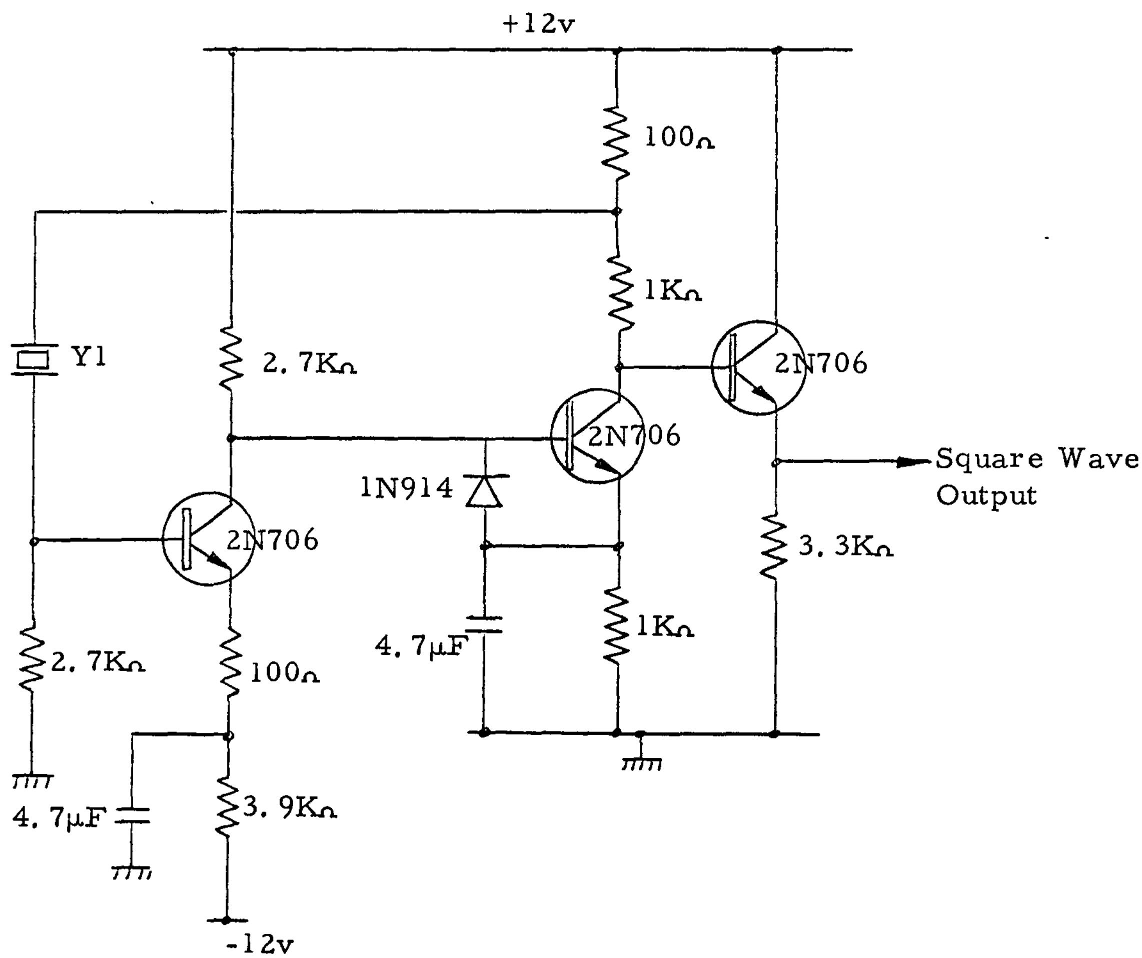

Y1: 25 KHz Crystal Operating In Series Mode.

2. <u>3-Stage Shift Register</u>

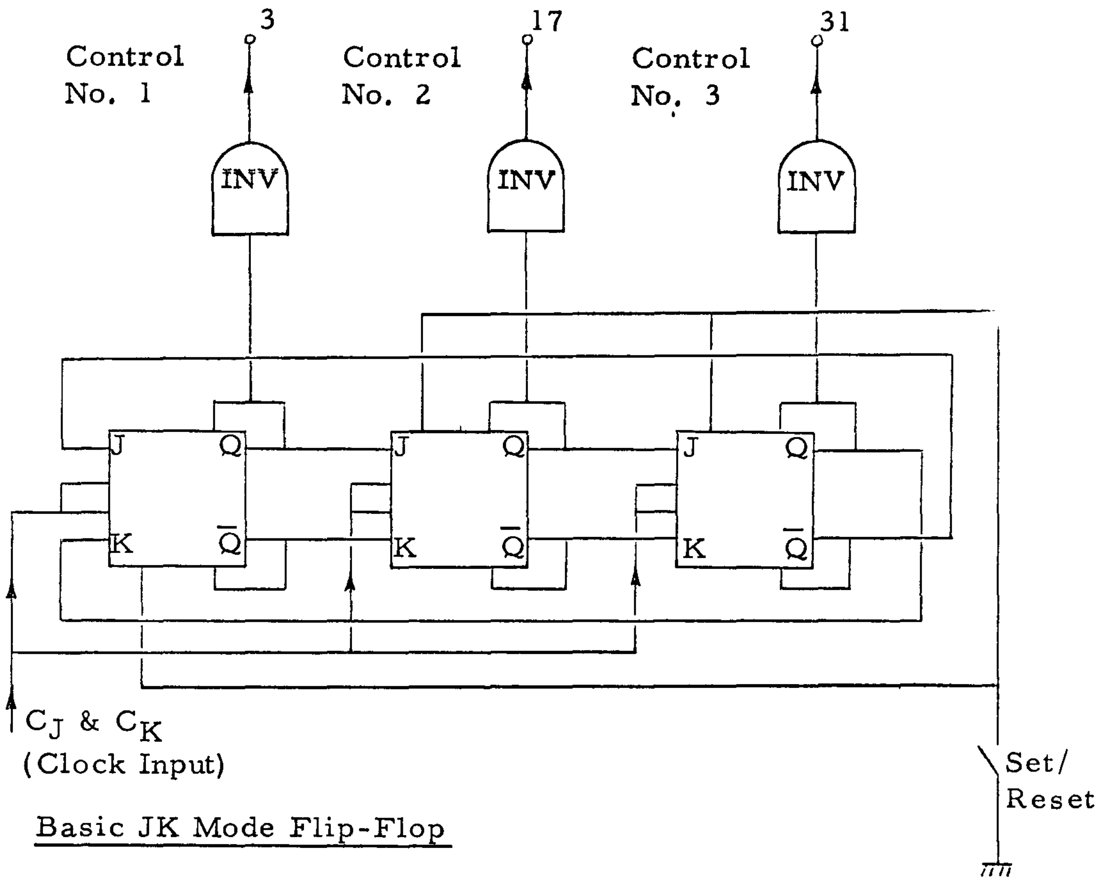

Basic JK Mode Flip-Flop

(Westinghouse Type WM 215T)

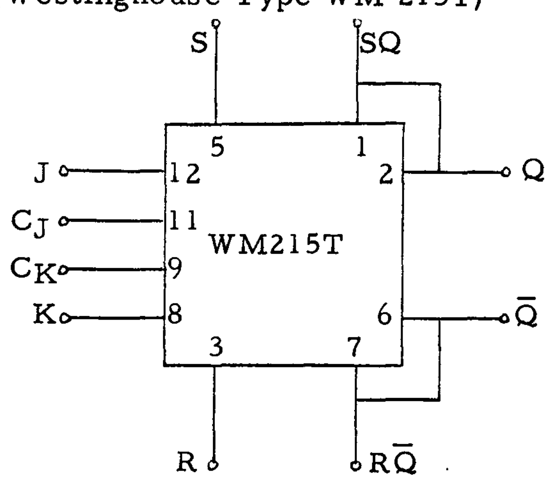

3. Bistable Circuit and Gate

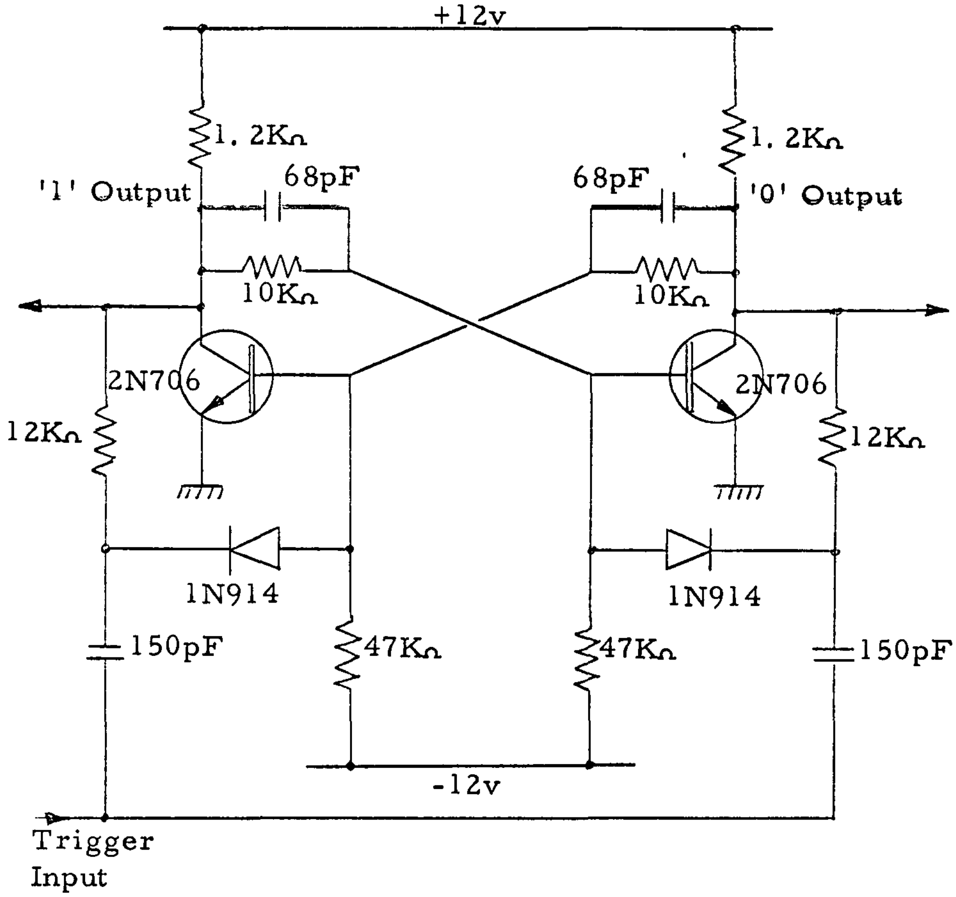

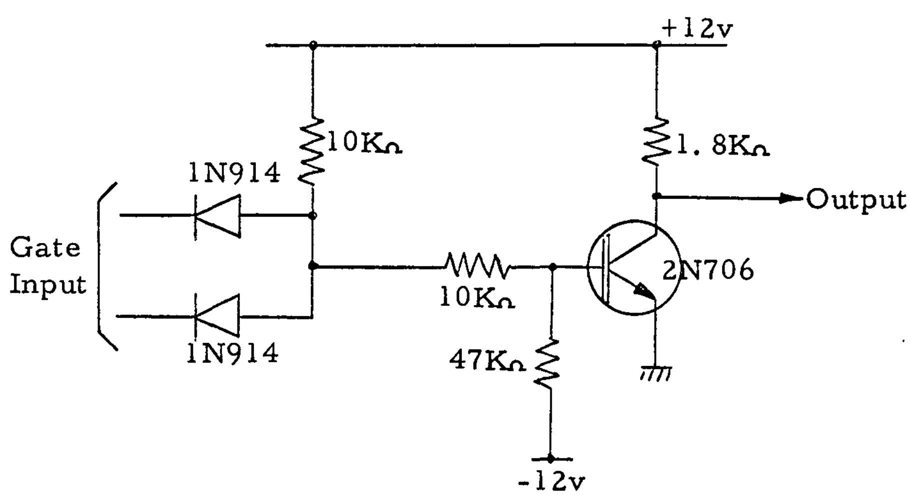

4. Tuned Amplifier

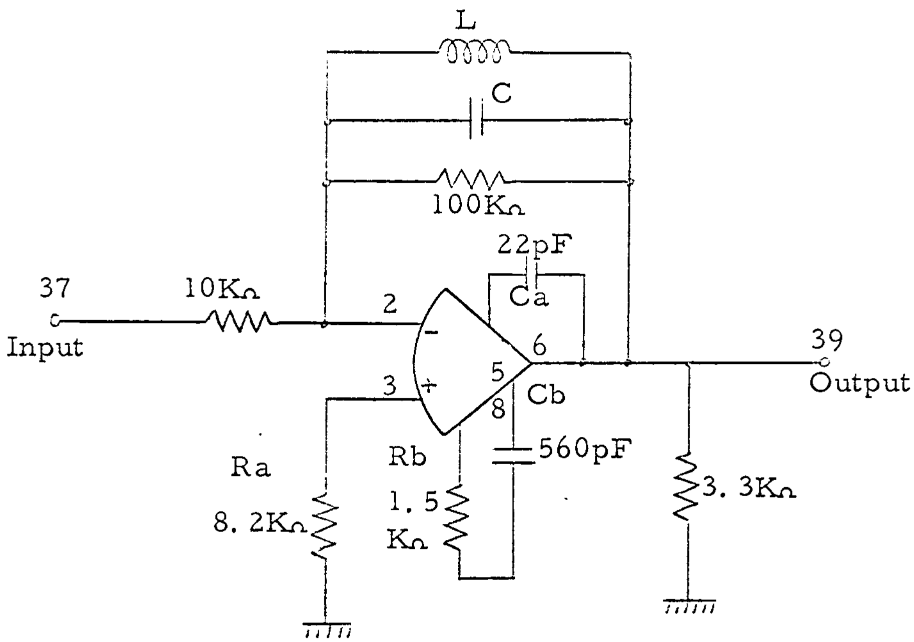

Centre Frequency f_o	L mH	C pF	3 dB Bandwidth	Gain at f_o -dB
8333 Hz	228 mH	1590 pF	$\simeq$1 KHz	$\simeq$20 dB
40 KHz	9.92 mH	1590 pF	$\simeq$1 KHz	$\simeq$20 dB

Components Ra and Rb, Ca and Cb are for off-set voltage minimization and frequency compensation of the operational amplifier, type μA709, respectively.

5. RC-Active Band-Pass Network

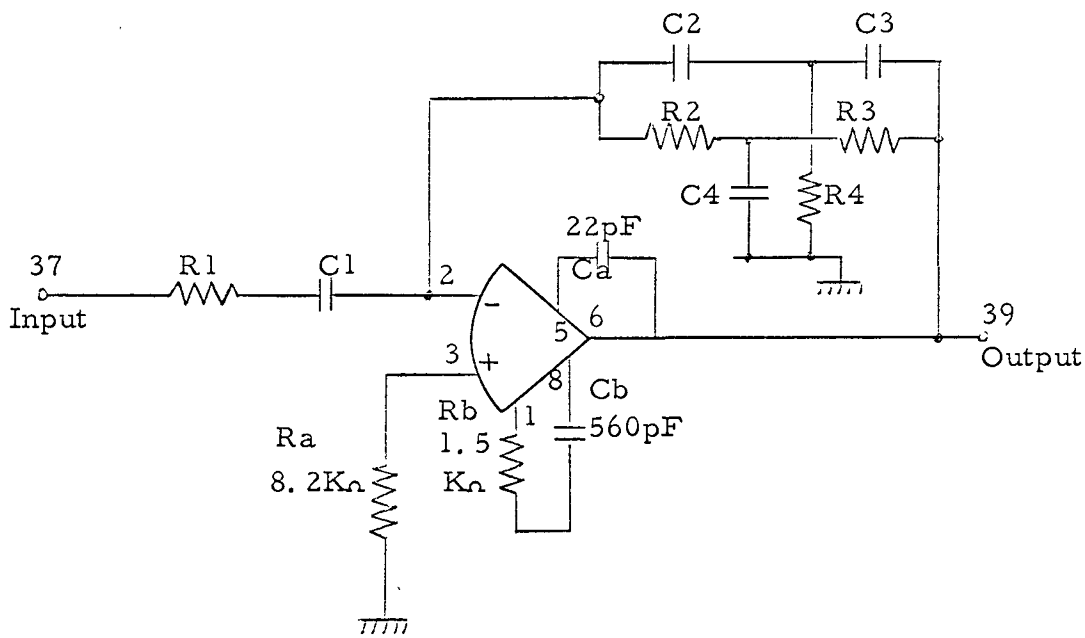

f_o = 8333 Hz.

3 dB Bandwidth $\simeq$ 1 KHz.

Gain at f_o $\simeq$ 40 dB.

R1 = 10 KΩ
R2 = 79.6 KΩ
R3 = 20.3 KΩ
R4 = 17.8 KΩ

C1 = 1905 pF
C2 = 239 pF
C3 = 940 pF
C4 = 1070 pF

As in the previous tuned amplifier, components Ra and Rb, Ca and Cb are for off-set voltage minimization and frequency compensation of the operational amplifier, type μA709, respectively.

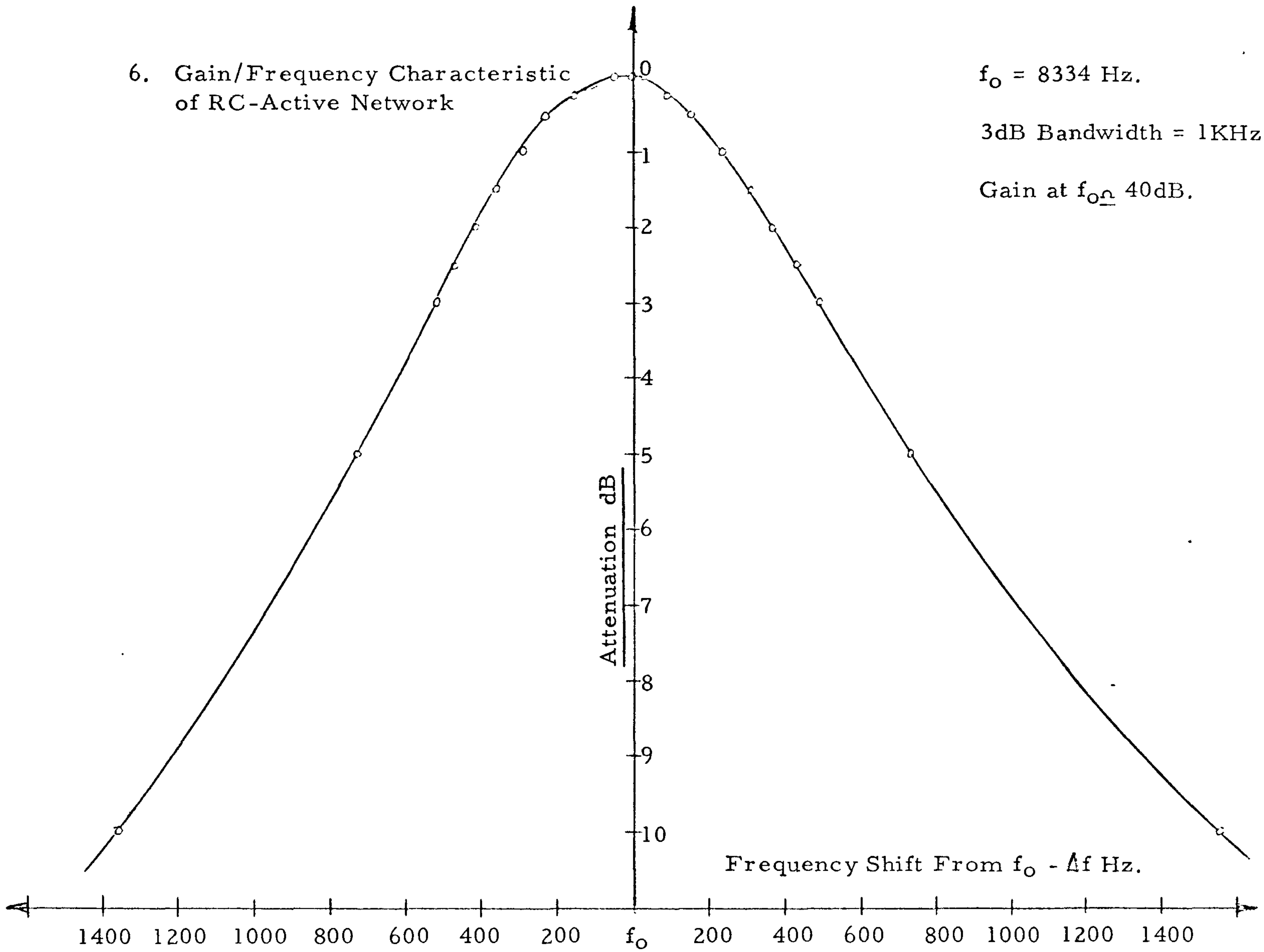

6. Gain/Frequency Characteristic of RC-Active Network

APPENDIX II

SYNTHESIS OF THE LOW-PASS NETWORK

The synthesis procedure for the passive low-pass network presented here is due to E. S. Kuh [7]. It has the advantage that the gain constant of the passive RC network is optimized to the maximum value. A third order network is considered having a transfer function

$$G_{12}(s) = \frac{H}{(s + 1)(s + 1.5)(s + 2)}$$

where H is the gain constant to be optimized. The network is to operate between specified load and source resistances and are included in the network below.

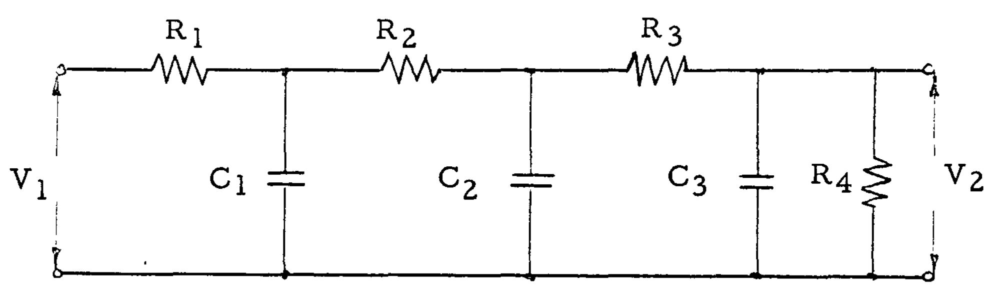

$$G_{12} = \frac{V_2}{V_1} = \frac{H}{(s + 1)(s + 1.5)(s + 2)} \text{ and } R_1 = 1, \; R_4 = 5$$

$$G_{12} = -y_{12}R_4$$

$$-y_{12} = \frac{G_{12}}{R_4} = \frac{H}{R_4} \cdot \frac{1}{(s + 1)(s + 1.5)(s + 2)}$$

The partial fraction expansion of this function for an RC network is

$$\frac{-y_{12}}{s} = \frac{H}{R_4}\left[\frac{k_{12}^{(0)}}{s} + \frac{k_{12}^{(1)}}{s+1} + \frac{k_{12}^{(2)}}{s+1.5} + \frac{k_{12}^{(3)}}{s+2}\right].$$

$$= \frac{H}{5}\left[\frac{.3333}{s} + \frac{-2}{s+1} + \frac{2.6667}{s+1.5} + \frac{-1}{s+2}\right]$$

From this equation we may select y_{11} and y_{22} to satisfy the residue condition with the equals sign i.e. when $k_{11}^{(i)} \cdot k_{22}^{(i)} = \left[k_{12}^{(i)}\right]^2$, giving

$$\frac{-y_{12}}{s} = \frac{H}{5}\left[\frac{\alpha_0}{s} + \frac{\alpha_1}{s+1} + \frac{\alpha_2}{s+1.5} + \frac{\alpha_3}{s+2}\right]$$

$$\frac{y_{11}}{s} = \frac{H}{5}\left[\frac{\alpha_0}{s} + \frac{x_1}{s+1} + \frac{x_2}{s+1.5} + \frac{x_3}{s+2}\right]$$

and $$\frac{y_{22}}{s} = \frac{H}{5}\left[\frac{\alpha_0}{s} + \frac{\alpha_1^{\,2}/x_1}{s+1} + \frac{\alpha_2^{\,2}/x_2}{s+1.5} + \frac{\alpha_3^{\,2}/x_3}{s+2}\right]$$

letting $\left|k_{12}^{(i)}\right| = \alpha_i$ and $k_{11}^{(i)} = x_i$

where $i = 0, 1, 2, 3$

then $$k_{22}^{(i)} = \frac{\alpha_i^{\,2}}{x_i}$$

Then we obtain for y_{11} and y_{22},

$$\frac{y_{11}}{s} = \frac{H}{5}\left[\frac{.3333}{s} + \frac{x_1}{s+1} + \frac{x_2}{s+1.5} + \frac{x_3}{s+2}\right].$$

and $$\frac{y_{22}}{s} = \frac{H}{5}\left[\frac{.3333}{s} + \frac{4/x_1}{s+1} + \frac{(2.6667)^2/x_2}{s+1.5} + \frac{1}{s+2}\right]$$

At infinite frequency,

$$y_{11} = 1 \text{ and } y_{22} = \frac{1}{5}$$

i.e. $$\frac{H}{5}\left[\frac{1}{3} + x_1 + x_2 + x_3\right] = 1$$

and $$\frac{H}{5}\left[\frac{1}{3} + \frac{4}{x_1} + \frac{(2.6667)^2}{x_2} + \frac{1}{x_3}\right] = \frac{1}{5}$$

Use is made of the Lagrange multiplier rule from the 'Calculus of Variations' in order to solve for x_1, x_2 and x_3 such that the gain constant H is maximized. Kuh has shown that, from this rule

$$\frac{x_1}{\alpha_1} = \frac{x_2}{\alpha_2} = \frac{x_3}{\alpha_3} = X$$

where X must satisfy the quadratic equation

$$X^2 + \frac{\alpha_0}{A}\left\{1 - \frac{R_4}{R_1}\right\}X - \frac{R_4}{R_1} = 0$$

where $$A = \sum_{i=1}^{3} |\alpha i|$$

Solving for X and taking the positive value only, we obtain

$$X = 2.40681280$$

Hence the values of x_1, x_2 and x_3 may be determined and are

$$x_1 = 4.8136256$$

$$x_2 = 6.4181675$$

$$x_3 = 2.4068128$$

The maximum value of H is,

$$H_{max} = \frac{R_4/R_1}{\alpha_0+X\cdot A} = \frac{R_4}{\alpha_0+x_1+x_2+x_3}$$

$$= \frac{5}{13.9719392} = 0.35786012$$

Substituting for H, α_0, x_1, x_2 and x_3 we have for y_{11},

$$\frac{y_{11}}{s} = \frac{0.35786012}{5}\left[\frac{1}{3s} + \frac{4.8136256}{s+1} + \frac{6.4181675}{s+1.5} + \frac{2.4068128}{s+2}\right]$$

From which z_{11} is found to be,

$$z_{11} = \frac{s^3 + 4.5s^2 + 6.5s + 3}{s^3 + 3.1219162\,s^2 + 2.3657488\,s + 0.07157202}$$

The continued fraction expansion of this impedance is

$$z_{11} = 1 + \cfrac{1}{.7256s + \cfrac{1}{11.3035 + \cfrac{1}{.08628s + \cfrac{1}{24.414 + \cfrac{1}{.1555s + \frac{1}{5}}}}}}$$

Thus the normalized network will be as given below

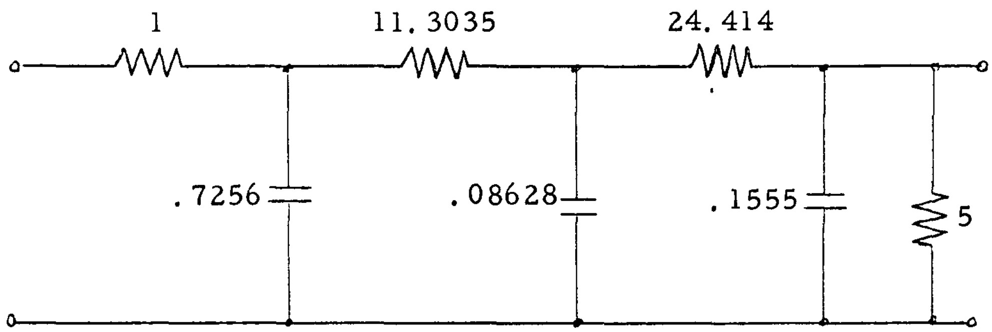

The network loss at s = 0

= $\underline{0.124 = 18.15 \text{ dB}}$

To denormalize, the

Resistors are multiplied by 2.2KΩ and

Capacitors are multiplied by $\frac{1}{R\omega_o}$

APPENDIX III

COMPUTER PROGRAMS

```
C     NTH ORDER LOW PASS FILTER (N=1 TO 5)
      READ(5,1) A5,A4,A3,A2,A1,A0,H,RIPL
      READ(5,2) FR1,FR2,FX1,FX2
      READ(5,8) F0
      WRITE(6,3) A5,A4,A3,A2,A1,A0,H,RIPL
      WRITE(6,4)
      COMPLEX S,G
      F=0.
      W0=2.*3.14159*F0
    5 W=2.*3.14159*F
      S=CMPLX(0.0,W)
      G=H/(A5*(S/W0)**5+A4*(S/W0)**4+A3*(S/W0)**3+A2*(S/W0)**2+A1*(S/W0)
     1+A0)
      GABS=CABS(G)
      THETA=180./3.14159*ATAN2(AIMAG(G),REAL(G))
      GDBS=20.*ALOG10(GABS)
      GDBS0=20.*ALOG10(H/A0)
      GDBSN=GDBS-GDBS0
      WRITE(6,7) F,GDBS,GDBSN,THETA
      IF(F.GE.FR2)GO TO 6
      IF(F.GE.FR1)F=F+FX2
      IF(F.LT.FR1)F=F+FX1
      GO TO 5
    6 CONTINUE
    1 FORMAT(6F11.7/2F5.2)
    2 FORMAT(2F7.1,2F5.1)
    8 FORMAT(F6.1)
    3 FORMAT(1H0,10X,3HA5=,F11.7,5X,3HA4=,F11.7,5X,3HA3=,F11.7/11X,3HA2=
     1,F11.7,5X,3HA1=,F11.7,5X,3HA0=,F11.7/11X,2HH=,F5.2,5X,16HPASSBAND
     2RIPPLE=,F5.2,1X,2HDB)
    4 FORMAT(1H0,10X,8HFREQ(HZ),10X,8HGAIN(DB),10X,11HGAINORM(DB),10X,10
     1HPHASE(DEG))
    7 FORMAT(1H ,10X,F7.1,11X,F8.4,11X,F8.4,13X,F8.3)
      STOP
      END
```

```
C             BANDPASS CHARACTERISTICS OF THE SAMPLED DATA FILTER
C             USING AN NTH ORDER LOW PASS FILTER (N=1 TO 5)
C             IN M IDENTICAL PARALLEL CHANNELS
      READ(5,1) A5,A4,A3,A2,A1,A0,H,RIPL,F0
      READ(5,2) FR1,FR2,FR3,FR4,FX1,FX2,CHN,FC,D1,D2
      WRITE(6,3) A5,A4,A3,A2,A1,A0,H,RIPL,F0
      WRITE(6,4) CHN,FC,D1,D2
      WRITE(6,5)
      T=1./FC
      CK=(CHN)*D2/T
      PW=(3.14159/T)*(D1-D2)
      COMPLEX S,SC,GD,GS,TRF,FP,CA1,CCA1
      FP=CMPLX(0.0,PW)
      CA1=(CEXP(FP))*((SIN(3.14159*D1/T))/(3.14159*D1/T))*((SIN(3.14159*
     1D2/T))/(3.14159*D2/T))
      CCA1=CONJG(CA1)
      FC=1./T
      F=FR1
      VOABS=1.
      W0=2.*3.14159*F0
      WC=2.*3.14159*FC
    6 W=2.*3.14159*F
      S=CMPLX(0.0,W)
      SC=CMPLX(0.0,WC)
      GD=H/(A5*((S-SC)/W0)**5+A4*((S-SC)/W0)**4+A3*((S-SC)/W0)**3+A2*((S
     1-SC)/W0)**2+A1*(S-SC)/W0+A0)
      GS=H/(A5*((S+SC)/W0)**5+A4*((S+SC)/W0)**4+A3*((S+SC)/W0)**3+A2*((S
     1+SC)/W0)**2+A1*(S+SC)/W0+A0)
      TRF=CK*((CA1*GD)+(CCA1*GS))
      VRABS=CABS(TRF)
      THETA=180./3.14159*ATAN2(AIMAG(TRF),REAL(TRF))
      IF(F.EQ.FC) VOABS=CABS(TRF)
      VRDBO=20.*ALOG10(VOABS)
      VRDBS=20.*ALOG10(VRABS)
      VRDBN=VRDBS-VRDBO
      WRITE(6,7) F,VRDBS,VRDBN,THETA
      IF(F.GE.FR4)GO TO 8
      IF(F.GE.FR3)F=F+FX2
      IF(F.GE.FR2.AND.F.LT.FR3)F=F+FX1
      IF(F.LT.FR2)F=F+FX2
      GO TO 6
    8 CONTINUE
    1 FORMAT(6F11.7/3F7.2)
    2 FORMAT(4F7.0,2F4.0,F3.0,F7.0,2F8.6)
    3 FORMAT(1H0,10X,3HA5=,F11.7,5X,3HA4=,F11.7,5X,3HA3=,F11.7/11X,3HA2=
     1,F11.7,5X,3HA1=,F11.7,5X,3HA0=,F11.7/11X,2HH=,F5.2,5X,16HPASSBAND
     2RIPPLE=,F5.2,1X,2HDB/11X,7HLOWPASS,1X,7HCUTOFF=,F7.2,1X,2HHZ)
    4 FORMAT(1H0,10X,6HNUMBER,1X,2HOF,1X,9HCHANNELS=,F3.0/11X,6HCENTRE,1
     1X,10HFREQUENCY=,F7.0,1X,2HHZ/11X,3HI/P,1X,8HSAMPLING,1X,9HINTERVAL
     2=,F9.6,1X,3HSEC/11X,3HO/P,1X,8HSAMPLING,1X,9HINTERVAL=,F9.6,1X,3HS
     3EC)
    5 FORMAT(1H0,10X,8HFREQ(HZ),10X,8HGAIN(DB),10X,11HGAINORM(DB),10X,10
     1HPHASE(DEG))
    7 FORMAT(1H ,10X,F7.0,11X,F8.4,11X,F8.4,13X,F8.3)
      STOP
      END
```

APPENDIX IV

TEST EQUIPMENT

1. Power Supplies (DC)

   Hewlett-Packard, Harrison 6206B, Serial No. 6J1466 and Serial No. 6J1461. McMaster No. 5285 and 5284.

2. RC-Oscillator, 20 Hz - 500 Hz

   General Radio Co., Type No. 1210-C. McMaster No. 4945.

3. RMS Voltmeter

   Hewlett-Packard, Type 3400A, Serial No. 528-05863. McMaster No. 5243.

4. Wave Analyzer

   Hewlett-Packard, Model 302A, Serial No. 528-05467. McMaster No. 5202.

5. Oscilloscope

   Tektronix Inc., Type 547, Serial No. 003487, McMaster No. 5278, with Type 1A2 Dual-Trace Plug In Unit, Serial No. 002626, McMaster No. 5279.

6. Electronic Counter

   Hewlett-Packard, Type 5233L, Serial No. E413-00146. McMaster No. 5126.

7. Test Oscillator

   Hewlett-Packard, Model 651A, Serial No. 434-01160. McMaster No. 5141.

8. Dumont Oscilloscope Camera

   Type 353, Serial No. 602. McMaster No. 4275.

REFERENCES

1. N. F. Barber,

   "Narrow Band-Pass Filter Using Modulation",

   Wireless Engineer, Vol. 20, pp. 132-135, May 1947.

2. G. B. Madella,

   "Single-Phase and Polyphase Filtering Devices Using Modulation",

   Wireless Engineer, Vol. 24, p. 310, October 1947.

3. I. F. Macdiarmid and D. G. Tucker,

   "Polyphase Modulation As A Solution Of Certain Filtration Problems In Telecommunication",

   Proceedings I. E. E., Vol. 97, Part 3, pp. 349-358, September 1950.

4. D. K. Weaver Jr.,

   "A Third Method Of Single-Sideband Generation And Reception",

   Proceedings I. R. E., Vol. 44, pp. 1703-1705, December 1956.

5. H. Paris,

   "Utilization Of The Quadrature Functions As A Unique Approach To Electronic Filter Design",

   I. R. E. Convention Record, Part 9, p. 204, 1960.

6. L. E. Franks and I. W. Sandberg,

"An Alternative Approach To The Realization Of Network Transfer Functions: The N-Path Filter",

B.S.T.J., Vol. 39, pp. 1321-1350, September 1960.

7. E.S. Kuh,

"Synthesis Of RC Grounded Two Parts",

I.R.E. Transactions, Vol. CT-5, pp. 55-61, 1958.

8. F.H. Blecher,

"Application Of Synthesis Techniques To Electronic Circuit Design",

I.R.E. Transactions On Circuit Theory, Vol. CT-7, p. 79, August 1960.

9. S.S. Haykim,

"A Synthesis Procedure Of RC-Active Filters Using Unity-Gain Current And Voltage Amplifiers",

Int. J. Control, Vol. 3, No. 6, pp. 553-564, 1966.

10. R.K.P. Galpin et al,

"A Practical Thin Film Single-Sideband Demodulator Using RC-Time Varying And Active Networks",

I.E.E.E. Journal Of Solid-State Circuits, Vol. SC-2, No. 1, pp. 26-31, March 1967.

11. A. Acampora,

"The Generalized Transfer Function And Pole-Zero Migrations In Switched Networks",

RCA Review, Vol. XXVII, No. 2, pp. 245-262, June 1966.

12. P. F. Panter,

"Modulation, Noise and Spectral Analysis",

McGraw-Hill, Inc., 1965; Section 2.5, p. 36-37.